Title
Transcriptional Regulation of Metabolic Genes by Glucocorticoid Receptor

Author
Kuo, Taiyi

Publication Date
2012

Peer reviewed|Thesis/dissertation

Transcriptional Regulation of Metabolic Genes by Glucocorticoid Receptor

By

Taiyi Kuo

A dissertation submitted in partial satisfaction of the requirements for

the degree of

Doctor of Philosophy

in

Endocrinology

in the

Graduate Division

of the

University of California, Berkeley

Committee in Charge:

Professor Jen-chywan Wally Wang
Professor Gary Firestone
Professor Terry Machen

Fall 2012

Table of Contents

Introduction

Glucocorticoids are steroid hormones involved in diverse cell type-specific physiological processes such as metabolic and immune responses. Their circulating levels are raised upon stress conditions, such as starvation and fasting. They exert essential adaptive physiological processes to ensure the survival of mammals, including preserving plasma glucose levels for brain. The endogenous glucocorticoid hormone in humans is cortisol while in rodents is corticosterone. Glucocorticoids are secreted from the adrenal cortex, under the control of a neuroendocrine feedback system, the hypothalamo-pituitary-adrenal (HPA) axis. The HPA axis starts with the secretion of the hypothalamic corticotropin-releasing hormone (CRH). In response to CRH, the pituitary pro-opiomelanocortin (POMC) gene transcription is activated. The secretion of POMC gives rise to adrenocorticotropic hormon (ACTH), which further stimulate the synthesis of glucocorticoids in the adrenal glands. Glucocorticoids, through negative feedback loop, can terminate the stress response by acting on the hypothalamus and the pituitary gland.

A. The Biological Effect of Glucocorticoids

Glucocorticoids affect almost every cell type and exert a wide range of physiological processes in mammals. The name of glucocorticoids is originated from their effects on carbohydrate metabolism. In addition to glucose homeostasis, glucocorticoids also regulate lipid and protein metabolism. The metabolic effects of glucocorticoids will be discussed in detail in next section.

Glucocorticoids have a profound effect on immune system. Glucocorticoids contain potent anti-inflammatory and immunosuppressive effects. For the former, glucocorticoids are able to increase the production of anti-inflammatory protein expression, and in the same time reduce the expression of pro-inflammatory proteins, such as cytokines and chemokines, induced by inflammatory stimuli and infection. For the latter, glucocorticoids can induce the apoptosis of immune cells, and also regulate T-cell development. Notably, because of these specific effects on immune system glucocorticoids are frequently used to treat inflammatory and immune diseases, such as arthritis, asthma and lupus.

Glucocorticoids also play a key role in fetal development. They are required for the maturation of lung development and the production of surfactant. Mice lacking glucocorticoid receptor (GR), a protein that mainly conveys glucocorticoid response, die after birth because of lung failure (1). Glucocorticoids are essential for maturation of the central nervous system development. Glucocorticoid-responsive genes mediate neurotransmitter release, exocytosis and turnover, axonal transport, neuronal structure, neurite outgrowth, and spine formation (2-5). It is established that glucocorticoids inhibit neuronal differentiation while promote oligodendrite differentiation. In addition, glucocorticoids act on many parts of the mature brain, such as hippocampus, amygdala, and frontal lobes, and have profound effects on many aspects of brain physiology. Glucocorticoids reduce the ability of memory and increase anxiety. They also affect feeding behavior. However, the detailed mechanisms behind these effects are still unclear.

Glucocorticoids affect many other organs. Here, I will concentrate on the metabolic effects of glucocorticoids, as they are the main focus of my research.

B. Metabolic effects of glucocorticoids

The major metabolic goal of glucocorticoids is to maintain plasma glucose level. They accomplish such by exerting different effects in three tissues: liver, adipose tissue and skeletal muscle. In liver, glucocorticoids enhance the expression of enzymes involved in gluconeogenesis. In adipose tissue, glucocorticoids stimulate fat breakdown by increasing lipolysis, decreasing glucose uptake. In skeletal muscle, glucocorticoids promote protein breakdown, decrease protein synthesis and glucose utilization. The free fatty acids released from lipolysis are used for energy production in muscle cells through β-oxidation. The released glycerol provides as another substrate for gluconeogenesis in the liver, and the amino acids from protein breakdown in muscle cells can also be used for gluconeogenesis (Fig.1). Simultaneously, Glucocorticoids inhibit glucose utilization in skeletal muscle and adipose tissue to preserve plasma glucose level. To achieve so, glucocorticoids need to antagonize the effect of insulin, a hormone that is secreted from pancreas β cells upon fed state to promote glucose utilization (Fig.1).

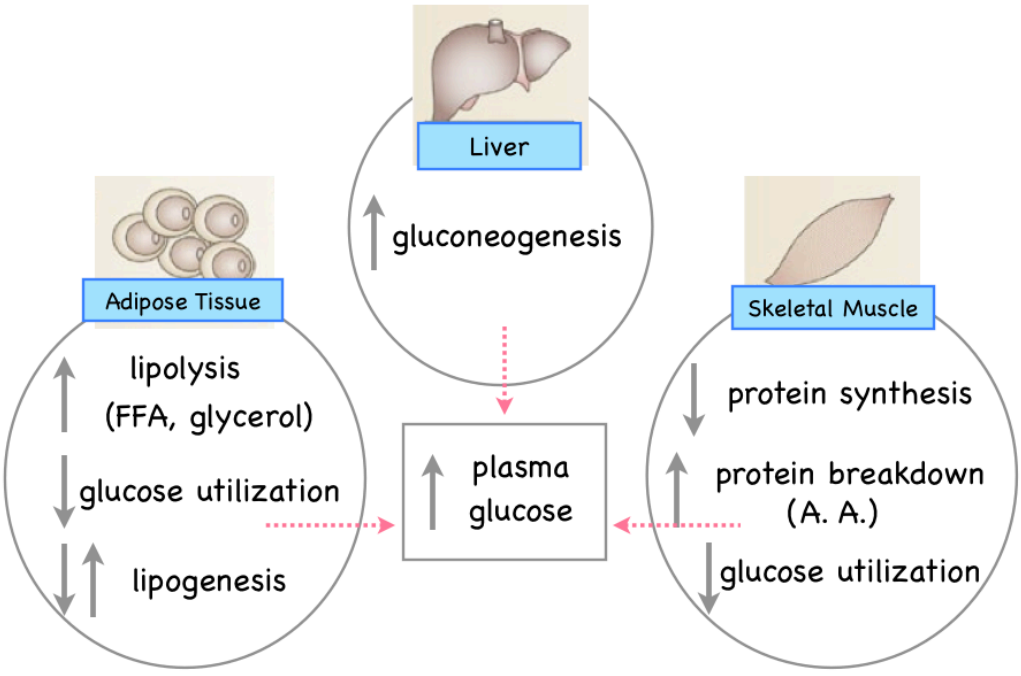

Fig. 1. Metabolic target tissues of glucocorticoids: liver, adipose tissue, and skeletal muscle and the metabolic action of glucocorticoids.

The effects of glucocorticoids on lipid metabolism are more complex. Glucocorticoids can also increase lipogenesis (6, 7) under certain physiological conditions. Animals starved for a period of 36-56 hours and then fed with high glucose diet showed an increase of hepatic lipids and de

novo lipogenesis. These effects are reduced upon adrenalectomy and restored after glucocorticoids are administered (6, 7). These results suggest that glucocorticoids play a role in the efficiency of storing nutrients as fat through potentiating lipogenesis. Moreover, in liver-specific glucocorticoid receptor (GR) knockout mice, lipid accumulation in liver is markedly reduced (8). Using a stable isotope labeling technique, we previously showed that, in mice, 4-day glucocorticoid treatment increased the rate of triglyceride (TG) synthesis in the inguinal fat depot (9). More intriguingly, adipose TG synthesis and lipolysis exhibit coupling, partly reflecting re-esterification of free fatty acids in adipocytes.

As mentioned above, glucocorticoids are widely used to suppress various allergic, inflammatory, and autoimmune disorders. Although glucocorticoids are beneficial to improve the symptoms of these inflammatory diseases, excess and/or chronic glucocorticoid exposure cause undesired adverse effects, which include many metabolic disorders, such as insulin resistance, hyperglycemia, hyperlipidemia and muscle atrophy. Endogenous glucocorticoids exert their metabolic effects upon physiological stimuli. Therefore, normal metabolic responses of glucocorticoids become problematic when mammals are exposed to them chronically and/or excessively, such as endogenously as in Cushing's Syndrome and exogenously as in glucocorticoid treatment. Rodent studies have shown that, elevating glucocorticoid signaling in liver, adipose tissue and skeletal muscle lead to metabolic disorders described above, whereas decreasing glucocorticoid signaling in these tissues markedly improve metabolic profiles and insulin sensitivity. In fact, compounds inhibiting the conversion of inactive cortisone to active cortisol are currently in the clinical trial for treating Type 2 diabetes. Thus, elucidating how glucocorticoids regulate metabolism not only is critical for the fundamental understanding of glucocorticoid biology, but also will provide important insight into the development of improved glucocorticoid therapy with reduced adverse effects and new approach in treating metabolic diseases.

C. Molecular Mechanism of Glucocorticoid Action

C-1. Transcriptional activation

To learn how glucocorticoids exert their biological effect, understanding their signaling pathway is vital. Glucocorticoids act through the intracellular glucocorticoid receptor (GR). GR protein contains 4 modules, as described in Fig. 2. The DNA binding domain (DBD) contains the dimerization domain, called the "D box", while "P box" in the DBD makes direct contact with DNA. The two activation function domains, AF-1 and AF-2 (Fig. 2), are required for transcriptional activation through interaction with coregulators. AF-2, located in the ligand-binding domain (LBD), is a ligand-dependent transactivation domain, as it only interacts with transcription cofactors upon ligand binding. In the absence of glucocorticoids, GR is located in the cytosol, and its LBD associates with heat shock protein 90 (Hsp90)-containing chaperone complex. This chaperon complex includes the Hsp90 and Hsp70, which aid GR folding, ligand binding, nuclear transport, and nuclear retention and degradation. The classical transcription

model is that a hormone-bound GR dimerizes at the glucocorticoid receptor binding site (GBS) or GRE (10) in the regulatory region of the target gene, thereby modulating its transcription.

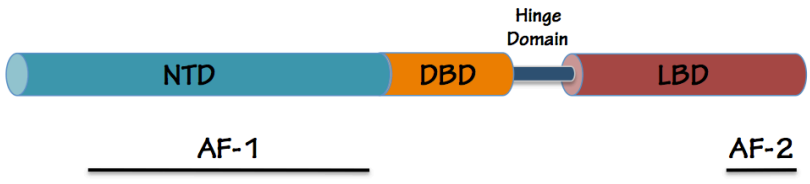

Fig.2. GR protein is composed of 4 modules: the N-terminal trans-activation domain (NTD), the DNA-binding domain (DBD), the hinge domain, and the C-terminal ligand-binding domain (LBD). Two activation functions, AF-1 and AF-2, are embedded in NTD and LBD, respectively. AF-1 binds coregulators and basal transcription machinery proteins, while AF-2 interaction with cofactors in a ligand-dependent manner.

These GBS/GRE are often part of composite regulatory elements or glucocorticoid response units (GRU) (11), composed of binding sites for several transcription factors. Although a classical consensus palindromic GR-binding sequence is represented as AGAACAnnnTGTTCT, where two GR bound to each six-nucleotide half-site of the palindrome as a homodimeric complex (12), the perfect consensus sequence is rarely found in native GBS/GRE. A number of genes are regulated by GBS/GRE half-sites; where only one-half of the classical palindrome is presented in the regulatory elements (13, 14). Other GR target genes have been described to contain degenerate but functional GBS/GRE (15, 16), where the nucleotides making contact with the GR protein are highly conserved compared to the rest of the nucleotides. The binding of GR to these degenerate but functional GBS/GRE could be stabilized by the other transcription factors in the GRU. For simplicity, I will now refer to GBS/GRE as GRE. Structural studies have shown that with only one base pair difference in different GRE differentially affect GR conformation and transcription activity (17), suggesting that DNA sequence serves as an allosteric regulator for GR. Different GR conformations expose specific surfaces of GR protein to associate with other transcriptional regulators, such as DNA-binding transcription factors and cofactors, which subsequently determine gene-specific GR transcription.

There are three major classes of transcriptional cofactors that participate in GR-activated gene transcription: chromatin-remodeling complexes, p160 family of transcription cofactors and histone acetyltransferase, and Mediator. Recent studies demonstrated that GR predominantly binds to nuclease-accessible sites in genome (18). The chromatin-remodeling complex, such as the hBrm-Brg1-Swi/Snf-containing complex, has been reported to help open up chromatin around GRE region for GR transcription (18). The hBrm-Brg1-Swi/Snf-containing complex possesses DNA-stimulated ATPase activity for destabilizing histone-DNA interactions in nucleosomes in an ATP-dependent manner. A role of Swi/Snf chromatin-remodeling complex is required for GR activity was first demonstrated in yeast (19). GR targets the hBrm-Brg1-Swi/Snf-containing complex at the GRE in yeast, disrupting local nucleosomal structure (20). Transfection of an ATPase and defective allele of either hBrm or Brg1 into mammalian cell lines decreased GR's ability to activate transcription (21, 22). Several members of Swi/Snf complex, such as Brg1-associated factor (BAF) 250 and BAF60A, have been shown to interact with GR in a ligand-independent manner. However, not all GR-induced genes require Swi/Snf complex.

Members of p160 family, include SRC1/NCoA-1, SRC2/TIF2/GRIP1, and SRC3/pCIP/ACTR/AIB-1/RAC-3/TRAM-1 (23-31), interact with the AF-2 of GR ; the interactions occur when agonist, but not antagonist, binds. These coactivators interact with LxxLL sequence motifs of GR (32-34). Members of p160 family contain trans-activation domains (AD1 and AD2) and a PAS domain. AD1 forms a docking platform for secondary coactivators, such as cAMP-response element binding protein (CREB)-binding protein (CBP) or its close homolog, p300, which harbors histone acetyltransferase (HAT) activity. Other HAT, such as GCN5, Tip60 and PCAF, have also been shown to co-activate gene transcription with GR in the synthetic reporter gene that contains the classical GRE. These HAT acetylate specific lysine residues of histone H3 and H4. Acetylation removes the positive charge on histones, decreasing the interaction of the N terminus of histone with the negatively charged phosphate groups of DNA. This results in a relaxed chromatin structure that is more accessible to DNA-binding transcription factors and favor transcriptional activation. The other activation domain of the p160 family, AD2, associates with CARM1, a histone methyltransferase (HMT) that specific methylates arginine 17 residue in histone H3. This modification is correlated with transcriptional activation. Notably, HMT and HAT can act together during the process of transcriptional activation. For example, acetylation of H3 tail by CBP enhanced the binding and enzymatic activity of CARM1 on H3. CARM1 can also methylates CBP/p300 to potentiate the transcriptional activity of GR (35). PAS domain of p160 also interacts with other transcriptional cofactors, such as G9a (a histone methyltransferase, (36)), CoCoA (coiled-coil coactivator, (37)), Flightless (Fli, (38)), and GAC63 (a GRIP-1-dependent coactivator, (39)). All these cofactors potentiate GR transcriptional activity in experiments using the synthetic reporter gene containing GRE.

Another transcriptional cofactor complex that interacts with GR is Mediator, which is a link to the basal transcription machinery. Mediator consists of more than 20 proteins. One of its members, MED1 (a.k.a. TRAP220), associates with AF-2 of GR. Another member, MED14 (a.k.a. DRIP150), interacts with AF-1 of GR. The former interaction is ligand-dependent, while the latter is ligand-independent. In MED1-lacking mouse embryonic fibroblast, glucocorticoid response is impaired. However, gene expression analysis indicates that not all GR-activated genes are affected by MED1 knockdown. Similar results are observed in U2OS osteosarcoma cell line, in which MED1 and MED14 reduction with RNA interference (RNAi) influenced the expression of distinct set of genes induced by glucocorticoids. The role of MED1 in glucocorticoid action in vivo is also supported by the fact that glucocorticoid-induced hepatic steatosis is markedly compromised in mice lacking MED1 gene specifically in the liver.

Intriguingly, because most genomic GRE are composite elements and the sequences of GRE are different, the transcription of each GR primary target gene is likely regulated by distinct mechanisms. If we could identify specific molecular feature of GR-containing transcriptional complex on each GRE, we could target specific GR gene. This approach could ultimately allow us to dissociate different biological effects of glucocorticoids. Indeed, stuies have shown that distinct compounds, such as Compound A, can suppress the reporter genes that coain different GRE (40, 41), although the mechanisms governing the effects of these compounds are unclear. These results confirm that it is possible to suppress the activity of particular GRE. To identify

specific molecular feature of each GRE, studying the transcriptional mechanism of GR primary target genes in detail is indispensible.

C-2. Transcriptional repression

In addition to activation, GR can also exert negative effect on gene transcription. The repressive effect of GR plays a key role in anti-inflammation and the modulation of HPA axis. Glucocorticoids repress inflammation by inducing the transcription of genes encoding anti-inflammatory proteins, and suppressing the transcription of pro-inflammatory genes, such as cytokines and chemokines. The latter is mainly due to the inhibitory action of GR on transcription factor, AP-1 (a heterodimers of Fos and Jun family of transcription factors) and NF-κB. Interestingly, chromatin immunoprecipitation (ChIP) experiments show that GR is recruited to AP-1 and NF-κB binding site through direct interaction with these transcription factors (42, 43). These are examples of the "tethering" GRE. GR likely act as a monomer on the tethering GRE, as a GR mutant with impaired dimerization ability can still repress AP-1 and NF-κB. In glucocorticoid-repressed collagenase-3 gene transcription, GR is recruited to the AP-1 site, and then recruits GRIP1/TIF2, which acts as a corepressor in this case (44). In glucocorticoid-inhibited IL-1β-increased GM-CSF gene in lung epithelial cells, GR occupied the NF-κB binding site and further recruit HDAC2 (45, 46), which deacetylates the chromatin region of the pro-inflammatory gene to repress its transcription. Notably, HDAC2 is also involved in the repressive effect of GR on the POMC gene, which is an important player in the HPA axis. In the case of POMC, Brg1 (the ATPase subunit of the Swi/Snf complex) is recruited to the tethering GRE to repress POMC transcription (47). In a case involving NF-κB, TNFα induces human IL-8 transcription in A549 lung epithelial cells. P-TEFβ, functions at a post-transcriptional step by phosphorylating the CTD of Pol II, is a required coactivator for NF-κB (48). Ligand–bound GR is tethered to the NF-κB binding site of the IL8 promoter and disrupts P-TEFβ and NF-κB interaction, thus blocking TNFα-induced activation and antagonizing NF-κB.

In addition to acting through the tethering GRE, GR can directly bind to DNA and repress gene transcription. GR represses corticotropin-related hormone (CRH) gene transcription through binding to the classical GRE sequence. A recent report has identified a negative GRE, whose sequences are entirely different from the classical GRE. Bioinformatic approach has identified several GR-repressed genes, such as the Thymic Stromal Lympho-Protein (TSLP), that contain such negative GRE (49).

D. Transcriptional regulation of GR primary target genes involved in metabolic regulation

D-1. Glucocorticoids and Insulin

In this section, I will discuss the mechanisms of glucocorticoid-regulated transcription of genes involved in the modulation of glucose, lipid and protein metabolism. In several cases, as

discussed above, glucocorticoids cross-talk with insulin. In mammals, insulin is synthesized in the pancreas within the β cells of the islets of Langerhans. Based on nutrient status, neural stimuli and levels of various hormones, insulin triggers the uptake of glucose in liver, muscle and adipose tissue, and inhibits the release of glucogon thus glycogenolysis and glyconeogenesis in liver (50-53). Glucose uptake is mediated by insulin receptor (IR) activation and signaling through the PI3 kinase-Akt phosphorylation pathway, resulting in the translocation of the glucose transporter protein GLUT4 to the plasma membrane. With Type 2 diabetes and metabolic syndrome, IR expression is elevated but signaling cascade is decreased, which leads to less GLUT4 translocation (51). Several studies have shown that exercise, contraction, and agents that activate trimeric GTP-binding proteins can all induce glucose uptake through GLUT4 translocation in skeletal muscle without any PI3 kinase activation (54, 55), while overexpressing constitutively active PI3 kinase can only partially stimulate GLUT4 translocation (56). These data suggest a second insulin signal that is independent of PI3 kinase to stimulate glucose transport.

In the liver, insulin enhances glycogen synthesis and de novo lipogenesis, and blocks gluconeogenesis. In the skeletal muscles, insulin promotes glucose transport and glycogen synthesis, as well as protein synthesis. In the adipose tissue, insulin increases lipogenesis and suppresses lipolysis. Most of these effects of insulin are opposite of those of glucocorticoids. In Type 2 diabetes, insulin signaling is impaired by ectopic lipid accumulation. These intramyocellular lipids further impairs insulin-mediate glucose uptake in skeletal muscles. As a result, the excess glucose is diverted to liver. However, increased lipid accumulation in liver hinders the ability of insulin to regulate gluconeogenesis and activate glycogen synthesis (46). In contrast, lipogenesis remains unaffected. With the increased glucose delivery from diets, increased lipogenesis worsens nonalcoholic fatty liver disease (NAFLD). Impaired insulin response in the adipose tissue leads to increased lipolysis, which promotes re-esterification of lipids in liver and others, and further exacerbates insulin resistance (57). Intriguingly, chronic or excess glucocorticoids treatment can lead to hyperglycemia, dyslipidemia, NAFLD, metabolic syndrome, and Type 2 diabetes, further demonstrating the opposing actions between insulin and glucocorticoids.

D-2. GR and Skeletal Muscle

In skeletal muscle, glucocorticoids inhibit protein synthesis and promote protein degradation. These catabolic effects glucocorticoids have been well documented both in vitro and in vivo (58, 59). (60). Moreover, muscle wasting is inhibited after adrenalectomy or by treating catabolic animals with glucocorticoid receptor antagonist (61). Notably, glucocortcoid treatment of cultured muscle cells results in reduced cell diameter, indicating that muscle atrophy is caused by cell autonomous effect, rather than systemic one of glucocorticoids.

Early studies have provided evidence that glucocorticoids affect protein metabolism by reducing protein synthesis and stimulating protein degradation in myotubes (62), although the detailed mechanism has not yet been elucidated. The ubiquitin-proteasomal pathway is the principal system for protein catabolism in the mammalian cytosol and nucleus. Ubiquitin-tagged substrate

proteins are targeted for proteasome-mediated degradation. The addition of ubiquitin to a protein substrate requires three distinct enzymatic components, an ubiquitin-activating E1, an ubiquitin-conjugating E2, and an ubiquitin ligase E3, which confers substrate specificity. During the process of the muscle atrophy, glucocorticoids significantly increase the expression of muscle-specific E3 ubiquitin ligases Muscle Ring Finger-1 (MuRF-1) and Muscle Atrophy F-box (MAFbx, a.k.a. atrogin-1), two E3 ligases implicated in muscle atrophy induced by various conditions (63-65). While mice lacking MuRF-1 gene showed a compromised glucocorticoid effect on muscle atrophy, glucocorticoid-induced muscle atrophy is not protected in mice lacking atrogin-1 gene. The GRE of MuRF-1 gene is located in (66). However, the GRE of atrogin-1 gene has not been found. Both MuRF-1 and atrogin-1 gene is activated by FoxO family of transcription factors, FoxO1 and FoxO3. For MuRF1 gene, GR cooperates with FoxO1 to induce its transcription. Notably, the expressions of FoxO1 and FoxO3 gene are induced by glucocorticoids. Thus, the induction of atrogin-1 gene by glucocorticoids may depend on FoxO1 and/or FoxO3. Whether FoxO1 and/or FoxO3 gene transcription is directly stimulated by glucocorticoids is one of the main topic of my dissertation. In addition to E3 ligases, glucocorticoids have been shown to activate other players involved in the ubiquitin-proteasomal pathway. ZNF216, a ubiquitin-binding protein containing a zinc finger, is such a factor. ZNF216 functions as a shuttle protein that presents poly-ubiquitylated proteins to the proteasome. *Znf216* expression is upregulated in skeletal muscle in models of muscle atrophy, and *Znf216*-deficient mice exhibit resistance to muscle atrophy accompanied by abnormal accumulation of poly-ubiquitylated proteins in skeletal muscle (67). Importantly, how glucocorticoids induce these genes is largely unclear. Although MuRF-1 appears to contain a GRE , GRE for atrogin-1 and ZNF216 have not been identified.

In addition to protein degradation, glucocorticoids also interfere with protein synthesis. The inhibition of protein synthesis by glucocorticoids partly results from the inhibition of mammalian target of rapamycin (mTOR), the serine/threonine protein kinase that phosphorylates ribosomal S6 kinase (S6K) and eukaryotic initiation factor-4E binding protein-1 (4E-BP1) (68). S6K phosphorylates ribosomal S6, which further regulates the translation of RNAs that contain an RNA 5' terminal oligopyrimidine sequence (69). mTOR phosphorylates and inhibits 4E-BP1 (70), a translation repression phosphoprotein. In a hypo-phosphorylated state, 4E-BP1 forms a tight complex with eIF4E and prevents its interaction with eIF4G and recruitment to the 43S pre-initiation complex. The association of 4E-BP1 with eIF4E represses translation (71, 72). In contrast, when phosphorylated, 4E-BP1 dissociates from eIF4E and allows the recruitment of 5' capped mRNA and translation initiation (72, 73). Since eIF4E is the least abundantly expressed subunit, this complex interaction is considered a rate-limiting step in protein synthesis (74). Therefore, by inhibiting 4E-BP1, mTOR activates protein synthesis. Studies have indicated that mTOR signaling is repressed by glucocorticoid-enhanced transcription of DDIT4 (75), leading to decreased phosphorylation of 4E-BP1 and decreased protein synthesis. However, the mechanism underlying the transcriptional regulation of DDIT4 by GR is also unclear, as GRE has not been identified.

The crosstalk between GR and mTOR was further examined in a report (76). KLF15, a GR primary target gene in skeletal muscle, inhibits mTOR activity. Also, KLF15 induces the expression of MuRF1 and atrogin-1 thus decreases myofiber size. Intriguingly, rapamycin significantly enhanced glucocorticoid-induced MuRF1, atrogin-1, and KLF15, suggesting that

blocking mTOR cascade elevated GR target genes. Therefore, mTOR seems to negatively regulate glucocorticoid-induced atrogenes (those induce muscle atrophy). This interaction between GR and mTOR adds another layer of complexity to the catabolic and anabolic balance in skeletal muscle.

D-3. GR and Adipose Tissue

In adipose tissues, glucocorticoids participate in the modulation of lipid and glucose homeostasis. As mentioned previously, glucocorticoids inhibits insulin-stimulated glucose uptake (77-79), while, depending on the nutrient status, glucocorticoids increase lipogenesis in the fed state (6, 7) and activate lipolysis in the fasted state (80-82). However, excess glucocorticoids in adipocytes can lead to central obesity, dyslipidemia and insulin resistance (83, 84). The central obesity phenotype is partly due to that fact that glucocorticoids promote redistribution of body fat (85), while the mobilization of fat during the process could contribute to dyslipidemia.

Glucocorticoids differentially regulate distinct fat depots. In peripheral fat depots, they reduce lipoprotein lipase (LPL) activity and increase lipolysis by inducing hormone-sensitive lipase (86). In central fat, they promote pre-adipocyte differentiation and pro-lipogenic signaling, leading to cellular hypertrophy (87, 88).

GR primary targets genes have been identified in a mouse 3T3-L1 adipocyte cell line (9). Many of these genes are involved in TG synthesis (Scd-1, 2, 3, GPAT3, GPAT4, Agpat2, Lpin1), lipolysis (Lipe, Mgll), lipid transport (Cd36, Lrp-1, Vldlr, Slc27a2) and storage (S3-12). Except Scd-3, the rest of the genes were induced by 4-day glucocorticoid treatment in mouse inguinal fat (9). Reporter assay further confirmed that, except Agpat2, the other 12 genes contain GR binding region(s) that can confer glucocorticoid response (9). Interestingly, short-term (4-day) glucocorticoid treatment increased TG synthesis and lipolysis simultaneously in inguinal fat. Although it is in agreement with the fact that glucocorticoids activated genes in both lipolytic and TG biosynthetic pathways depending on the fat depots and nutrient status, having these two opposing pathways happening at the same time in the same tissue in a futile cycle could have turned up the gain of additional hormonal signals, which would further inhibits TG synthesis or lipolysis alone (89).

D-4. GR and Liver

The liver plays a pivotal role in whole-body carbohydrate, lipid, and protein metabolic homeostasis. Chronic GR activation leads to excess triglyceride (TG) storage in the liver due to reduced catabolism of fatty acids (FA) via β-oxidation and reduced capacity to hydrolyse TG. In liver, adipose tissue and brain, 11 beta-Hydroxysteroid dehydrogensase type 1 (11β-HSD1) catalyses the regeneration of active glucocorticoids (cortisol in human and corticosterone in rodents) from inert 11-keto forms. Mice deficient in 11β-HSD1 resist metabolic syndrome that

develops with dietary obesity (90) and glucocorticoid-associated cognitive impairments that develop with ageing (91). Downregulation of liver, but not adrenal gland, hypothalamus or pituitary, GR expression by antisense oligonucleotide treatment improved fasting hyperglycemia and systemic glucose homeostasis in diabetic mice without affecting blood glucocorticoid levels (92). Excess GR activity leads to hyperglycemia and blunted insulin-induced suppression of hepatic glucose production by heightened gene activation and expression of gluconeogenic genes phosphoenolpyruvate carboxyknase (PEPCK) and glucose-6-phosphatase (G6Pase). PEPCK is a gluconeogenic enzyme, which converts oxaloacetate into phosphoenolpyruvate and CO_2. Glucocorticoids induce hepatic PEPCK gene transcription through two low-affinity GRE (93). These two GREs cannot confer glucocorticoid response when they are inserted into a synthetic reporter gene. They require additional binding sites for DNA-binding transcription factors for transcription activation. These binding sites include HNF-4/COUP-TF, CREB and FoxA, which FoxO protein can also bind. Insulin represses PEPCK gene transcription, at least in part, through the FoxO/FoxA element. Both FoxA2 and FoxO1 may be able to confer accessory activity for glucocorticoid response, but FoxO1 likely is the protein that mediates the insulin action. In mice lacking FoxO1, the ability of insulin to repress PEPCK gene is significantly reduced.

G6Pase hydrolyzes glucose-6-phosphate, resulting in a phosphate group and a free glucose, and completes the final step in gluconeogenesis and glycogenolysis. Two GRE, located within the region of 300 bp upstream from the G6Pase transcription start site, were reported (94). However, a complete glucocorticoid response also requires the participation of HNF-1 and FoxA/FoxO. Similar to the composite GRE in PEPCK gene, both FoxA2 and FoxO1 likely serve as accessory factors for glucocorticoid-activated G6Pase gene transcription. Again, FoxO1 is the protein that mediates the suppressive effect of insulin, as the ability of insulin to represses G6Pase gene is diminished in mice lacking FoxO1.

The insulin like growth factor (IGF) binding proteins (IGF-BP) are a family of proteins that bind IGF-1 and 2 to modulate their actions (95-97). IGF-BP1 mRNA is increased in insulin-deficient diabetes (98, 99). Phosphorylated IGF-BP1 binds IGF-1 with high affinity to form inactive complexes that inhibits IGF-1 action (100-102). Glucocorticoids increased IGF-BP1 mRNA abundance and gene transcription in rat liver and H4IIE rat hepatoma cells (103, 104). A GRE (nt -91 to -77) and four accessory regulatory sites: a hepatocytes nuclear factor-1 (HNF-1, nt -62 to -50), an insulin response element (nt -108 to -99) and an upstream site (nt -252 to -236) were identified (104). The GR and HNF-1 have been shown to synergistically activate transcription of IGF-BP1 gene (104). The insulin response element is a FoxA/FoxO binding site. Similar to PEPCK and G6Pase gene, FoxO1 likely mediates insulin response on IGFBP-1 gene the FoxA/FoxO response element.

E. The Goal of Dissertation Research

The goal of my research is to elucidate the mechanisms governing the transcription regulation of genes involved in metabolic regulation. I started my tenure in the laboratory to study the transcriptional regulation of angiopoietin-like 4 (Angptl4) gene, which encodes a secreted protein that inhibits extracellular lipoprotein lipase activity and promote intracellular lipolysis in

adipocytes. We hypothesized that Angptl4 mediates glucocorticoid-regulated lipid metabolism. In Chapter 3, I will show the mechanism of glucocorticoid-induced Angptl4 transcription and how insulin affects this process. I will present its vivo studies as well as transcriptional regulation by GR.

To figure how glucocorticoids induce metabolic side effects, the first step is to find the primary target genes of glucocorticoids. The first chapter of my dissertation identified genome-wide GR primary target genes in a skeletal muscle cell line, as skeletal muscle is one of the metabolic target tissue of glucocorticoids. Markedly, many genes that participate in the crosstalk between glucocorticoids and insulin signaling pathway were isolated. I then focused on one gene, p85α (the regulatory subunit of PI3 kinase), for its mechanistic and signal transduction studies..

The second chapter is the transcriptional study of another GR primary target in skeletal muscle, FoxO3, a gene that could partly explain glucocorticoid-mediated muscle atrophy. FoxO3 is recognized as one of the master regulators of muscle atrophy, as overexpressing FoxO3 alone can decrease myofiber size. In Chapter 2, three GR binding regions of FoxO3 gene were identified. I then studied and compared the mechanism of GR-mediated gene activation for these GR binding regions. As discuss above, FoxO family members are key players in insulin signaling pathway. Many studies showed that FoxO1 mediates insulin effect in liver, whereas FoxO3 plays a role in insulin-regulated protein metabolism in skeletal muscle. Rodent studies suggest that these two factors likely play a redundant role in mediating insulin action. Identifyinf FoxO3 as a GR primary target gene provides another layer for the interaction between glucocorticoids and insulin signaling.

Overall, I hope that my research has provided important pioneer works that will facilitate future identification of specific molecular features of GR primary target genes mediating the metabolic effects, allowing the separation of the anti-inflammatory and adverse actions of glucocorticoids.

References

1. Cole TJ*, et al.* (1995) Targeted disruption of the glucocorticoid receptor gene blocks adrenergic chromaffin cell development and severely retards lung maturation. *Genes & development* 9(13):1608-1621.
2. Datson NA, Morsink MC, Meijer OC, & de Kloet ER (2008) Central corticosteroid actions: Search for gene targets. *European journal of pharmacology* 583(2-3):272-289.
3. Datson NA, van der Perk J, de Kloet ER, & Vreugdenhil E (2001) Identification of corticosteroid-responsive genes in rat hippocampus using serial analysis of gene expression. *The European journal of neuroscience* 14(4):675-689.
4. Morsink MC*, et al.* (2006) Acute activation of hippocampal glucocorticoid receptors results in different waves of gene expression throughout time. *Journal of neuroendocrinology* 18(4):239-252.
5. Li Y, Gonzalez P, & Zhang L (2012) Fetal stress and programming of hypoxic/ischemic-sensitive phenotype in the neonatal brain: Mechanisms and possible interventions. *Progress in neurobiology* 98(2):145-165.
6. Berdanier CD (1989) Role of glucocorticoids in the regulation of lipogenesis. *FASEB journal : official publication of the Federation of American Societies for Experimental Biology* 3(10):2179-2183.
7. Wang Y*, et al.* (2004) The human fatty acid synthase gene and de novo lipogenesis are coordinately regulated in human adipose tissue. *The Journal of nutrition* 134(5):1032-1038.
8. Shteyer E, Liao Y, Muglia LJ, Hruz PW, & Rudnick DA (2004) Disruption of hepatic adipogenesis is associated with impaired liver regeneration in mice. *Hepatology* 40(6):1322-1332.
9. Yu CY*, et al.* (2010) Genome-wide analysis of glucocorticoid receptor binding regions in adipocytes reveal gene network involved in triglyceride homeostasis. *PLoS One* 5(12):e15188.
10. Yamamoto KR (1985) Steroid receptor regulated transcription of specific genes and gene networks. *Annu Rev Genet* 19:209-252.
11. Schoneveld OJ, Gaemers IC, & Lamers WH (2004) Mechanisms of glucocorticoid signalling. *Biochim Biophys Acta* 1680(2):114-128.
12. Tsai MJ & O'Malley BW (1994) Molecular mechanisms of action of steroid/thyroid receptor superfamily members. *Annu Rev Biochem* 63:451-486.
13. Bristeau A, Catherin AM, Weiss MC, & Faust DM (2001) Hormone response of rodent phenylalanine hydroxylase requires HNF1 and the glucocorticoid receptor. *Biochem Biophys Res Commun* 287(4):852-858.
14. Faust DM*, et al.* (1996) The activity of the highly inducible mouse phenylalanine hydroxylase gene promoter is dependent upon a tissue-specific, hormone-inducible enhancer. *Mol Cell Biol* 16(6):3125-3137.
15. Sugiyama T, Scott DK, Wang JC, & Granner DK (1998) Structural requirements of the glucocorticoid and retinoic acid response units in the phosphoenolpyruvate carboxykinase gene promoter. *Mol Endocrinol* 12(10):1487-1498.

16. Rozansky DJ, Wu H, Tang K, Parmer RJ, & O'Connor DT (1994) Glucocorticoid activation of chromogranin A gene expression. Identification and characterization of a novel glucocorticoid response element. *J Clin Invest* 94(6):2357-2368.
17. Meijsing SH*, et al.* (2009) DNA binding site sequence directs glucocorticoid receptor structure and activity. *Science* 324(5925):407-410.
18. John S*, et al.* (2008) Interaction of the glucocorticoid receptor with the chromatin landscape. *Molecular cell* 29(5):611-624.
19. Yoshinaga SK, Peterson CL, Herskowitz I, & Yamamoto KR (1992) Roles of SWI1, SWI2, and SWI3 proteins for transcriptional enhancement by steroid receptors. *Science* 258(5088):1598-1604.
20. Ostlund Farrants AK, Blomquist P, Kwon H, & Wrange O (1997) Glucocorticoid receptor-glucocorticoid response element binding stimulates nucleosome disruption by the SWI/SNF complex. *Molecular and cellular biology* 17(2):895-905.
21. Muchardt C & Yaniv M (1993) A human homologue of Saccharomyces cerevisiae SNF2/SWI2 and Drosophila brm genes potentiates transcriptional activation by the glucocorticoid receptor. *The EMBO journal* 12(11):4279-4290.
22. Chiba H, Muramatsu M, Nomoto A, & Kato H (1994) Two human homologues of Saccharomyces cerevisiae SWI2/SNF2 and Drosophila brahma are transcriptional coactivators cooperating with the estrogen receptor and the retinoic acid receptor. *Nucleic acids research* 22(10):1815-1820.
23. Onate SA, Tsai SY, Tsai MJ, & O'Malley BW (1995) Sequence and characterization of a coactivator for the steroid hormone receptor superfamily. *Science* 270(5240):1354-1357.
24. Hong H, Kohli K, Trivedi A, Johnson DL, & Stallcup MR (1996) GRIP1, a novel mouse protein that serves as a transcriptional coactivator in yeast for the hormone binding domains of steroid receptors. *Proceedings of the National Academy of Sciences of the United States of America* 93(10):4948-4952.
25. Voegel JJ, Heine MJ, Zechel C, Chambon P, & Gronemeyer H (1996) TIF2, a 160 kDa transcriptional mediator for the ligand-dependent activation function AF-2 of nuclear receptors. *The EMBO journal* 15(14):3667-3675.
26. Yao TP, Ku G, Zhou N, Scully R, & Livingston DM (1996) The nuclear hormone receptor coactivator SRC-1 is a specific target of p300. *Proceedings of the National Academy of Sciences of the United States of America* 93(20):10626-10631.
27. Anzick SL*, et al.* (1997) AIB1, a steroid receptor coactivator amplified in breast and ovarian cancer. *Science* 277(5328):965-968.
28. Chen H*, et al.* (1997) Nuclear receptor coactivator ACTR is a novel histone acetyltransferase and forms a multimeric activation complex with P/CAF and CBP/p300. *Cell* 90(3):569-580.
29. Li H, Gomes PJ, & Chen JD (1997) RAC3, a steroid/nuclear receptor-associated coactivator that is related to SRC-1 and TIF2. *Proceedings of the National Academy of Sciences of the United States of America* 94(16):8479-8484.
30. Torchia J*, et al.* (1997) The transcriptional co-activator p/CIP binds CBP and mediates nuclear-receptor function. *Nature* 387(6634):677-684.
31. Lonard DM & O'Malley B W (2007) Nuclear receptor coregulators: judges, juries, and executioners of cellular regulation. *Molecular cell* 27(5):691-700.
32. Darimont BD*, et al.* (1998) Structure and specificity of nuclear receptor-coactivator interactions. *Genes & development* 12(21):3343-3356.

33. Ding XF, *et al.* (1998) Nuclear receptor-binding sites of coactivators glucocorticoid receptor interacting protein 1 (GRIP1) and steroid receptor coactivator 1 (SRC-1): multiple motifs with different binding specificities. *Mol Endocrinol* 12(2):302-313.
34. Kalkhoven E, Valentine JE, Heery DM, & Parker MG (1998) Isoforms of steroid receptor co-activator 1 differ in their ability to potentiate transcription by the oestrogen receptor. *The EMBO journal* 17(1):232-243.
35. Xu W, *et al.* (2001) A transcriptional switch mediated by cofactor methylation. *Science* 294(5551):2507-2511.
36. Lee DY, Northrop JP, Kuo MH, & Stallcup MR (2006) Histone H3 lysine 9 methyltransferase G9a is a transcriptional coactivator for nuclear receptors. *The Journal of biological chemistry* 281(13):8476-8485.
37. Kim JH & Stallcup MR (2004) Role of the coiled-coil coactivator (CoCoA) in aryl hydrocarbon receptor-mediated transcription. *The Journal of biological chemistry* 279(48):49842-49848.
38. Lee YH, Campbell HD, & Stallcup MR (2004) Developmentally essential protein flightless I is a nuclear receptor coactivator with actin binding activity. *Molecular and cellular biology* 24(5):2103-2117.
39. Chen YH, Kim JH, & Stallcup MR (2005) GAC63, a GRIP1-dependent nuclear receptor coactivator. *Molecular and cellular biology* 25(14):5965-5972.
40. De Bosscher K, *et al.* (2005) A fully dissociated compound of plant origin for inflammatory gene repression. *Proceedings of the National Academy of Sciences of the United States of America* 102(44):15827-15832.
41. Liberman AC, *et al.* (2012) Compound A, a dissociated glucocorticoid receptor modulator, inhibits T-bet (Th1) and induces GATA-3 (Th2) activity in immune cells. *PloS one* 7(4):e35155.
42. Necela BM & Cidlowski JA (2004) Mechanisms of glucocorticoid receptor action in noninflammatory and inflammatory cells. *Proceedings of the American Thoracic Society* 1(3):239-246.
43. Newton R & Holden NS (2007) Separating transrepression and transactivation: a distressing divorce for the glucocorticoid receptor? *Molecular pharmacology* 72(4):799-809.
44. Rogatsky I, Zarember KA, & Yamamoto KR (2001) Factor recruitment and TIF2/GRIP1 corepressor activity at a collagenase-3 response element that mediates regulation by phorbol esters and hormones. *The EMBO journal* 20(21):6071-6083.
45. Ito K, Barnes PJ, & Adcock IM (2000) Glucocorticoid receptor recruitment of histone deacetylase 2 inhibits interleukin-1beta-induced histone H4 acetylation on lysines 8 and 12. *Mol Cell Biol* 20(18):6891-6903.
46. Ito K, *et al.* (2006) Histone deacetylase 2-mediated deacetylation of the glucocorticoid receptor enables NF-kappaB suppression. *J Exp Med* 203(1):7-13.
47. Bilodeau S, *et al.* (2006) Role of Brg1 and HDAC2 in GR trans-repression of the pituitary POMC gene and misexpression in Cushing disease. *Genes & development* 20(20):2871-2886.
48. Luecke HF & Yamamoto KR (2005) The glucocorticoid receptor blocks P-TEFb recruitment by NFkappaB to effect promoter-specific transcriptional repression. *Genes & development* 19(9):1116-1127.

49. Surjit M*, et al.* (2011) Widespread negative response elements mediate direct repression by agonist-liganded glucocorticoid receptor. *Cell* 145(2):224-241.
50. O'Brien RM, Streeper RS, Ayala JE, Stadelmaier BT, & Hornbuckle LA (2001) Insulin-regulated gene expression. *Biochemical Society transactions* 29(Pt 4):552-558.
51. Saltiel AR & Pessin JE (2002) Insulin signaling pathways in time and space. *Trends in cell biology* 12(2):65-71.
52. Saltiel AR & Kahn CR (2001) Insulin signalling and the regulation of glucose and lipid metabolism. *Nature* 414(6865):799-806.
53. Newton R (2000) Molecular mechanisms of glucocorticoid action: what is important? *Thorax* 55(7):603-613.
54. Cortright RN & Dohm GL (1997) Mechanisms by which insulin and muscle contraction stimulate glucose transport. *Canadian journal of applied physiology = Revue canadienne de physiologie appliquee* 22(6):519-530.
55. Lund S, Holman GD, Schmitz O, & Pedersen O (1995) Contraction stimulates translocation of glucose transporter GLUT4 in skeletal muscle through a mechanism distinct from that of insulin. *Proceedings of the National Academy of Sciences of the United States of America* 92(13):5817-5821.
56. Martin SS*, et al.* (1996) Activated phosphatidylinositol 3-kinase is sufficient to mediate actin rearrangement and GLUT4 translocation in 3T3-L1 adipocytes. *The Journal of biological chemistry* 271(30):17605-17608.
57. Samuel VT & Shulman GI (2012) Mechanisms for insulin resistance: common threads and missing links. *Cell* 148(5):852-871.
58. Odedra BR, Bates PC, & Millward DJ (1983) Time course of the effect of catabolic doses of corticosterone on protein turnover in rat skeletal muscle and liver. *Biochem J* 214(2):617-627.
59. Kayali AG, Young VR, & Goodman MN (1987) Sensitivity of myofibrillar proteins to glucocorticoid-induced muscle proteolysis. *Am J Physiol* 252(5 Pt 1):E621-626.
60. Auclair D, Garrel DR, Chaouki Zerouala A, & Ferland LH (1997) Activation of the ubiquitin pathway in rat skeletal muscle by catabolic doses of glucocorticoids. *Am J Physiol* 272(3 Pt 1):C1007-1016.
61. Hall-Angeras M, Angeras U, Zamir O, Hasselgren PO, & Fischer JE (1991) Effect of the glucocorticoid receptor antagonist RU 38486 on muscle protein breakdown in sepsis. *Surgery* 109(4):468-473.
62. Menconi M*, et al.* (2007) Role of glucocorticoids in the molecular regulation of muscle wasting. *Crit Care Med* 35(9 Suppl):S602-608.
63. Clarke BA*, et al.* (2007) The E3 Ligase MuRF1 degrades myosin heavy chain protein in dexamethasone-treated skeletal muscle. *Cell Metab* 6(5):376-385.
64. Bodine SC*, et al.* (2001) Identification of ubiquitin ligases required for skeletal muscle atrophy. *Science* 294(5547):1704-1708.
65. Lecker SH*, et al.* (2004) Multiple types of skeletal muscle atrophy involve a common program of changes in gene expression. *Faseb J* 18(1):39-51.
66. Waddell DS*, et al.* (2008) The glucocorticoid receptor and FOXO1 synergistically activate the skeletal muscle atrophy-associated MuRF1 gene. *American journal of physiology. Endocrinology and metabolism* 295(4):E785-797.
67. Hishiya A*, et al.* (2006) A novel ubiquitin-binding protein ZNF216 functioning in muscle atrophy. *Embo J* 25(3):554-564.

68. Schakman O, Gilson H, & Thissen JP (2008) Mechanisms of glucocorticoid-induced myopathy. *J Endocrinol* 197(1):1-10.
69. Hay N & Sonenberg N (2004) Upstream and downstream of mTOR. *Genes Dev* 18(16):1926-1945.
70. Hara K*, et al.* (2002) Raptor, a binding partner of target of rapamycin (TOR), mediates TOR action. *Cell* 110(2):177-189.
71. Khaleghpour K, Pyronnet S, Gingras AC, & Sonenberg N (1999) Translational homeostasis: eukaryotic translation initiation factor 4E control of 4E-binding protein 1 and p70 S6 kinase activities. *Mol Cell Biol* 19(6):4302-4310.
72. Schalm SS, Fingar DC, Sabatini DM, & Blenis J (2003) TOS motif-mediated raptor binding regulates 4E-BP1 multisite phosphorylation and function. *Curr Biol* 13(10):797-806.
73. Rhoads RE (1999) Signal transduction pathways that regulate eukaryotic protein synthesis. *J Biol Chem* 274(43):30337-30340.
74. Duncan R, Milburn SC, & Hershey JW (1987) Regulated phosphorylation and low abundance of HeLa cell initiation factor eIF-4F suggest a role in translational control. Heat shock effects on eIF-4F. *J Biol Chem* 262(1):380-388.
75. Wang H, Kubica N, Ellisen LW, Jefferson LS, & Kimball SR (2006) Dexamethasone represses signaling through the mammalian target of rapamycin in muscle cells by enhancing expression of REDD1. *J Biol Chem* 281(51):39128-39134.
76. Shimizu N*, et al.* (2011) Crosstalk between glucocorticoid receptor and nutritional sensor mTOR in skeletal muscle. *Cell metabolism* 13(2):170-182.
77. Rizza RA, Mandarino LJ, & Gerich JE (1982) Cortisol-induced insulin resistance in man: impaired suppression of glucose production and stimulation of glucose utilization due to a postreceptor detect of insulin action. *The Journal of clinical endocrinology and metabolism* 54(1):131-138.
78. Dinneen S, Alzaid A, Miles J, & Rizza R (1993) Metabolic effects of the nocturnal rise in cortisol on carbohydrate metabolism in normal humans. *The Journal of clinical investigation* 92(5):2283-2290.
79. Sakoda H*, et al.* (2000) Dexamethasone-induced insulin resistance in 3T3-L1 adipocytes is due to inhibition of glucose transport rather than insulin signal transduction. *Diabetes* 49(10):1700-1708.
80. Gravholt CH, Dall R, Christiansen JS, Moller N, & Schmitz O (2002) Preferential stimulation of abdominal subcutaneous lipolysis after prednisolone exposure in humans. *Obesity research* 10(8):774-781.
81. Tomlinson JW*, et al.* (2007) Inhibition of 11beta-hydroxysteroid dehydrogenase type 1 activity in vivo limits glucocorticoid exposure to human adipose tissue and decreases lipolysis. *The Journal of clinical endocrinology and metabolism* 92(3):857-864.
82. Samra JS*, et al.* (1998) Effects of physiological hypercortisolemia on the regulation of lipolysis in subcutaneous adipose tissue. *The Journal of clinical endocrinology and metabolism* 83(2):626-631.
83. Masuzaki H*, et al.* (2001) A transgenic model of visceral obesity and the metabolic syndrome. *Science* 294(5549):2166-2170.
84. Masuzaki H*, et al.* (2003) Transgenic amplification of glucocorticoid action in adipose tissue causes high blood pressure in mice. *The Journal of clinical investigation* 112(1):83-90.

85. Macfarlane DP, Forbes S, & Walker BR (2008) Glucocorticoids and fatty acid metabolism in humans: fuelling fat redistribution in the metabolic syndrome. *The Journal of endocrinology* 197(2):189-204.
86. Slavin BG, Ong JM, & Kern PA (1994) Hormonal regulation of hormone-sensitive lipase activity and mRNA levels in isolated rat adipocytes. *Journal of lipid research* 35(9):1535-1541.
87. Gaillard D, Wabitsch M, Pipy B, & Negrel R (1991) Control of terminal differentiation of adipose precursor cells by glucocorticoids. *Journal of lipid research* 32(4):569-579.
88. Samra JS, Summers LK, & Frayn KN (1996) Sepsis and fat metabolism. *The British journal of surgery* 83(9):1186-1196.
89. Wang JC, Gray NE, Kuo T, & Harris C (2012) Regulation of triglyceride metabolism by glucocorticoid receptor. *Cell & bioscience* 2(1):19.
90. Morton NM*, et al.* (2004) Novel adipose tissue-mediated resistance to diet-induced visceral obesity in 11 beta-hydroxysteroid dehydrogenase type 1-deficient mice. *Diabetes* 53(4):931-938.
91. Yau JL*, et al.* (2001) Lack of tissue glucocorticoid reactivation in 11beta -hydroxysteroid dehydrogenase type 1 knockout mice ameliorates age-related learning impairments. *Proceedings of the National Academy of Sciences of the United States of America* 98(8):4716-4721.
92. Liang Y*, et al.* (2005) Antisense oligonucleotides targeted against glucocorticoid receptor reduce hepatic glucose production and ameliorate hyperglycemia in diabetic mice. *Metabolism: clinical and experimental* 54(7):848-855.
93. Granner D & Pilkis S (1990) The genes of hepatic glucose metabolism. *The Journal of biological chemistry* 265(18):10173-10176.
94. Lin B, Morris DW, & Chou JY (1998) Hepatocyte nuclear factor 1alpha is an accessory factor required for activation of glucose-6-phosphatase gene transcription by glucocorticoids. *DNA and cell biology* 17(11):967-974.
95. Rechler MM (1993) Insulin-like growth factor binding proteins. *Vitamins and hormones* 47:1-114.
96. Jones JI & Clemmons DR (1995) Insulin-like growth factors and their binding proteins: biological actions. *Endocrine reviews* 16(1):3-34.
97. Oh Y*, et al.* (1996) Synthesis and characterization of insulin-like growth factor-binding protein (IGFBP)-7. Recombinant human mac25 protein specifically binds IGF-I and -II. *The Journal of biological chemistry* 271(48):30322-30325.
98. Suikkari AM*, et al.* (1988) Insulin regulates the serum levels of low molecular weight insulin-like growth factor-binding protein. *The Journal of clinical endocrinology and metabolism* 66(2):266-272.
99. Ooi GT*, et al.* (1990) Different tissue distribution and hormonal regulation of messenger RNAs encoding rat insulin-like growth factor-binding proteins-1 and -2. *Mol Endocrinol* 4(2):321-328.
100. Elgin RG, Busby WH, Jr., & Clemmons DR (1987) An insulin-like growth factor (IGF) binding protein enhances the biologic response to IGF-I. *Proceedings of the National Academy of Sciences of the United States of America* 84(10):3254-3258.
101. Jones JI, D'Ercole AJ, Camacho-Hubner C, & Clemmons DR (1991) Phosphorylation of insulin-like growth factor (IGF)-binding protein 1 in cell culture and in vivo: effects on

affinity for IGF-I. *Proceedings of the National Academy of Sciences of the United States of America* 88(17):7481-7485.

102. Westwood M, Gibson JM, & White A (1997) Purification and characterization of the insulin-like growth factor-binding protein-1 phosphoform found in normal plasma. *Endocrinology* 138(3):1130-1136.
103. Conover CA, Divertie GD, & Lee PD (1993) Cortisol increases plasma insulin-like growth factor binding protein-1 in humans. *Acta endocrinologica* 128(2):140-143.
104. Suh DS & Rechler MM (1997) Hepatocyte nuclear factor 1 and the glucocorticoid receptor synergistically activate transcription of the rat insulin-like growth factor binding protein-1 gene. *Mol Endocrinol* 11(12):1822-1831.

Chapter 1

Genome-Wide Analysis of Glucocorticoid Receptor Binding Sites in Myotubes Identifies Gene Networks Modulating Insulin Signaling

Abstract

Glucocorticoids elicit a variety of biological responses in skeletal muscle, including inhibiting protein synthesis and insulin-stimulated glucose uptake and promoting proteolysis. Thus, excess or chronic glucocorticoid exposure leads to muscle atrophy and insulin resistance. Glucocorticoids propagate their signal mainly through glucocorticoid receptors (GR), which, upon binding to ligands, translocate to the nucleus and bind to genomic glucocorticoid response elements (GRE) to regulate the transcription of nearby genes. Using a combination of chromatin immunoprecipitation sequencing (ChIPseq) and microarray, we identified 173 genes in mouse C2C12 myotubes. The mouse genome contains GR binding regions (GBR) in or near these genes and the genes' expression was regulated by glucocorticoids. Eight of these genes encode proteins known to regulate distinct signaling events in insulin/insulin-like growth factor 1 (IGF-1) pathways. We found that overexpression of p85α, one of these eight genes, caused a decrease in C2C12 myotube diameters, mimicking the effect of glucocorticoids. Moreover, reducing p85α expression by RNA interference in C2C12 myotubes significantly compromised the ability of glucocorticoids to inhibit Akt and p70 S6 kinase activity and reduced glucocorticoid induction of IRS-1 phosphorylation at serine 307. This phosphorylation is associated with insulin resistance. Furthermore, decreasing p85α expression abolished glucocorticoid inhibition of protein synthesis and compromised glucocorticoid-induced reduction of cell diameters in C2C12 myotubes. Finally, a GRE was identified in the p85α GBR. In summary, our studies identified GR-regulated transcriptional networks in myotubes and showed that p85α plays a critical role in glucocorticoid-induced insulin resistance and muscle atrophy in C2C12 myotubes.

Introduction

Glucocorticoids perform vital metabolic functions in skeletal muscle: inhibiting protein synthesis and insulin-stimulated glucose uptake and promoting protein degradation. These effects are critical during stress, producing amino acid precursors for gluconeogenesis, which provides glucose for the brain. Initially, muscle insulin resistance maintains adequate circulating glucose to fuel the brain; however, these effects are deleterious if chronic. Treating animals with glucocorticoids causes a decrease in skeletal muscle size (1-4). Mice treated with glucocorticoids have reduced insulin-stimulated glucose uptake and GLUT4 translocation in myotubes (5-7). Circulating glucocorticoid levels are higher in obese *ob/ob* and *db/db* mice than in normal mice. Adrenalectomy in these obese mice improves insulin-stimulated muscle glucose disposal (8). These changes are in part due to the direct effect of glucocorticoids on myotubes, as glucocorticoid treatment in cultured myotubes reduces cell diameters (9-11) and inhibits insulin-stimulated glucose utilization (5, 12).

While the metabolic effects of glucocorticoids in skeletal muscle are well known, the underlying mechanisms are not fully understood. One way glucocorticoids affect glucose and protein metabolism is to antagonize the insulin/insulin-like growth factor-1 (IGF-1) pathway (5, 13), which promotes protein synthesis and glucose utilization. Insulin/IGF-1 acts by binding to membrane receptors, tyrosine kinases that autophosphorylate and phosphorylate insulin receptor substrates (IRS) (14). Tyrosine-phosphorylated IRS associate with insulin receptors (IR) and activate signaling pathways (14). Mice treated with glucocorticoids have reduced levels of tyrosine-phosphorylated IR and total IRS-1 in skeletal muscle (5). The activity of phosphatidylinositol 3-kinase (PI3K) and Akt, two signaling molecules downstream of IR and IRS-1, is also decreased (5). Glucocorticoids also reduce the activity of mammalian target of rapamycin (mTOR), a protein kinase downstream of Akt and upstream of p70 S6 kinase (p70S6K) (15). Furthermore, glucocorticoid treatment increases the phosphorylation of serine 307 of IRS-1 (pSer307-IRS-1) (5), which disrupts the association of IR and IRS-1, reducing the insulin/IGF-1 response (16). The mechanism by which glucocorticoids inhibit the insulin/IGF-1 pathway is unclear.

Although certain glucocorticoid effects are independent of intracellular glucocorticoid receptor (GR) (17), the majority are mediated by GR, which upon binding to its ligand moves to the nucleus and interacts with genomic GR response elements (GRE). It is critical to identify genes directly regulated by GR in order to learn the physiological mechanisms of glucocorticoids. Here, we used a combination of chromatin immunoprecipitation sequencing (ChIPseq) and microarray to identify direct targets of GR in mouse C2C12 myotubes. We identified potential GR primary targets previously shown to modulate distinct steps of insulin/IGF-1 signaling. We focused on one potential GR primary target, p85α. Experiments were conducted to identify its GRE and its role in the suppressive effects of glucocorticoids on myotube diameters, protein synthesis, and insulin/IGF-1 signaling pathway.

Results

Identification of potential GR primary target genes in C2C12 myotubes

Microarray analyses were conducted in C2C12 myotubes treated for 6 or 24 h with dexamethasone (Dex), a synthetic glucocorticoid, or ethanol (EtOH), a vehicle control. Combining data from both time points, we found that Dex induced the expression of 363 genes by more than 1.5 fold and inhibited the expression of 218 genes by more than 1.5 fold (Supporting Information (SI) Dataset S1). To learn which of these genes contain GR binding regions (GBR) in or near their genomic regions, ChIPseq was performed with C2C12 myotubes treated with Dex or EtOH for 1 h. We located 2,251 genomic positions with sequencing reads significantly enriched in Dex-treated samples compared to EtOH-treated ones, with a p-value threshold of 10^{-5}. We utilized PinkThing to assign these genomic GBR to mouse genes based on proximity, and grouped target sites based on their relative position to the nearest gene (GBR are listed in SI Dataset S2). We found 42% of GBR in the intron regions, and 29% are found either 25 kb upstream of TSS or downstream of stop codons (Fig. 1A). In contrast, only 5% of GBR are located within 5kb upstream from TSS (Fig. 1A). Overall, we identified 147 Dex-activated genes and 26 Dex-repressed genes containing GBR in or near their genomic regions (SI Table S1, SI Dataset S3).

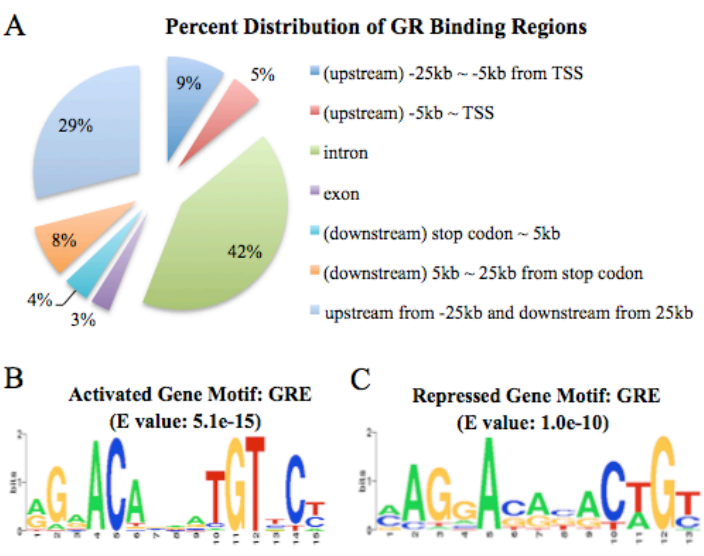

Fig. 1 Genomic distribution of GBR and GRE motifs within GBR. A) Percentage distribution of all identified GBR in different genomic regions. B) For GBR of glucocorticoid-induced genes, Bioprospector analysis identified a motif that is similar to the consensus GRE in STAMP. C) For GBR of glucocorticoid-repressed genes, Bioprospector analysis also identified a motif that is similar to the consensus GRE in STAMP. For 1B, C) The Expect value (E) is a parameter that describes the number of hits one can expect to see by random chance when searching a database of a particular DNA element.

The top categories of gene annotation from gene ontology analysis of 173 GR-regulated genes include those encoding proteins involved in the receptor tyrosine kinase signaling pathway, blood vessel development, apoptosis, muscle organ development and cytoskeletal organization (SI Dataset S4). We performed a combination of Bioprospector and STAMP analyses to search for consensus motifs within GBR located in or near genes that were regulated by glucocorticoids. For glucocorticoid-activated genes, the classical GRE was the most represented motif in these analyses based on E values (Fig. 1B). Binding motifs for HSF, AP-1, NF-E2, MAF, NRF-2, Core-binding, AML, PEBP, FOXP3, HNF3α, T3R and RREB-1 were all significantly represented (SI Table S2). For glucocorticoid-repressed genes, the classical GRE motif was also highly represented (Fig. 1C). Moreover, HSF, SMAD3, T3R, XBP-1, ELF-1, HAC-1, ID-1, FOXP3, AbaA, XPF-1, Bach1 and AP-1 were all high on the list of binding motifs (SI Table S3).

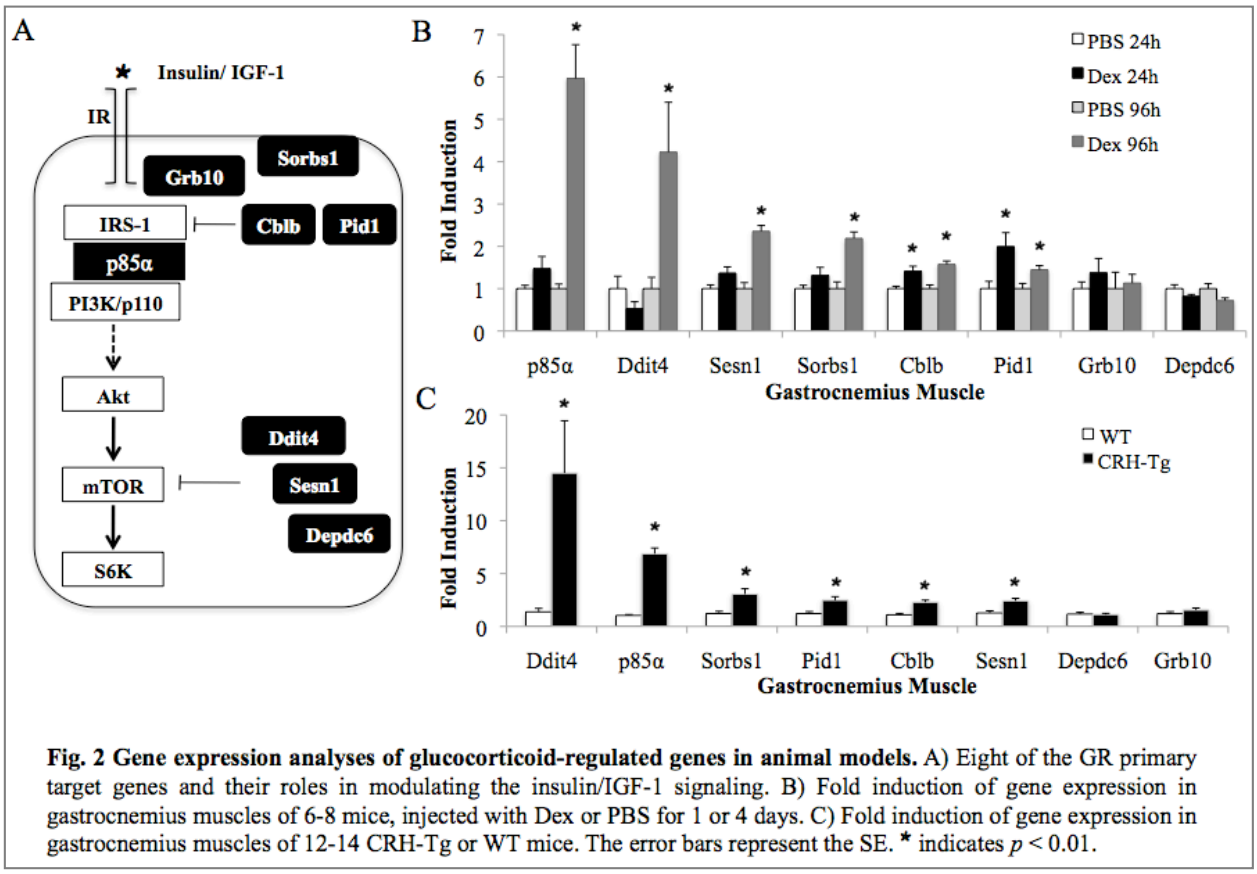

Fig. 2 Gene expression analyses of glucocorticoid-regulated genes in animal models. A) Eight of the GR primary target genes and their roles in modulating the insulin/IGF-1 signaling. B) Fold induction of gene expression in gastrocnemius muscles of 6-8 mice, injected with Dex or PBS for 1 or 4 days. C) Fold induction of gene expression in gastrocnemius muscles of 12-14 CRH-Tg or WT mice. The error bars represent the SE. * indicates $p < 0.01$.

Glucocorticoid-controlled genes involved in insulin/IGF-1 signaling

Gene ontology analysis revealed that many glucocorticoid-regulated genes affect receptor tyrosine kinase signaling. We analyzed the potential GR primary targets that can specifically inhibit the insulin/IGF-1 pathway, which propagates through receptor tyrosine kinases. As shown in Fig. 2A, at least 8 glucocorticoid-regulated genes encode proteins that can modulate the activity of this pathway. One of these genes, Cblb, encodes a ubiquitin E3 ligase involved in IRS-1 degradation (18). Pid-1 inhibits the tyrosine phosphorylation of IRS-1 (19). Grb10 inhibits the physical interaction between IR and IRS-1 (20). Overexpression of p85α induces insulin resistance in vitro and in vivo (21-23). Sesn 1 (24), Ddit4 (15) and Depdc6 (25) inhibit mTOR. Finally, mice with bone-marrow-specific deletion of Sorbs1 are protected from high fat diet-induced insulin resistance (26), indicating that overexpression of Sorbs1 could induce insulin resistance. To learn whether these genes were regulated by glucocorticoids in vivo, mice were injected with Dex or phosphate buffered saline (PBS) control for 24 or 96 h. We found that mice injected with Dex for 24 h had significantly higher expression of Cblb and Pid1 than those injected with PBS in gastrocnemius muscles (Fig. 2B). Furthermore, the expression of Cblb, Pid1, p85α, Sesn1, Ddit4 and Sorbs1 was increased in mice treated with Dex for 96 h compared to the control (Fig. 2B). To determine the effect of chronic glucocorticoid exposure, we utilized transgenic mice overexpressing corticotropin-releasing hormone (CRH-Tg). CRH causes an increased secretion of adrenocorticotropic hormone, which further stimulates the secretion of adrenal corticosterone. In CRH-Tg mice, the expression of Cblb, Pid1, p85α, Ddit4, Sorbs1 and Sesn1 was markedly elevated in gastrocnemius muscles (Fig. 2C). In summation, at least 6 of the potential GR primary targets can inhibit insulin/IGF-1 signaling in vivo.

A critical criterion for determining GR primary targets is that GR directly regulates their transcription. Thus, these GBR should be able to mediate the glucocorticoid response. To validate the GBR identified near these 8 genes, each GBR was inserted upstream of a TATA box of a heterologous reporter plasmid, pGL4.10-E4TATA, which drives a firefly luciferase gene. A collection of plasmids used is listed in SI Dataset S5. We found that all GBR tested could mediate glucocorticoid responses (Fig. 3A), suggesting these 8 glucocorticoid-regulated genes are primary targets of GR.

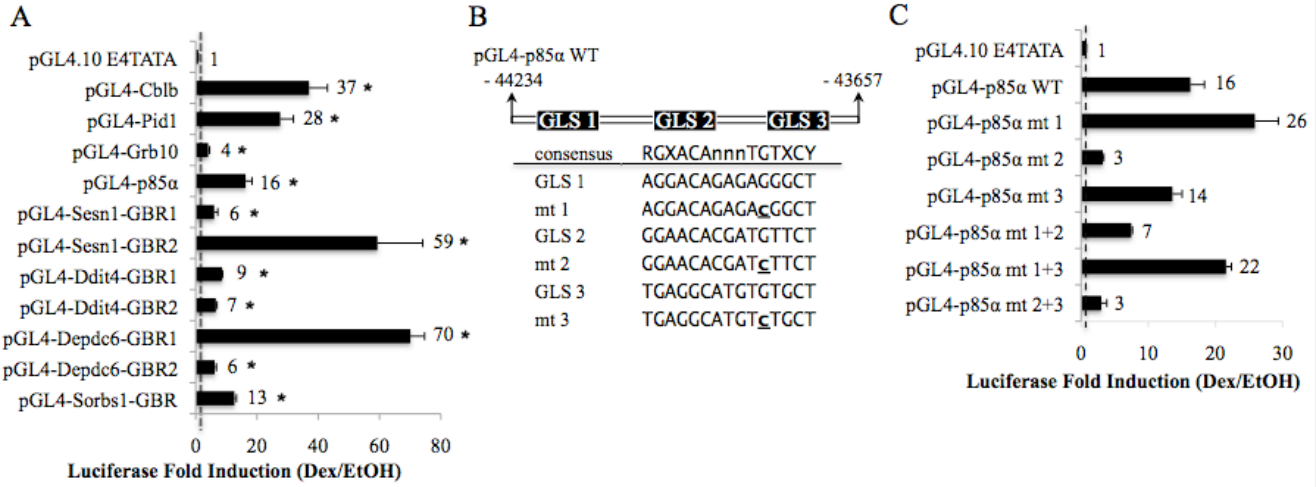

Fig. 3 Glucocorticoid response of GBR. A) Reporter plasmids harboring different GBR were co-transfected with pcDNA3-hGR and pRL Renilla into C2C12 myoblasts, with $n > 6$ per group. Renilla luciferase expression was used to normalize for transfection efficiency. After 24 h of transfection, cells were treated with Dex or EtOH for 16-20 h, and assayed for firefly and Renilla luciferase activities. Data shows fold induction of normalized luciferase activity (Dex/EtOH-treated samples) from at least 6 experiments. * indicates $p < 0.05$. The error bars represent the SE for the fold induction, and the dashed line marks a one-fold induction. B) pGL4-p85α WT harbors nucleotide (nt) -44234 to -43657 of p85α genomic region. Based on the consensus GRE shown, three GRE-like sequences (GLS) were identified. The locations of GLS are: nt -44003 to -43989 (GLS 1), nt -43938 to -43924 (GLS 2), and nt -43913 to 43899 (GLS 3). Point mutation, where the mutated nt is underlined, is made in each GLS to generate mutant (mt). Mt 1 has nt -43993 mutated from G to C; mt 2, nt -43928 from G to C; and mt 3, nt -43903 from G to C. C) Reporter assay, as described in Fig. 3A, was carried with WT and mt p85α GBR plasmid. pGL4-p85α mt 1+2 represents double mt of GLS 1 and 2; pGL4-p85α mt 1+3, double mt of GLS 1 and 3; and pGL4-p85α mt 2+3, double mt of GLS 2 and 3.

The role of p85α in glucocorticoid-regulated insulin signaling

The induction of p85α by glucocorticoids in vivo (Fig. 2B, 2C) prompted further analysis into its role in mediating glucocorticoid responses in muscle. First, we identified the GRE in the p85α GBR. We searched for DNA sequences matching at least 7 nucleotides to the consensus GRE motif identified from Bioprospector/STAMP (RGXACAnnnTGTXCY, Fig. 1C) in the p85α GBR. Three potential GRE-like sequences (GLS) were found, and for each GLS we mutated the nucleotide from G to C at position 11, which makes direct contact with GR (27) (Fig. 3B). With the reporter assay, we found that GLS 2 mutants had an 80% reduction in the Dex response. While the GLS 3 mutation had no significant effect, the GLS 1 mutation moderately potentiated the Dex response (Fig. 3C). Double mutations of GLS 2 and GLS 3 had similar effects as GLS 2 single mutations, and double mutations of GLS 1 and GLS 2 resulted in a slight increase in Dex response compared to GLS 2 single mutations (Fig. 3C). These results indicated that, while GLS 1 may be suppressive, GLS 2 plays a central role in mediating the glucocorticoid response. Furthermore, we used TFSEARCH to identify transcription factor binding

motifs in the p85α GBR. We found SRY, GATA, USF and Ikaros binding sites located in the vicinity of GLS 2 (SI Figure S1).

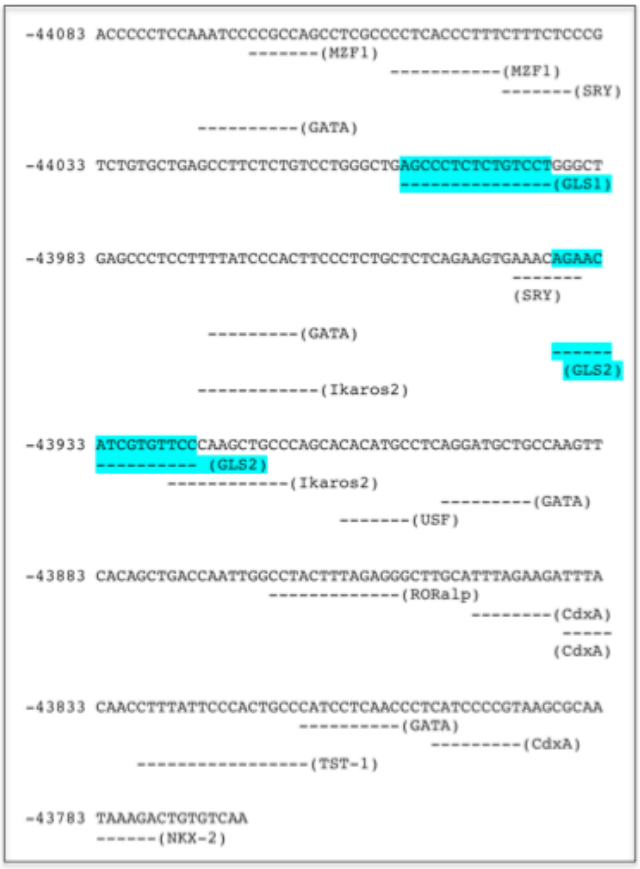

Supporting Information Figure S1. **Additional transcription factor binding motifs in Pik3r1 GBR.** The number indicates the nucleotide location relative to the transcription start site of Pik3r1 gene. The identified motifs are underlined and labeled. GRE-like sequence (GLS) 1 and 2 of Pik3r1 gene are highlighted in blue.

Next, we examined the role of p85α on glucocorticoid-induced inhibition of signaling molecules participating in the insulin/IGF-1 pathway. We used lentiviral-mediated small hairpin RNA (shRNA) to decrease p85α expression (sh-p85α) in C2C12 cells. Control cells were infected with lentiviruses expressing shRNA with scramble sequences (sh-scr). Cells were then treated with Dex or EtOH for 72 h. In sh-scr cells, p85α protein levels were increased upon Dex treatment (Fig. 4A). In sh-p85α cells, p85α levels were reduced approximately 90% in both Dex- and EtOH-treated cells (Fig. 4A).

We monitored the phosphorylation status of serine 473 of Akt (pSer473-Akt) and threonine 389 of p70S6K (pThr389-S6K). These phosphorylations are required to potentiate their kinase activity. In contrast, pSer307-IRS-1 disrupts its interaction with insulin/IGF-1 receptor. In sh-scr cells, pSer473-Akt and pThr389-S6K levels were reduced upon Dex treatment (Fig. 4A). While pSer307-IRS-1 levels were comparable between Dex- and EtOH-treated cells, IRS-1 protein expression was decreased upon Dex treatment in sh-scr cells (Fig. 4A). After normalizing to the IRS-1 protein present, there was a significant increase of pSer307-IRS-1 in Dex-treated sh-scr cells. In sh-p85α cells, Dex treatment did not suppress the levels of pSer473-Akt and pThr389-S6K (Fig. 4A, 4B). Although total IRS-1 protein levels decreased upon Dex treatment, this reduction was weaker than that of Dex-treated sh-scr cells (Fig. 4A, 4B). Considering the similarity of pSer307-IRS-1 levels and the difference in total IRS-1 levels between Dex- and EtOH-treated sh-scr and sh-p85α cells, the ability of Dex to induce pSer307-IRS-1 was significantly compromised by knocking down p85α (Fig. 4B). Notably, EtOH treatment resembles PBS-treated sh-scr and sh-p85α cells (Fig. 4B). Overall, our data indicated that reducing the expression of p85α compromised the ability of glucocorticoids to inhibit the activity of Akt and p70S6K, to reduce IRS-1 protein levels and to induce phosphorylation at serine 307 of IRS-1.

The role of p85α in glucocorticoid-induced muscle atrophy

We investigated whether p85α is involved in glucocorticoid-induced muscle atrophy. C2C12 myotubes were infected with adenoviruses expressing p85α (Ad-p85α) or a control of LacZ (Ad-LacZ). Cell

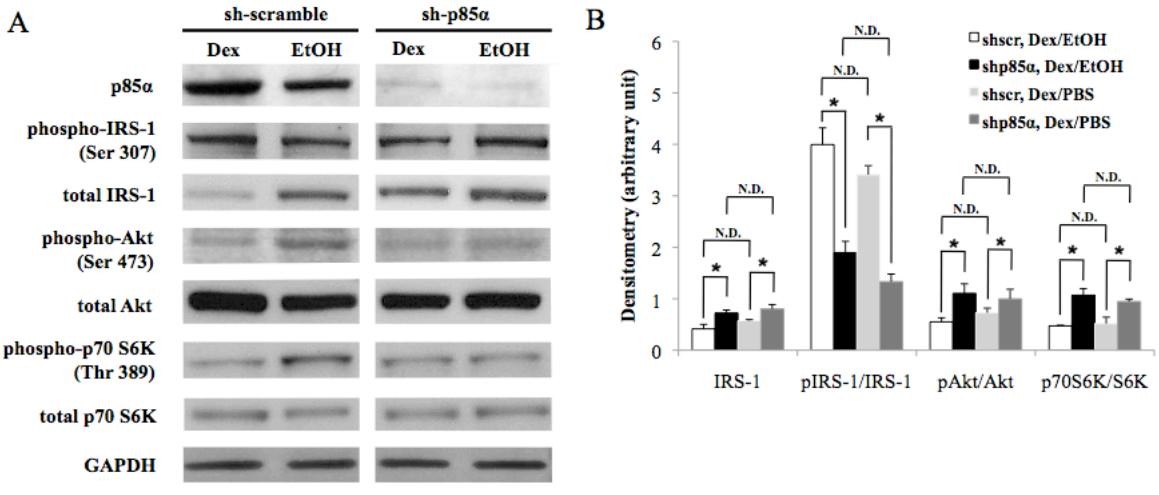

Fig. 4 The effect of p85α RNAi in glucocorticoid response. A) Sh-p85α and sh-scr C2C12 myotubes and treated with Dex or EtOH for 72 h. Immunoblots were used to detect the indicated proteins. B) Quantification of the densitometry of total IRS-1 and the ratio of pSer307-IRS-1, pSer473-Akt and pThr389-S6K bands to that of IRS-1, Akt and p70S6K bands, respectively, with Dex/EtOH or Dex/PBS. Data were normalized to GAPDH optical density. These results were averaged from at least 3 immunoblots. * indicates $p < 0.05$ and N.D. specifies no difference. The error bars represent the SE for the fold induction and relative abundance.

diameters were then measured 72 h after infection. p85α protein levels are approximately 4 fold higher in Ad-p85α than Ad-LacZ cells (Fig. 5A). We found that significantly more Ad-p85α myotubes had smaller cell diameters than Ad-LacZ ones (Fig. 5B). The average cell diameter of Ad-p85α myotubes was about 30% smaller than Ad-LacZ ones (Fig. 5C). These results demonstrate that overexpressing p85α mimics the effect of glucocorticoids in reducing C2C12 myotube diameters.

Following the treatment of sh-scr and sh-p85α myotubes with Dex, EtOH or PBS for 72 h, we measured cell diameters. The average diameter in Dex-treated sh-scr myotubes was 28% smaller than those of EtOH-treated sh-scr myotubes (Fig. 5D). A similar effect was observed in wild type (WT) myotubes, with no lentiviral infection, treated with Dex and EtOH (Fig. 5D). In contrast, the average diameter of Dex-treated sh-p85α myotubes was 14% smaller than those of EtOH-treated sh-p85α myotubes (Fig. 5D). Although glucocorticoids still decreased C2C12 myotube diameter, reduced p85α expression significantly compromised this decrease. Notably, the average myotube diameters of EtOH-treated WT, sh-scr and sh-p85α myotubes were comparable.

Furthermore, we investigated the effect of glucocorticoids on protein synthesis in sh-scr and sh-p85α myotubes. Myotubes were treated with Dex or EtOH for 72 h, and protein synthesis was measured using a fluorescence assay. We found that Dex-treated sh-scr myotubes had 13% lower nascent protein synthesis than EtOH-treated sh-scr myotubes (Fig. 5E). In contrast, Dex-treated sh-p85α myotubes had 14% higher nascent protein synthesis than EtOH-treated sh-p85α myotubes (Fig. 5E). Notably, the protein synthesis rates in EtOH-treated sh-scr and sh-p85α myotubes were similar. Our data suggest that p85α mediates glucocorticoid-reduced protein synthesis.

Previous studies have shown that, in myotubes, glucocorticoids stimulate the expression of atrogenes, such as FoxO1, FoxO3, atrogin-1 (a.k.a. MAFbx) and MuRF-1, which contribute to glucocorticoid-induced muscle atrophy (28, 29). We found that 72 h of Dex treatment induced FoxO3, atrogin-1 and MuRF-1 gene expression in sh-scr myotubes (Fig. 5F). However, this induction was diminished in sh-

p85α myotubes (Fig. 5F). These results indicate that p85α is involved in glucocorticoid-induced FoxO3, atrogin-1 and MuRF-1 gene expression. Immunoblotting showed that Dex treatment upregulated total FoxO1 and FoxO3 proteins, whereas the levels of phosphorylated-FoxO1 (pFoxO1) and FoxO3 (pFoxO3) were unchanged (Fig. 5G). Thus, the ratio of pFoxO1 to total FoxO1 and the ratio of pFoxO3 to total FoxO3 were reduced. However, these ratios were similar in sh-scr and sh-p85α myotubes.

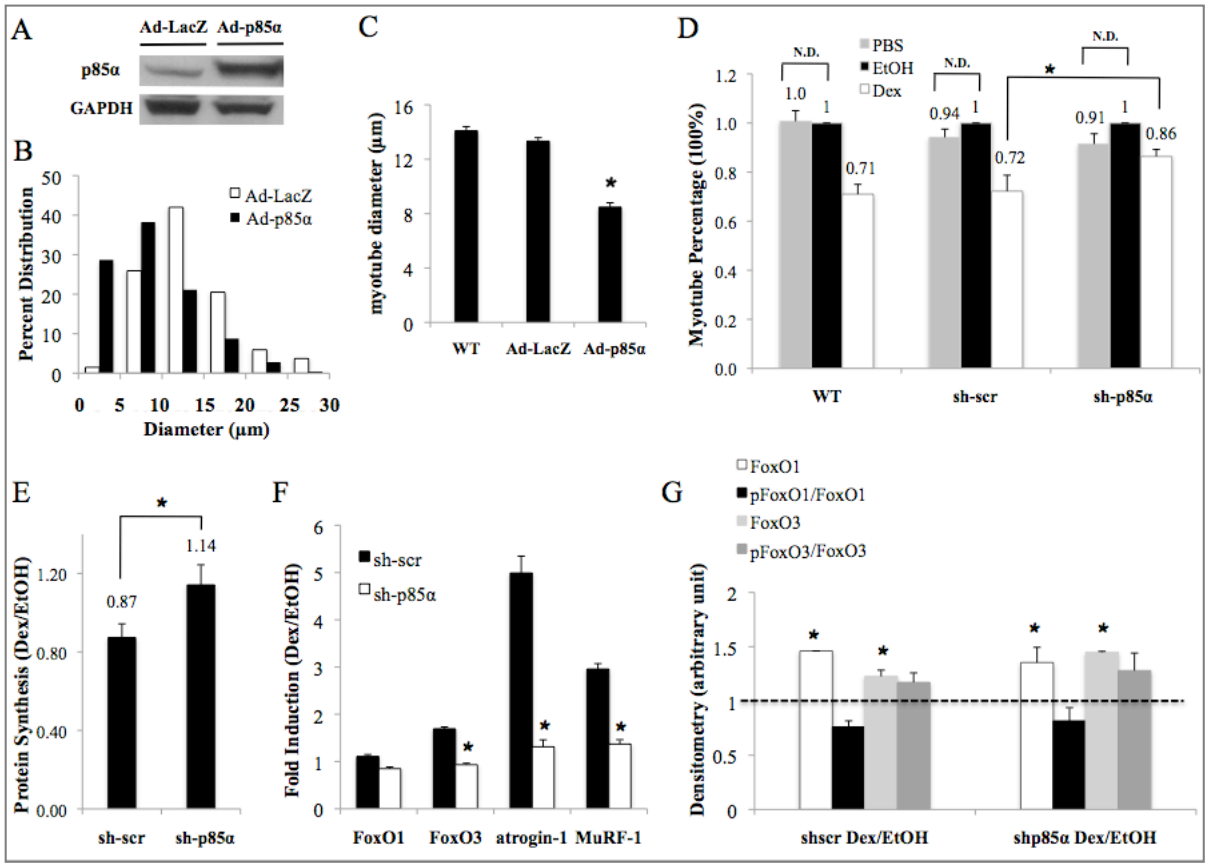

Fig. 5 The effect of p85α overexpression and knock-down on C2C12 myotube cell diameters. A) Immunoblot was performed in Ad-LacZ and Ad-p85α myotubes to detect p85α protein levels. B) The distribution of cell diameters in Ad-LacZ and Ad-p85α myotubes. C) The average cell diameter of WT, Ad-LacZ and Ad-p85α myotubes. D) WT, sh-scr and sh-p85α myotubes were treated with Dex, EtOH or PBS for 72 h, EtOH-treated WT, sh-scr and sh-p85α myotube diameters were set as 1 (100%) for Dex-treated or PBS-treated WT, sh-scr and sh-p85α myotubes, respectively. N.D. specifies no difference. E) Protein synthesis level was measured for sh-scr and sh-p85α myotubes, with EtOH-treated sh-scr and sh-p85α myotubes' protein synthesis level set as 1 for Dex-treated sh-scr and sh-p85α myotubes', respectively. F) FoxO1, FoxO3, atrogin-1 and MuRF-1 gene expressions are done in sh-scr and sh-p85α myotubes. Rpl19 primer was internal control. G) Protein levels of phosphorylated- and total- FoxO1 and FoxO3 are shown for sh-scr and sh-p85α myotubes. For 5C, D, E, F, G) * indicates $p < 0.05$. The error bars represent the SE for diameters. These results are averaged from at least 3 independent experiments.

Supporting Information: Table S1, S2, S3

Supporting Information Table S1. The Number of Genes Regulated by Glucocorticoids and Containing GBR in C2C12 Myotubes

	Glucocorticoid-regulated genes	Glucocorticoid-regulated genes containing GBR	% of glucocorticoid-regulated genes containing GBR
Activated	363	147	40%
Repressed	218	26	12%
Total	581	173	30%

Supporting Information Table S2. Activated Gene Motifs

Motifs	Factors	E values
NGAANNTTCNNTTC	HSF	2.8e-14
WNKNAGTCAN	AP-1	3.5e-11
GCTGAGTCAY	NF-E2	2.7e-10
NTGACTCANC	MAF	3.7e-10
TGCTGAGTCANN	NRF-2	4.2e-10
WNACCAC	Core-binding	1.1e-8
NNWRACCACANNNN	AML	2.0e-8
NNNNYTGTGGTNAN	PEBP	2.6e-6
NTMTGNNANAACNNNW	FOXP3	3.5e-6
NWRARCAAAY	HNF3alpha	3.6e-6
NAGGWCAN	T3R	8.1e-6
CCCAAACCACCCC	RREB-1	8.5e-6

Supporting Information Table S3. Repressed Gene Motifs

Motifs	Factors	E values
NGAANNTTCNNTTC	HSF	3.7e-11
AGNCAGAC	SMAD3	5.5e-7
NNNNNNGGAATGNRRNNN	AbaA	2.0e-5
--NNNATGACTCATNN	Bach1	2.8e-5
---GKTSNYCNG--	XPF-1	2.9e-5
NAGGWCAN	T3R	3.1e-5
NWNNNMCACGTCANCN	XBP-1	3.6e-5
WNNNGTTNTNNCAKAN	FOXP3	3.6e-5
TTGTCSTTWT	ID-1	3.7e-5
-----NTGASTCA	AP-1	5.2e-5
AYTTCCTCTTN	ELF-1	9.0e-5
GACACGCTGKC	HAC-1	9.7e-5

Discussion

In this Chapter, we present several novel findings. First, we identified potential GR primary target genes in C2C12 myotubes. Identification will facilitate future studies into the mechanisms underlying glucocorticoid actions in skeletal muscle physiology. Second, through ChIPseq, we localized genome-wide GBR in C2C12 myotubes, which is the first step in understanding the mechanisms governing GR-regulated gene transcription. Finally, we found 8 potential GR primary targets that can modulate distinct steps in insulin/IGF-1 signaling. Specifically, we have shown that p85α induction plays a key role in mediating glucocorticoid inhibition of the insulin/IGF-1 response.

We previously identified GBR in another mouse cell type, 3T3-L1 adipocytes (30). The distribution of GBR in genomic regions is similar between adipocytes and myotubes. Whereas only 5% of GBR lie within 5 kb upstream of TSS, many are localized in introns, greater than 25 kb upstream of TSS or greater than 25 kb downstream of stop codons. In motif analyses of GBR from glucocorticoid-activated genes, classical GRE sequences were highly represented. AP-1 and HNF3α, two binding motifs that have been shown to act with GR for maximal activation of transcription (31, 32) also scored highly. The binding site of HNF3α is similar to that of FoxO1 and FoxO3, which perform similar metabolic functions to GR in myotubes, as they promote proteolysis, reduce protein synthesis and reduce glucose utilization (33). Therefore, GR and FoxO may act together to transcriptionally regulate genes involved in these physiological processes. The classical GRE sequence is also highly represented in GBR of genes repressed by glucocorticoids, but the mechanism is unclear. The AP-1 element, which mediates glucocorticoid repression (34), was highly represented in the GBR of glucocorticoid-repressed genes. Most motifs identified in GBR of glucocorticoid-regulated genes have not been linked to transcriptional repression by GR.

Gene ontology analysis recognized some GR primary targets involved in the regulation of apoptosis. In myotubes, glucocorticoids were shown to potentiate apoptosis (35). This analysis also identified gene groups involved in muscle organ development and cytoskeletal organization, suggesting that glucocorticoids may modulate mechanical properties of muscle, a concept that has not been extensively studied. Genes involved in blood vessel development were also highly represented. Many of these genes regulate angiogenesis, which plays an important role in modulating skeletal muscle health (36). The role of glucocorticoids in angiogenesis has been described (37), but the impact of this function on skeletal muscle is not entirely clear.

We focused on gene clusters that modulate insulin/IGF-1 receptor tyrosine kinase signaling, as glucocorticoids decrease insulin-stimulated glucose utilization and protein synthesis, and increase proteolysis. In skeletal muscle, glucocorticoids affect multiple steps in the insulin/IGF-1 signaling pathway. Therefore, it is conceivable that glucocorticoids induce a group of genes to mediate these effects. We focused on elucidating the role of p85α, the regulatory subunit of PI3K, in glucocorticoid-inhibited insulin signaling. Excess p85α can compete with PI3K (a heterodimer of p85α and the catalytic subunit of PI3K) to interact with IRS-1 (23, 38), resulting in a decrease in insulin response. In contrast, reducing the expression of p85α improves insulin sensitivity (39). Moreover, the induction of p85α gene expression by glucocorticoids and the functional interaction between GR and p85α /PI3K pathway were previously described (40-42). We demonstrated that p85α is a GR primary target by identifying a GRE in the p85α GBR. We used RNAi to decrease p85α expression in C2C12 cells in

order to analyze its role in glucocorticoid responses. The levels of pSer473-Akt and pThr389-S6K were a little lower in EtOH-treated sh-p85α cells compared to EtOH-treated sh-scr cells (Fig. 4B), suggesting that the reduction of p85α expression decreased the activity of Akt and p70S6K. However, previous studies indicated that Pik3r2, another regulatory subunit of PI3K, can compensate for p85α function in skeletal muscle-specific p85α knockout mice (43). In our sh-p85α myotubes, Pik3r2 and the remaining p85α should be enough to support downstream activities. Therefore, the reduced suppressive effect of glucocorticoids was unlikely due to the lack of activity in insulin/IGF-1 signaling.

Our results from p85α RNAi experiments raised several interesting points. First, p85α reduction limited the ability of Dex to decrease IRS-1 protein expression; however, IRS-1 gene expression was unchanged after 6 or 24h Dex treatment according to microarray. Therefore, Dex likely reduced IRS-1 protein stability, but the mechanism of p85α in glucocorticoid-promoted IRS-1 degradation is unclear. Second, p85α reduction decreased Dex-induced phosphorylation of IRS-1 at serine 307. Several kinases, including IκB kinase β (IKKβ), p70S6K, c-Jun N-terminal kinases (JNK) and PKCθ, have been shown to phosphorylate IRS-1 at serine 307 (16). To our knowledge, there are no reports that glucocorticoids can increase IKKβ activity. Since glucocorticoids decrease p70S6K activity, p70S6K is unlikely to mediate this event. Interestingly, in obese and type 2 diabetic patients, p85α protein expression correlates with the activity of JNK, PKCθ and pSer307-IRS-1 (44). Establishing the link between glucocorticoids, p85α, JNK and PKCθ requires further study.

Our studies have shown that p85α is involved in glucocorticoid-induced atrophy and glucocorticoid-inhibited protein synthesis in C2C12 myotubes. Dex treatment resulted in a 50% smaller reduction of myotube diameter in sh-p85α cells than in control cells. The remaining Dex-induced reduction of diameter in sh-p85α myotubes may be due to residual p85α. Alternatively, other GR-regulated genes might contribute to the Dex effect. Supporting this alternative, a study showed that reducing Ddit4 expression attenuates glucocorticoid-inhibited protein synthesis in L6 myotubes (15). This study suggests that additional genes, such as the remaining 6 GR primary targets, may also have nonredundant effect and could mediate glucocorticoid-induced muscle atrophy by suppressing insulin/IGF-1 signaling.

The ability of Dex to decrease cell diameters in sh-p85α myotubes may be due to Dex-induced protein degradation, as the inhibitory effect of Dex on protein synthesis was abolished in these cells. Glucocorticoids have been shown to increase the expression of MuRF-1 and atrogin-1, two ubiquitin E3 ligases implicated as causes of muscle atrophy (40). In mice lacking MuRF1, the ability of glucocorticoids to induce muscle atrophy is compromised (3). The previously identified MuRF1 GRE (45) was not found in our ChIPseq; however, it is possible that our GR antibody did not recognize the conformation of GR while bound to the MuRF1 GRE. FoxO1 is required for maximal glucocorticoid-activated MuRF1 gene transcription. Although we did not find any GBR near or within the atrogin-1 gene, its transcription is activated by FoxO1 and FoxO3 (11). In agreement with previous reports, we observed reduced ratio of pFoxO1 to total FoxO1 upon Dex treatment (29). Also, we found decreased ratio of pFoxO3 to total FoxO3. However, these ratios were similar between sh-scr and sh-p85α myotubes, despite the reduced ability of Dex to suppress Akt activity in the latter. Since Dex increased total FoxO1 and FoxO3 proteins, it added another layer of complexity for the calculation and comparison between their phosphorylation status in sh-scr and sh-p85α cells. The immunoblotting just might not be sensitive enough to consistently detect the difference. Upon 72 h Dex treatment, FoxO3, MuRF-1 and atrogin-1 expressions were reduced in sh-p85α myotubes, but levels of total FoxO3 protein in sh-scr and sh-p85α myotubes were similar. A longer Dex treatment could be required to observe a

change in FoxO3 protein level. Nonetheless, the fact that p85α is involved in Dex-activated atrogene expression suggests it has a role in glucocorticoid-induced protein degradation.

In summary, we have identified GR-controlled transcriptional networks in myotubes and focused on one that can modulate the insulin/IGF-1 signaling. We highlighted the role of p85α in this crosstalk between glucocorticoid and insulin action. Future studies will test other GR primary targets to complete the picture of glucocorticoid-induced insulin resistance and muscle atrophy in skeletal muscle.

Materials and Methods

Cell culture: The C2C12 cells were purchased from the Cell and Tissue Culture Facility at the University of California, Berkeley. They were maintained in Dulbecco's modified Eagle's medium (DMEM; Mediatech) containing 10% fetal bovine serum (FBS; Tissue Culture Biologicals) and incubated at 37°C with 5% CO_2. The 95~100 % confluent C2C12 myoblasts were differentiated into myotubes with 2% horse serum (J.R. Scientific) in DMEM. The C2C12 cells were maintained in 2% horse serum-containing DMEM, changed every 2 days, until fully differentiated into myotubes, taking about 4-6 days. For all cell culture experiments, C2C12 myotubes were treated with 1 μM Dex, an equal volume (0.05% v/v of media) of vehicle control ethanol (EtOH) or phosphate buffer saline (PBS).

Animals: The protocol is described in SI Text S1. The Office of Laboratory Animal Care at the University of California, Berkeley (#R306-0111) approved all animal experiments conducted in this paper. Male 8-week-old C57BL/6 mice were purchased from Charles River. Mice were injected with 5 mg/kg/day Dex (Sigma) or PBS for 1 or 4 days. After the treatment, gastrocnemius muscles were isolated from mice. CRH-Tg mice were provided by Mary Stenzel-Poore (46). The Office of Laboratory Animal Care at the University of California, Berkeley (#R306-0111) approved all animal experiments conducted in this paper.

ChIPseq: Fully differentiated C2C12 myotubes were treated with 1μM Dex or control EtOH for 1h, cross-linked in 2% formaldehyde for 3 min at 37°C. The reactions were quenched with 0.125M glycine. The cell were then washed with 1X PBS, and scraped and lysed in cell lysis buffer (50 mM HEPES-KOH at pH 7.4, 1 mM EDTA, 150 mM NaCl, 10% glycerol, 0.5% Triton X-100), supplemented with protease inhibitor cocktails (Calbiochem). The cell lysate was incubated for 1h at 4°C, and the crude nuclear extract was collected by centrifugation at 600xg for 5 min at 4°C. The nuclei were resuspended in 1 mL of ice-cold RIPA buffer (10 mM Tris-HCL at pH 8.0, 1 mM EDTA, 150 mM NaCl, 5% glycerol, 1% Triton X-100, 0.1% sodium deoxycholate, 0.1% SDS, supplemented with protease inhibitor). The chromatin was fragmented with Branson Sonifier 250 sonicator (13 min total, 20 sec pulse at 35% power followed by 40 sec pause) on ice. To remove insoluble components, we centrifuged the samples at 13,000 rpm for 15 min at 4°C and recovered the supernatant. One μg of rabbit polyclonal anti-GR (N499, provided by Keith R. Yamamoto laboratory, UCSF) antibody was add to the supernatant to immunoprecipitate GR-bound chromatin at 4°C overnight. The next day, 100 μl of 50% protein A/G plus-agarose bead slurry (Santa Cruz Biotechnology) was added into each immunoprecipitation and incubated it for 2 h at 4°C. The beads were then washed twice with RIPA buffer; three times with RIPA buffer containing 500 mM NaCl, twice with LiCl buffer (20 mM Tris at pH 8.0, 1 mM EDTA, 250 mM LiCl, 0.5% NP-40, 0.5% sodiumdeoxycholate), and one time RIPA buffer, all supplemented with protease inhibitor. After removing the remaining wash buffer, 75 μl of proteinase K solution (TE pH 8.0, 0.7% SDS, 200 μg/ml proteinase K) was added to each IP reaction, followed by incubation at 55°C for 3 h and 65°C for overnight to reverse formaldehyde cross-linking. ChIP DNA fragments were purified with QIAquick PCR purification kit (Qiagen), eluting in 30 μl of Qiagen Elution Buffer.

We followed the procedures of Illumina's and Dr. Samantha Cooper's protocols (*http://samanthacooper.dreamhosters.com/mywiki/index.php?title=SolexaChIP*) for genomic DNA library preparation. In brief, ChIP DNA fragments were blunted and ligated to sequencing adapters, kindly provided by Samantha Cooper. One μl of highly pure T4 DNA ligase (Enzymatics) was used to

ligate the adapters to ChIP DNA, incubated at 16°C overnight. The next morning, another 1μl of T4 DNA ligase was added to the reaction to boost the ligation efficiency. Adapter-ligated ChIP fragments became circular, and UDG is used to digest the U in the adapter to linearize the DNA fragments. This adapter design allows maximal reads for each ChIPseq library. The linearized adapter-ligated DNA was then amplified with 25 rounds of PCR. The PCR products were cleaned with Agencourt AMPure PCR purification kit (*http://www.agencourt.com/technical/*). DNA quality control was done with Bioanalyzer (Agilent). The resulting ChIP DNA libraries were sequenced on the Illumina Genome Analyzer (Vincent J. Coates Genomic Sequencing Laboratory, University of California, Berkeley). The reads that have passed Illumina's internal quality filter were retained for further analysis. Reads were aligned to mm9 assembly of mouse genome by Illumina's default aligner ELAND (allowing up to 2 mismatches in first 32 bps). The aligned reads were given as input to peak-finding software Model-based Analysis of ChIPseq (MACS). The default p-value cutoff criterion was at 10^{-5} (the effective genome size was set to 2.2 Gb). The underlying DNA sequences of the identified peak regions were obtained with a python script and further analyzed with web-based motif-finding tools.

Annotation of genes: The distribution of GR-binding sites, relative to nearest genes, was determined by PinkThing (http://pinkthing.cmbi.ru.nl). PinkThing identifies the closest genes to each GBR within 1000 kb upstream of TSS or downstream of stop codons. All sequences associated with the peaks were obtained from the *Mus musculus* NCBI m37 genome assembly (mm9; July 2007).

Motif search and gene ontology analysis: BioProspector (47) was used to search for 14- or 8-bp motifs in the ChIPseq data. The top 10-20 scoring output motifs from BioProspector were then compared to known binding sites in the TRANSFAC V11.3 database using STAMP (48). A motif discovery program, cis-regulatory element annotation system (CEAS) (http://ceas.cbi.pku.edu.cn) (49), was also used to obtain the enriched transcription factor motifs located in ChIPseq-identified GBR. The Expect value (E) from STAMP research is a parameter that describes the number of hits one can expect to see by chance when searching a database of a particular element. The lower the E-value, the more significant the match is.

The Database for Annotation, Visualization and Integrated Discovery (DAVID) (http://david.abcc.ncifcrf.gov/home.jsp) was used to perform gene ontology analysis. Below is the list of categories selected for analysis: Disease: OMIM_DISEASE, Functional Categories: OMIM_DISEASES, COG_ONTOLOGY, SP_PIR_KEYWORDS, UP_SEQ_FEATURE, Gene_Ontology: GOTERM_BP_FAT, GOTERM_CC_FAT, GOTERM_MF_FAT, Pathway: BBID, BIOCARTA, KEGG_PATHWAY.

TFSEARCH (http://www.cbrc.jp/research/db/TFSEARCH.html) was used to locate transcription factor binding motifs in p85α GBR using default threshold score of 85.

Microarrays and Data Analysis: Fully differentiated C2C12 myotubes were treated with 1 μM Dex or an equal volume (0.05% v/v of media) of vehicle control ethanol for 6 h or 24h at 37°C in DMEM supplemented with 2% horse serum. Total RNA was isolated with NucleoSpin RNA II kit (Macherey-Nagel), following their protocol. RNA isolates were first quantified by standard spectrophotometry, and then qualitatively evaluated by capillary electrophoresis employing the Bio-Rad Experion system per the manufacturer's instruction. Biotin-labeled cRNA samples were prepared with 750 ng of total RNA template. Following synthesis and purification, the biotin-labeled samples were evaluated by both

260/280 absorbance spectrophotometry and capillary electrophoresis. The final labeled cRNA samples were hybridized overnight against 48,000 transcripts using MouseWG-6 BeadChip arrays (Illumina, San Diego, CA). The Illumina microarrays were processed at the UCSF Genomics Core. All treatments were done in triplicates and the same batch of microarrays was used for all treatments. The Illumina expression arrays were pre-processed using lumi package (50). The differential expression analysis was performed using the Limma package (51). These packages are all available in R/BioConductor. Probes were selected for further analysis if the fold-induction was greater than 1.5, and multiple testing adjusted the p-value to less than 0.05 using Benjamini and Hochberg procedure (BH-adjusted p-value) (52). The heatmaps of log intensities of genes across different experiments were produced using Cluster and TreeView software (53). The microaray data is available at the Gene Expression Omnibus Web site (*http://www.ncbi.nlm.nih.gov/geo/*) under accession No. GSE28840.

RNA isolation and quantitative PCR: Total RNA was isolated from mouse gastrocnemius muscles using TRI Reagent® RT (Molecular Research Center, Inc.). To synthesize randomly primed cDNA, 0.5 μg of total RNA, 4 μl of 2.5 mM dNTP and 2 μl of random primers (New England Biolabs) were mixed at a volume of 16 μl, and incubated at 70°C for 10 min. Then, a 4-μl cocktail containing 25 units of Moloney Murine Leukemia Virus (M-MuLV) Reverse Transcriptase (New England Biolabs), 10 units of RNasin (Promega) and 2 μl of 10X reaction buffer (New England Biolabs) was added and incubated at 42°C for 1 h and then 95°C for 5 min. The cDNA was diluted and used to perform real-time quantitative PCR (qPCR) using the EVA QPCR SuperMix Kit (Biochain) following manufacturer's protocol. qPCR was performed in either a 7900HT, 7500HT or StepOne PCR System (Applied Biosystems) and analyzed with the ΔΔ-Ct method, as supplied by the manufacturer (Applied Biosystems). *Rpl19* gene expression was used for internal normalization. Primer sequences are listed in supporting information Dataset S5.

Plasmids, transfection, and luciferase reporter assay: Reporter plasmids harboring different GBR were co-transfected with pcDNA3-hGR (150 ng) and pRL Renilla (100 ng) into C2C12 myoblasts in a 12-well plate. pGL4.10-E4TATA reporter plasmid was generated by insertion of a 50-bp minimal *E4* TATA promoter sequence (Lin et al. 1988) into the *Bgl* II to *Hind* III sites of vector pGL4.10 to drive luciferase expression (Bolton et al. 2007). Each chosen GBR fragment, extending 100-150 bp upstream and downstream of the GBR, was amplified from genomic C2C12 DNA (primer sequences are listed in supporting information Dataset S5) using the Expand Long Template PCR System (Roche Applied Science) and cloned into the pGL4.10-E4TATA vector with *Kpn* I/*Xho* I sites. The QuikChange Lightning mutagenesis kit (Stratagene) was used to make site-directed mutations per the manufacturer's instructions. Primer sequences are listed in supporting information Dataset S5. Lipofectamine 2000 (Invitrogen) was used to transfect C2C12 myoblast according to the technical manual. Twenty-four hours post-transfection, cells were treated with either 1 μM Dex or control EtOH in differentiation media for 16-20 h. Cells were then harvested, and their luciferase activities were measured with the Dual-Luciferase Reporter Assay kit (Promega) according to the technical manual.

Lentiviral infection and Western Blot: Mouse C2C12 myoblasts were infected with p85α shRNA lentiviral particle (sc-36217-V, Santa Cruz Biotechnology), sh-p85α; or control shRNA lentiviral particle (sc-108080, Santa Cruz Biotechnology), sh-scr, and selected for with 5μg/ml puromycin for several days. Sh-p85α and sh-scr C2C12 myoblasts were then differentiated into myotubes. Three days after differentiation, 1 μM Dex or EtOH were added to sh-p85α or sh-scr myotubes for 72 h, with replenishment of media and treatment every 24 h. Each 10-cm plate of myotubes were washed twice

with 1x PBS, and scraped and divided into two portions: one for gene expression, and the other for Western blotting. For gene expression, total RNA was isolated with NucleoSpin RNA II kit (Macherey-Nagel), following the manufacturer's instruction, and reverse transcription and quantitative PCR (described in *RNA isolation and quantitative PCR*) were done to check knockdown efficiency. For Western blotting, RIPA buffer (10 mM Tris-HCl, pH 8.0, 1mM EDTA, 150 mM NaCl, 5% glycerol, 0.1% sodium deoxycholate, 0.1% SDS, and 1% Triton X-100), supplemented with protease inhibitors, was added to cell pellet. The mixture was gently rocked at 4°C for 1 h. The supernatant was then collected as protein sample. NuPAGE Novex Bis-Tris mini gels (Invitrogen) were used, following the manufaturer's protocol, and proteins were transferred to nitrocellulose membranes (Amersham) using semidry transfer (Bio-Rad) overnight. The next day, membranes were blocked for 4 h at room temperature with 10% (wt/vol) nonfat milk in TBS (50 mM Tris-base, 200 mM NaCl, pH 7.5). Membranes were then incubated in 5% milk in TBS with appropriate primary antibody with gentle rocking overnight at 4°C. The next day, membranes were washed with TBS plus 0.5% Tween-20 at pH 7.5 (TBST), and then incubated in 5% milk in TBS containing appropriate secondary antibody for at least 2 h at room temperature. The membranes were then washed with TBST, and proteins were detected by chemiluminescence (Western Lighting Plus-ECL, Perkin Elmer). For additional protein detection on the same membrane, membranes were soaked in TBS overnight at 4°C, and stripped for 30 min in PBS with 7 μl/ml β-mercaptoethanol, followed by 30min in PBS only, and 4 h in 10% milk in TBS before re-probing with other primary antibodies. The following antibodies were used: PI3 kinase p85 (4292, Cell Signaling), phospho-IRS1 (Ser 307) (07-247, Millipore), IRS-1 (06-248, Millipore), phospho-Akt (Ser 473) (9271, Cell Signaling), Akt (9272, Cell Signaling), p70 S6 kinase (9202, Cell Signaling), phospho-p70 S6 kinase (Thr 389) (9205, Cell Signaling), FoxO1 (sc-11350, Santa Cruz Biotechnology), phospho-FoxO1 Ser-256 (#9461S, Cell Signaling), FoxO3 (07-702, Millipore), phospho-FoxO3 Thr-32 (sc-12357-R, Santa Cruz Biotechnology), GAPDH (abcam, ab9483), anti-rabbit IgG_1-HRP (Cell Signaling) and anti-goat IgG-HRP (sc-2768; Santa Cruz Biotechnology). Blots were scanned and analyzed with Image J software (*http://rsbweb.nih.gov/ij*). GAPDH was used as an internal control.

Muscle Atrophy Assay: Fully differentiated C2C12 myotubes were infected with adenovirus overexpressing LacZ (Ad-LacZ) or p85α (Ad-p85α, provided by Ron Kahn, Joslin Diabetes Center) for 72 h. WT, sh-scr, and sh-p85α C2C12 myotubes (differentiation day 3) were treated with 1 μM Dex or EtOH for 72 h with replenishment of media and treatment every 24 h. The cells were fixed with 3.7% formaldehyde in 2% horse serum-containing DMEM, and incubated at 37°C for 15 min, followed by two PBS washes. The fixed cells were visualized and photographed with phase-contrast microscopy and 300nM DAPI (Invitrogen) in PBS, and incubated at 37°C for 15 min. The stained cells were then washed with PBS twice before imaging. Zeiss Axio Imager was used for fluorescent imaging. Three short-axis measurements were taken along the length of a given myotube, and at least one hundred myotubes were analyzed using iVision software (BioVision Technologies) for each adenovirus construct.

Protein Synthesis Assay: Sh-p85α and sh-scr C2C12 myoblasts were grown in 96-well plates, and differentiated into myotubes. Protein synthesis assay (Click-iT AHA Alexa Fluor 488 Protein Synthesis HCS Assay, catalog no. C10289, Invitrogen) was carried out per manufacturer's instruction.

Acknowledgements

This work is supported by the NIH (R01DK083591) and the Muscular Dystrophy Association (186068). T.K. is supported by the Dissertation Award Fellowship from the University of California Tobacco-Related Diseases Research Program.

References

1. Hu Z, Wang H, Lee IH, Du J, & Mitch WE (2009) Endogenous glucocorticoids and impaired insulin signaling are both required to stimulate muscle wasting under pathophysiological conditions in mice. *J Clin Invest* 119(10):3059-3069.
2. Auclair D, Garrel DR, Chaouki Zerouala A, & Ferland LH (1997) Activation of the ubiquitin pathway in rat skeletal muscle by catabolic doses of glucocorticoids. *Am J Physiol* 272(3 Pt 1):C1007-1016.
3. Baehr LM, Furlow JD, & Bodine SC (2011) Muscle sparing in muscle RING finger 1 null mice: response to synthetic glucocorticoids. *J Physiol* 589(Pt 19):4759-4776.
4. Shimizu N*, et al.* (2011) Crosstalk between glucocorticoid receptor and nutritional sensor mTOR in skeletal muscle. *Cell Metab* 13(2):170-182.
5. Morgan SA*, et al.* (2009) 11beta-hydroxysteroid dehydrogenase type 1 regulates glucocorticoid-induced insulin resistance in skeletal muscle. *Diabetes* 58(11):2506-2515.
6. Dimitriadis G*, et al.* (1997) Effects of glucocorticoid excess on the sensitivity of glucose transport and metabolism to insulin in rat skeletal muscle. *Biochem J* 321 (Pt 3):707-712.
7. Weinstein SP, Wilson CM, Pritsker A, & Cushman SW (1998) Dexamethasone inhibits insulin-stimulated recruitment of GLUT4 to the cell surface in rat skeletal muscle. *Metabolism: clinical and experimental* 47(1):3-6.
8. Ohshima K, Shargill NS, Chan TM, & Bray GA (1989) Effects of dexamethasone on glucose transport by skeletal muscles of obese (ob/ob) mice. *Int J Obes* 13(2):155-163.
9. Menconi M, Gonnella P, Petkova V, Lecker S, & Hasselgren PO (2008) Dexamethasone and corticosterone induce similar, but not identical, muscle wasting responses in cultured L6 and C2C12 myotubes. *J Cell Biochem* 105(2):353-364.
10. Stitt TN*, et al.* (2004) The IGF-1/PI3K/Akt pathway prevents expression of muscle atrophy-induced ubiquitin ligases by inhibiting FOXO transcription factors. *Mol Cell* 14(3):395-403.
11. Sandri M*, et al.* (2004) Foxo transcription factors induce the atrophy-related ubiquitin ligase atrogin-1 and cause skeletal muscle atrophy. *Cell* 117(3):399-412.
12. Gathercole LL, Bujalska IJ, Stewart PM, & Tomlinson JW (2007) Glucocorticoid modulation of insulin signaling in human subcutaneous adipose tissue. *J Clin Endocrinol Metab* 92(11):4332-4339.
13. Schakman O, Gilson H, & Thissen JP (2008) Mechanisms of glucocorticoid-induced myopathy. *J Endocrinol* 197(1):1-10.
14. Lee YH & White MF (2004) Insulin receptor substrate proteins and diabetes. *Arch Pharm Res* 27(4):361-370.

15. Wang H, Kubica N, Ellisen LW, Jefferson LS, & Kimball SR (2006) Dexamethasone represses signaling through the mammalian target of rapamycin in muscle cells by enhancing expression of REDD1. *J Biol Chem* 281(51):39128-39134.
16. Gual P, Le Marchand-Brustel Y, & Tanti JF (2005) Positive and negative regulation of insulin signaling through IRS-1 phosphorylation. *Biochimie* 87(1):99-109.
17. Song IH & Buttgereit F (2006) Non-genomic glucocorticoid effects to provide the basis for new drug developments. *Mol Cell Endocrinol* 246(1-2):142-146.
18. Nakao R*, et al.* (2009) Ubiquitin ligase Cbl-b is a negative regulator for insulin-like growth factor 1 signaling during muscle atrophy caused by unloading. *Mol Cell Biol* 29(17):4798-4811.
19. Wu WL*, et al.* (2011) Over-expression of NYGGF4 (PID1) inhibits glucose transport in skeletal myotubes by blocking the IRS1/PI3K/AKT insulin pathway. *Mol Genet Metab* 102(3):374-377.
20. Wick KR*, et al.* (2003) Grb10 inhibits insulin-stimulated insulin receptor substrate (IRS)-phosphatidylinositol 3-kinase/Akt signaling pathway by disrupting the association of IRS-1/IRS-2 with the insulin receptor. *J Biol Chem* 278(10):8460-8467.
21. Barbour LA*, et al.* (2005) Increased P85alpha is a potent negative regulator of skeletal muscle insulin signaling and induces in vivo insulin resistance associated with growth hormone excess. *J Biol Chem* 280(45):37489-37494.
22. Ueki K*, et al.* (2003) Positive and negative roles of p85 alpha and p85 beta regulatory subunits of phosphoinositide 3-kinase in insulin signaling. *J Biol Chem* 278(48):48453-48466.
23. Draznin B (2006) Molecular mechanisms of insulin resistance: serine phosphorylation of insulin receptor substrate-1 and increased expression of p85alpha: the two sides of a coin. *Diabetes* 55(8):2392-2397.
24. Budanov AV & Karin M (2008) p53 target genes sestrin1 and sestrin2 connect genotoxic stress and mTOR signaling. *Cell* 134(3):451-460.
25. Peterson TR*, et al.* (2009) DEPTOR is an mTOR inhibitor frequently overexpressed in multiple myeloma cells and required for their survival. *Cell* 137(5):873-886.
26. Lesniewski LA*, et al.* (2007) Bone marrow-specific Cap gene deletion protects against high-fat diet-induced insulin resistance. *Nat Med* 13(4):455-462.
27. Luisi BF*, et al.* (1991) Crystallographic analysis of the interaction of the glucocorticoid receptor with DNA. *Nature* 352(6335):497-505.
28. Bodine SC*, et al.* (2001) Identification of ubiquitin ligases required for skeletal muscle atrophy. *Science* 294(5547):1704-1708.
29. Zhao W*, et al.* (2009) Dependence of dexamethasone-induced Akt/FOXO1 signaling, upregulation of MAFbx, and protein catabolism upon the glucocorticoid receptor. *Biochemical and biophysical research communications* 378(3):668-672.
30. Yu CY*, et al.* (2010) Genome-wide analysis of glucocorticoid receptor binding regions in adipocytes reveal gene network involved in triglyceride homeostasis. *PloS one* 5(12):e15188.
31. Wang JC, Stromstedt PE, O'Brien RM, & Granner DK (1996) Hepatic nuclear factor 3 is an accessory factor required for the stimulation of phosphoenolpyruvate carboxykinase gene transcription by glucocorticoids. *Mol Endocrinol* 10(7):794-800.
32. Miner JN & Yamamoto KR (1991) Regulatory crosstalk at composite response elements. *Trends Biochem Sci* 16(11):423-426.
33. Gross DN, van den Heuvel AP, & Birnbaum MJ (2008) The role of FoxO in the regulation of metabolism. *Oncogene* 27(16):2320-2336.

34. De Bosscher K, Vanden Berghe W, & Haegeman G (2003) The interplay between the glucocorticoid receptor and nuclear factor-kappaB or activator protein-1: molecular mechanisms for gene repression. *Endocr Rev* 24(4):488-522.
35. Lee MC, Wee GR, & Kim JH (2005) Apoptosis of skeletal muscle on steroid-induced myopathy in rats. *J Nutr* 135(7):1806S-1808S.
36. Hudlicka O, Brown M, & Egginton S (1992) Angiogenesis in skeletal and cardiac muscle. *Physiol Rev* 72(2):369-417.
37. Logie JJ*, et al.* (2010) Glucocorticoid-mediated inhibition of angiogenic changes in human endothelial cells is not caused by reductions in cell proliferation or migration. *PLoS One* 5(12):e14476.
38. Barbour LA*, et al.* (2004) Human placental growth hormone increases expression of the p85 regulatory unit of phosphatidylinositol 3-kinase and triggers severe insulin resistance in skeletal muscle. *Endocrinology* 145(3):1144-1150.
39. Mauvais-Jarvis F*, et al.* (2002) Reduced expression of the murine p85alpha subunit of phosphoinositide 3-kinase improves insulin signaling and ameliorates diabetes. *J Clin Invest* 109(1):141-149.
40. Zheng B, Ohkawa S, Li H, Roberts-Wilson TK, & Price SR (2010) FOXO3a mediates signaling crosstalk that coordinates ubiquitin and atrogin-1/MAFbx expression during glucocorticoid-induced skeletal muscle atrophy. *Faseb J* 24(8):2660-2669.
41. Fujita T, Fukuyama R, Enomoto H, & Komori T (2004) Dexamethasone inhibits insulin-induced chondrogenesis of ATDC5 cells by preventing PI3K-Akt signaling and DNA binding of Runx2. *Journal of cellular biochemistry* 93(2):374-383.
42. Andrade MV, Hiragun T, & Beaven MA (2004) Dexamethasone suppresses antigen-induced activation of phosphatidylinositol 3-kinase and downstream responses in mast cells. *J Immunol* 172(12):7254-7262.
43. Luo J*, et al.* (2006) Loss of class IA PI3K signaling in muscle leads to impaired muscle growth, insulin response, and hyperlipidemia. *Cell Metab* 3(5):355-366.
44. Bandyopadhyay GK, Yu JG, Ofrecio J, & Olefsky JM (2005) Increased p85/55/50 expression and decreased phosphotidylinositol 3-kinase activity in insulin-resistant human skeletal muscle. *Diabetes* 54(8):2351-2359.
45. Waddell DS*, et al.* (2008) The glucocorticoid receptor and FOXO1 synergistically activate the skeletal muscle atrophy-associated MuRF1 gene. *American journal of physiology. Endocrinology and metabolism* 295(4):E785-797.
46. Stenzel-Poore MP, Cameron VA, Vaughan J, Sawchenko PE, & Vale W (1992) Development of Cushing's syndrome in corticotropin-releasing factor transgenic mice. *Endocrinology* 130(6):3378-3386.
47. Liu X, Brutlag DL, & Liu JS (2001) BioProspector: discovering conserved DNA motifs in upstream regulatory regions of co-expressed genes. *Pac Symp Biocomput*:127-138.
48. Mahony S & Benos PV (2007) STAMP: a web tool for exploring DNA-binding motif similarities. *Nucleic Acids Res* 35(Web Server issue):W253-258.
49. Ji X, Li W, Song J, Wei L, & Liu XS (2006) CEAS: cis-regulatory element annotation system. *Nucleic acids research* 34(Web Server issue):W551-554.
50. Du P, Kibbe WA, & Lin SM (2008) lumi: a pipeline for processing Illumina microarray. *Bioinformatics* 24(13):1547-1548.
51. Smyth GK (2004) Linear models and empirical bayes methods for assessing differential expression in microarray experiments. *Stat Appl Genet Mol Biol* 3:Article3.

52. Dudoit S, Gentleman RC, & Quackenbush J (2003) Open source software for the analysis of microarray data. *Biotechniques* Suppl:45-51.
53. Eisen MB, Spellman PT, Brown PO, & Botstein D (1998) Cluster analysis and display of genome-wide expression patterns. *Proc Natl Acad Sci U S A* 95(25):14863-14868.

Genome-wide analysis of glucocorticoid receptor-binding sites in myotubes identifies gene networks modulating insulin signaling

Taiyi Kuo[a,b], Michelle J. Lew[b], Oleg Mayba[c], Charles A. Harris[d,e], Terence P. Speed[c], and Jen-Chywan Wang[a,b,1]

[a]Endocrinology Graduate Program, [b]Department of Nutritional Science and Toxicology, and [c]Department of Statistics, University of California, Berkeley, CA 94720; [d]Gladstone Institute for Cardiovascular Disease, San Francisco, CA 94158; and [e]Department of Medicine, University of California, San Francisco, CA 94143

Edited by Gordon L. Hager, National Cancer Institute, Bethesda, MD, and accepted by the Editorial Board May 30, 2012 (received for review July 15, 2011)

Glucocorticoids elicit a variety of biological responses in skeletal muscle, including inhibiting protein synthesis and insulin-stimulated glucose uptake and promoting proteolysis. Thus, excess or chronic glucocorticoid exposure leads to muscle atrophy and insulin resistance. Glucocorticoids propagate their signal mainly through glucocorticoid receptors (GR), which, upon binding to ligands, translocate to the nucleus and bind to genomic glucocorticoid response elements to regulate the transcription of nearby genes. Using a combination of chromatin immunoprecipitation sequencing and microarray analysis, we identified 173 genes in mouse C2C12 myotubes. The mouse genome contains GR-binding regions in or near these genes, and gene expression is regulated by glucocorticoids. Eight of these genes encode proteins known to regulate distinct signaling events in insulin/insulin-like growth factor 1 pathways. We found that overexpression of p85α, one of these eight genes, caused a decrease in C2C12 myotube diameters, mimicking the effect of glucocorticoids. Moreover, reducing p85α expression by RNA interference in C2C12 myotubes significantly compromised the ability of glucocorticoids to inhibit Akt and p70 S6 kinase activity and reduced glucocorticoid induction of insulin receptor substrate 1 phosphorylation at serine 307. This phosphorylation is associated with insulin resistance. Furthermore, decreasing p85α expression abolished glucocorticoid inhibition of protein synthesis and compromised glucocorticoid-induced reduction of cell diameters in C2C12 myotubes. Finally, a glucocorticoid response element was identified in the p85α GR-binding regions. In summary, our studies identified GR-regulated transcriptional networks in myotubes and showed that p85α plays a critical role in glucocorticoid-induced insulin resistance and muscle atrophy in C2C12 myotubes.

Glucocorticoids perform vital metabolic functions in skeletal muscle: inhibiting protein synthesis and insulin-stimulated glucose uptake and promoting protein degradation. These effects are critical during stress, producing amino acid precursors for gluconeogenesis, which provides glucose for the brain. Initially, muscle insulin resistance maintains adequate circulating glucose to fuel the brain; however, these effects are deleterious if chronic. Treating animals with glucocorticoids causes a decrease in skeletal muscle size (1–4). Mice treated with glucocorticoids have reduced insulin-stimulated glucose uptake and GLUT4 translocation in myotubes (5–7). Circulating glucocorticoid levels are higher in obese *ob*/*ob* and *db*/*db* mice than in normal mice. Adrenalectomy in these obese mice improves insulin-stimulated muscle glucose disposal (8). These changes are in part due to the direct effect of glucocorticoids on myotubes, as glucocorticoid treatment in cultured myotubes reduces cell diameters (9–11) and inhibits insulin-stimulated glucose utilization (5, 12).

Although the metabolic effects of glucocorticoids in skeletal muscle are well known, the underlying mechanisms are not fully understood. One way in which glucocorticoids affect glucose and protein metabolism is to antagonize the insulin/insulin-like growth factor 1 (IGF1) pathway (5, 13), which promotes protein synthesis and glucose utilization. Insulin/IGF1 acts by binding to membrane receptors, tyrosine kinases that autophosphorylate and phosphorylate insulin receptor substrates (IRS) (14). Tyrosine-phosphorylated IRS associate with insulin receptors (IR) and activate signaling pathways (14). Mice treated with glucocorticoids have reduced levels of tyrosine-phosphorylated IR and total IRS-1 in skeletal muscle (5). The activity of phosphatidylinositol 3-kinase (PI3K) and Akt, two signaling molecules downstream of IR and IRS-1, is also decreased (5). Glucocorticoids also reduce the activity of mammalian target of rapamycin (mTOR), a protein kinase downstream of Akt and upstream of p70 S6 kinase (p70S6K) (15). Furthermore, glucocorticoid treatment increases the phosphorylation of serine 307 of IRS-1 (pSer307-IRS-1) (5), which disrupts the association of IR and IRS-1, reducing the insulin/IGF1 response (16). However, the mechanism by which glucocorticoids inhibit the insulin/IGF1 pathway is unclear.

Although certain glucocorticoid effects are independent of intracellular glucocorticoid receptors (GR) (17), the majority are mediated by GR, which, upon binding to its ligand, moves to the nucleus and interacts with genomic GR response elements (GRE). It is critical to identify genes directly regulated by GR to learn the physiological mechanisms of glucocorticoids. Here, we used a combination of chromatin immunoprecipitation sequencing (ChIPseq) and microarray analysis to identify direct targets of GR in mouse C2C12 myotubes. We identified potential GR primary targets previously shown to modulate distinct steps of insulin/IGF1 signaling. We focused on one potential GR primary target, p85α. Experiments were conducted to identify its GRE and its role in the suppressive effects of glucocorticoids on myotube diameters, protein synthesis, and the insulin/IGF1-signaling pathway.

Results

Identification of Potential GR Primary Target Genes in C2C12 Myotubes. Microarray analyses were conducted in C2C12 myotubes treated for 6 or 24 h with dexamethasone (Dex), a synthetic glucocorticoid, or ethanol (EtOH), a vehicle control. Combining data from both time points, we found that Dex induced the expression of 363 genes by more than 1.5-fold and inhibited the expression of 218 genes by more than 1.5-fold (Dataset S1). To learn which of these genes contains GR-binding regions (GBR) in or near their genomic regions, ChIPseq was performed with C2C12 myotubes treated with Dex or EtOH for 1 h. We located 2,251 genomic positions with sequencing reads significantly enriched in Dex-treated samples compared with EtOH-treated ones, with a *P* value

Author contributions: T.K. and J.-C.W. designed research; T.K. and M.J.L. performed research; C.A.H. contributed new reagents/analytic tools; T.K., O.M., T.P.S., and J.-C.W. analyzed data; and T.K. and J.-C.W. wrote the paper.

The authors declare no conflict of interest.

This article is a PNAS Direct Submission. G.L.H. is a guest editor invited by the Editorial Board.

Data deposition: The microarray data reported in this paper have been deposited in the Gene Expression Omnibus (GEO) database, http://www.ncbi.nlm.nih.gov/geo/ (accession no. GSE28840).

[1]To whom correspondence should be addressed. E-mail: walwang@berkeley.edu.

This article contains supporting information online at www.pnas.org/lookup/suppl/doi:10.1073/pnas.1111334109/-/DCSupplemental.

threshold of 10^{-5}. We used PinkThing to assign these genomic GBR to mouse genes on the basis of proximity and grouped target sites on the basis of their relative position to the nearest gene (GBR are listed in Dataset S2). We found 42% of GBR in the intron regions and 29% either 25 kb upstream of transcription start site (TSS) or downstream of stop codons (Fig. 1*A*). In contrast, only 5% of GBR are located within 5 kb upstream from TSS (Fig. 1*A*). Overall, we identified 147 Dex-activated genes and 26 Dex-repressed genes containing GBR in or near their genomic regions (Table S1, Dataset S3).

The top categories of gene annotation from gene ontology analysis of 173 GR-regulated genes include those encoding proteins involved in the receptor tyrosine kinase-signaling pathway, blood vessel development, apoptosis, muscle organ development, and cytoskeletal organization (Dataset S4). We performed a combination of BioProspector and STAMP analyses to search for consensus motifs within GBR located in or near genes that were regulated by glucocorticoids. For glucocorticoid-activated genes, the classical GRE was the most represented motif in these analyses on the basis of *E* values (Fig. 1*B*). Binding motifs for HSF, AP-1, NF-E2, MAF, NRF-2, core binding, AML, PEBP, FOXP3, HNF3α, T3R, and RREB-1 were all significantly represented (Table S2). For glucocorticoid-repressed genes, the classical GRE motif was also highly represented (Fig. 1*C*). Moreover, HSF, SMAD3, T3R, XBP-1, ELF-1, HAC-1, ID-1, FOXP3, AbaA, XPF-1, Bach1, and AP-1 were all high on the list of binding motifs (Table S3).

Glucocorticoid-Controlled Genes Involved in Insulin/IGF1 Signaling. Gene ontology analysis revealed that many glucocorticoid-regulated genes affect receptor tyrosine kinase signaling. We analyzed the potential GR primary targets that can specifically inhibit the insulin/IGF1 pathway, which propagates through receptor tyrosine kinases. As shown in Fig. 2*A*, at least eight glucocorticoid-regulated genes encode proteins that can modulate the activity of this pathway. One of these genes, Cblb, encodes a ubiquitin E3 ligase involved in IRS-1 degradation (18). Pid-1 inhibits the tyrosine phosphorylation of IRS-1 (19). Grb10 inhibits the physical interaction between IR and IRS-1 (20). Overexpression of p85α induces insulin resistance in vitro and in vivo (21–23). Sesn 1 (24), Ddit4 (15), and Depdc6 (25) inhibit mTOR. Finally, mice with bone-marrow-specific deletion of Sorbs1 are protected from high-fat-diet–induced insulin resistance (26), indicating that overexpression of Sorbs1 could induce insulin resistance. To learn whether these genes were regulated by glucocorticoids in vivo, mice were injected with Dex or PBS control for 24 or 96 h. We found that mice injected with Dex for 24 h had significantly higher expression of Cblb and Pid1 than those injected with PBS in gastrocnemius muscles (Fig. 2*B*). Furthermore, the expression of Cblb, Pid1, p85α, Sesn1, Ddit4, and Sorbs1 was increased in mice treated with Dex for 96 h compared with the control (Fig. 2*B*). To determine the effect of chronic glucocorticoid exposure, we used transgenic mice overexpressing corticotropin-releasing hormone (CRH-Tg). CRH causes an increased secretion of adrenocorticotropic hormone, which further stimulates the secretion of adrenal corticosterone. In CRH-Tg mice, the expression of Cblb, Pid1, p85α, Ddit4, Sorbs1, and Sesn1 was markedly elevated in gastrocnemius muscles (Fig. 2*C*). In summation, at least six of the potential GR primary targets can inhibit insulin/IGF1 signaling in vivo.

A critical criterion for determining GR primary targets is that GR directly regulates their transcription. Thus, these GBR should be able to mediate the glucocorticoid response. To validate the GBR identified near these eight genes, each GBR was inserted upstream of a TATA box of a heterologous reporter plasmid, pGL4.10-E4TATA, which drives a firefly luciferase gene. A collection of plasmids used is listed in Dataset S5. We found that all GBR tested could mediate glucocorticoid responses (Fig. 3*A*), suggesting these eight glucocorticoid-regulated genes are primary targets of GR.

Role of p85α in Glucocorticoid-Regulated Insulin Signaling. The induction of p85α by glucocorticoids in vivo (Fig. 2 *B* and *C*) prompted further analysis into its role in mediating glucocorticoid responses in muscle. First, we identified the GRE in the *p85α* GBR. We searched for DNA sequences matching at least seven nucleotides to the consensus GRE motif identified from BioProspector/STAMP (RGXACAnnnTGTXCY) (Fig. 1*C*) in the *p85α* GBR. Three potential GRE-like sequences (GLS) were found, and for each GLS, we mutated the nucleotide from G to C at position 11, which makes direct contact with GR (27) (Fig. 3*B*). With the reporter assay, we found that GLS-2 mutants had an 80% reduction in the Dex response. Although the GLS-3 mutation had no significant effect, the GLS-1 mutation moderately potentiated the Dex response (Fig. 3*C*). Double mutations of GLS-2 and GLS-3 had similar effects as GLS-2 single mutations, and double mutations of GLS-1 and GLS-2 resulted in a slight increase in Dex response compared with GLS-2 single mutations (Fig. 3*C*). These results indicated that, although GLS-1 may be suppressive, GLS-2 plays a central role in mediating the glucocorticoid response. Furthermore, we used TFSEARCH to identify transcription factor-binding motifs in the *p85α* GBR. We found SRY-, GATA-, USF-, and Ikaros-binding sites located in the vicinity of GLS-2 (Fig. S1).

Next, we examined the role of p85α on glucocorticoid-induced inhibition of signaling molecules participating in the insulin/IGF1 pathway. We used lentiviral-mediated small hairpin RNA (shRNA) to decrease p85α expression (sh-p85α) in C2C12 cells. Control cells were infected with lentiviruses expressing shRNA with scramble sequences (sh-scr). Cells were then treated with Dex or EtOH for 72 h. In sh-scr cells, p85α protein levels were increased upon Dex treatment (Fig. 4*A*). In sh-p85α cells, p85α levels were reduced ~90% in both Dex- and EtOH-treated cells (Fig. 4*A*).

We monitored the phosphorylation status of serine 473 of Akt (pSer473-Akt) and threonine 389 of p70S6K (pThr389-S6K). These phosphorylations are required to potentiate their kinase activity. In contrast, pSer307-IRS-1 disrupts its interaction with the insulin/IGF1 receptor. In sh-scr cells, pSer473-Akt and pThr389-S6K levels were reduced upon Dex treatment (Fig. 4*A*). Although pSer307-IRS-1 levels were comparable between Dex- and EtOH-treated cells, IRS-1 protein expression was decreased upon Dex treatment in sh-scr cells (Fig. 4*A*). After normalizing to the IRS-1 protein present, there was a significant increase of pSer307-IRS-1 in Dex-treated sh-scr cells. In sh-p85α cells, Dex

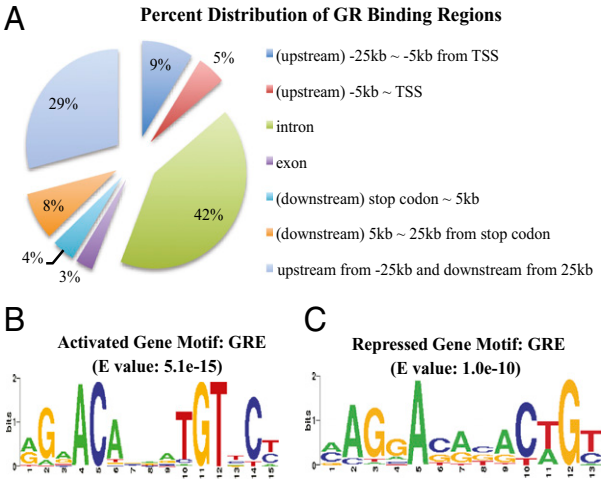

Fig. 1. Genomic distribution of GBR and GRE motifs within GBR. (*A*) Percentage distribution of all identified GBR in different genomic regions. (*B*) For GBR of glucocorticoid-induced genes, BioProspector analysis identified a motif that is similar to the consensus GRE in STAMP. (*C*) For GBR of glucocorticoid-repressed genes, BioProspector analysis also identified a motif that is similar to the consensus GRE in STAMP. (*B* and *C*) The *E* value is a parameter that describes the number of hits that one can expect to see by random chance when searching a database of a particular DNA element.

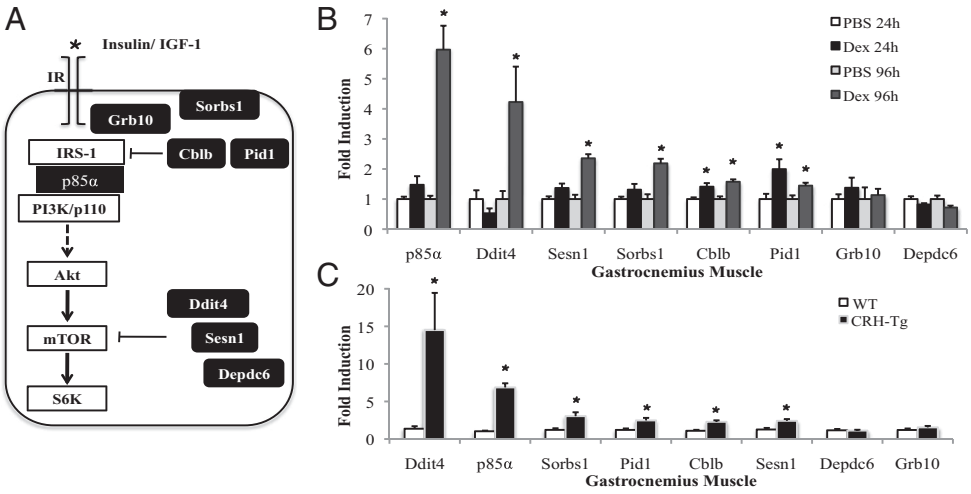

Fig. 2. Gene expression analyses of glucocorticoid-regulated genes in animal models. (*A*) Eight of the GR primary target genes and their roles in modulating the insulin/IGF1 signaling. (*B*) Fold induction of gene expression in gastrocnemius muscles of six to eight mice, injected with Dex or PBS for 1 or 4 d. (*C*) Fold induction of gene expression in gastrocnemius muscles of 12–14 CRH-Tg or WT mice. Error bars represent the SE. $*P < 0.01$.

treatment did not suppress the levels of pSer473-Akt and pThr389-S6K (Fig. 4 *A* and *B*). Although total IRS-1 protein levels decreased upon Dex treatment, this reduction was weaker than that of Dex-treated sh-scr cells (Fig. 4 *A* and *B*). Considering the similarity of pSer307-IRS-1 levels and the difference in total IRS-1 levels between Dex- and EtOH-treated sh-scr and sh-p85α cells, the ability of Dex to induce pSer307-IRS-1 was significantly compromised by knocking down p85α (Fig. 4*B*). Notably, EtOH treatment resembles PBS-treated sh-scr and sh-p85α cells (Fig. 4*B*). Overall, our data indicated that reducing the expression of p85α compromised the ability of glucocorticoids to inhibit the activity of Akt and p70S6K, to reduce IRS-1 protein levels, and to induce phosphorylation at serine 307 of IRS-1.

Role of p85α in Glucocorticoid-Induced Muscle Atrophy. We investigated whether p85α is involved in glucocorticoid-induced muscle atrophy. C2C12 myotubes were infected with adenoviruses expressing p85α (Ad-p85α) or a control of LacZ (Ad-LacZ). Cell diameters were then measured 72 h after infection. p85α protein levels are approximately fourfold higher in Ad-p85α than in Ad-LacZ cells (Fig. 5*A*). We found that significantly more Ad-p85α myotubes had smaller cell diameters than Ad-LacZ ones (Fig. 5*B*). The average cell diameter of Ad-p85α myotubes was about 30% smaller than Ad-LacZ ones (Fig. 5*C*). These results demonstrate that overexpressing p85α mimics the effect of glucocorticoids in reducing C2C12 myotube diameters.

Following the treatment of sh-scr and sh-p85α myotubes with Dex, EtOH, or PBS for 72 h, we measured cell diameters. The average diameter of Dex-treated sh-scr myotubes was 28% smaller than those of EtOH-treated sh-scr myotubes (Fig. 5*D*). A similar effect was observed in wild-type (WT) myotubes, with no lentiviral infection, treated with Dex and EtOH (Fig. 5*D*). In contrast, the average diameter of Dex-treated sh-p85α myotubes was 14% smaller than that of EtOH-treated sh-p85α myotubes (Fig. 5*D*). Although glucocorticoids still decreased C2C12 myotube diameter, reduced p85α expression significantly compromised this decrease. Notably, the average myotube diameters of EtOH-treated WT, sh-scr, and sh-p85α myotubes were comparable.

In addition, we investigated the effect of glucocorticoids on protein synthesis in sh-scr and sh-p85α myotubes. Myotubes were treated with Dex or EtOH for 72 h, and protein synthesis was measured using a fluorescence assay. We found that Dex-treated sh-scr myotubes had 13% lower nascent protein synthesis than EtOH-treated sh-scr myotubes (Fig. 5*E*). In contrast, Dex-treated sh-p85α myotubes had 14% higher nascent protein synthesis than EtOH-treated sh-p85α myotubes (Fig. 5*E*). Notably, the protein synthesis rates in EtOH-treated sh-scr and sh-p85α myotubes were similar. Our data suggest that p85α mediates glucocorticoid-reduced protein synthesis.

Previous studies have shown that, in myotubes, glucocorticoids stimulate the expression of atrogenes such as FoxO1, FoxO3, atrogin-1 (a.k.a. MAFbx), and MuRF-1, which contribute to glucocorticoid-induced muscle atrophy (28, 29). We found that

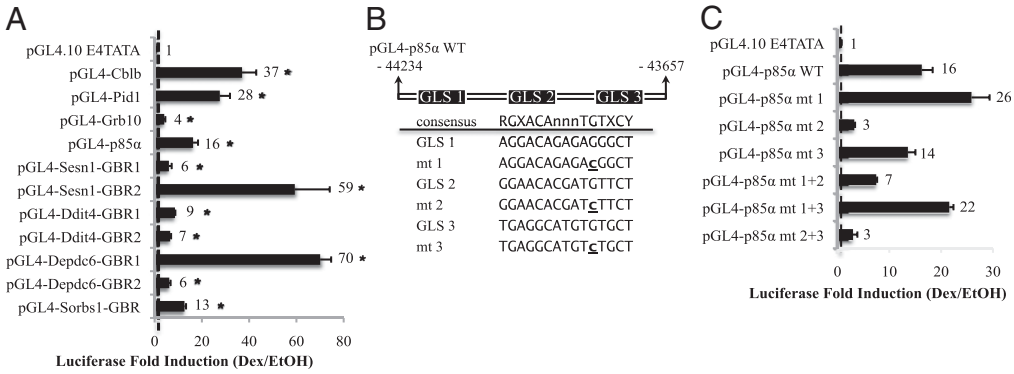

Fig. 3. Glucocorticoid response of GBR. (*A*) Reporter plasmids harboring different GBR were cotransfected with pcDNA3-hGR and pRL Renilla into C2C12 myoblasts ($n > 6$/group). Renilla luciferase expression was used to normalize for transfection efficiency. After 24 h of transfection, cells were treated with Dex or EtOH for 16–20 h and assayed for firefly and Renilla luciferase activities. Data show fold induction of normalized luciferase activity (Dex/EtOH-treated samples) from at least six experiments. $*P < 0.05$. The error bars represent the SE for the fold induction, and the dashed line marks a one-fold induction. (*B*) pGL4-p85α WT harbors nucleotide (nt) –44234 to –43657 of the *p85α* genomic region. On the basis of the consensus GRE shown, three GLS were identified. The locations of the GLS are the following: nt –44003 to –43989 (GLS-1), nt –43938 to –43924 (GLS-2), and nt –43913 to +43899 (GLS-3). Point mutation, indicated by underlining, is made in each GLS to generate a mutant (mt). Mt 1 has nt –43993 mutated from G to C; mt 2, nt –43928 from G to C; and mt 3, nt –43903 from G to C. (*C*) Reporter assay, as described in *A*, was carried with WT and mt *p85α* GBR plasmid. pGL4-p85α mt 1+2 represents a double mutant of GLS-1 and -2; pGL4-p85α mt 1+3, a double mutant of GLS-1 and -3; and pGL4-p85α mt 2+3, double mutant of GLS-2 and -3.

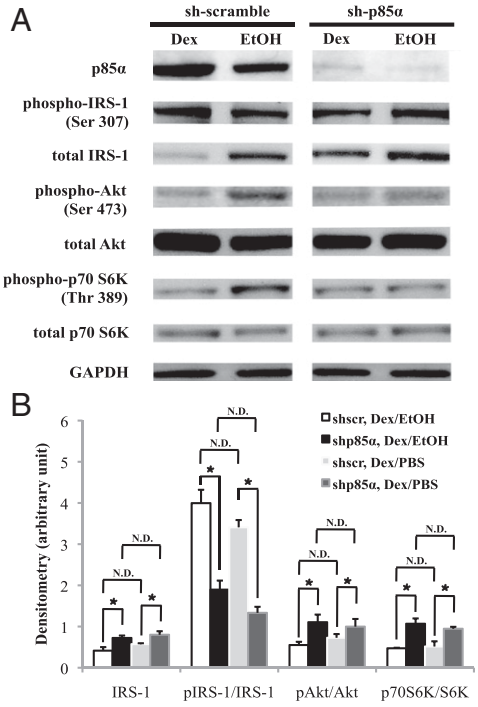

Fig. 4. Effect of p85α RNAi in glucocorticoid response. (*A*) Sh-p85α and sh-scr C2C12 myotubes treated with Dex or EtOH for 72 h. Immunoblots were used to detect the indicated proteins. (*B*) Quantification of the densitometry of total IRS-1 and the ratio of pSer307-IRS-1, pSer473-Akt, and pThr389-S6K bands to that of IRS-1, Akt, and p70S6K bands, respectively, with Dex/EtOH or Dex/PBS. Data were normalized to GAPDH optical density. These results were averaged from at least three immunoblots. $*P < 0.05$ and N.D. specifies "no difference." The error bars represent the SE for the fold induction and relative abundance.

72 h of Dex treatment induced FoxO3, atrogin-1, and MuRF-1 gene expression in sh-scr myotubes (Fig. 5*F*). However, this induction was diminished in sh-p85α myotubes (Fig. 5*F*). These results indicate that p85α is involved in glucocorticoid-induced FoxO3, atrogin-1, and MuRF-1 gene expression. Immunoblotting showed that Dex treatment up-regulated total FoxO1 and FoxO3 proteins, whereas the levels of phosphorylated-FoxO1 (pFoxO1) and FoxO3 (pFoxO3) were unchanged (Fig. 5*G*). Thus, the ratio of pFoxO1 to total FoxO1 and the ratio of pFoxO3 to total FoxO3 were reduced. However, these ratios were similar in sh-scr and sh-p85α myotubes.

Discussion

In this report, we present several findings. First, we identified potential GR primary target genes in C2C12 myotubes. Identification will facilitate future studies into the mechanisms underlying glucocorticoid actions in skeletal muscle physiology. Second, through ChIPseq, we localized genome-wide GBR in C2C12 myotubes, which is the first step in understanding the mechanisms governing GR-regulated gene transcription. Finally, we found eight potential GR primary targets that can modulate distinct steps in insulin/IGF1 signaling. Specifically, we have shown that p85α induction plays a key role in mediating glucocorticoid inhibition of the insulin/IGF1 response.

We previously identified GBR in another mouse cell type, 3T3-L1 adipocytes (30). The distribution of GBR in genomic regions is similar in adipocytes and myotubes. Whereas only 5% of GBR lie within 5 kb upstream of TSS, many are localized in introns greater than 25 kb upstream of TSS or greater than 25 kb downstream of stop codons. In motif analyses of GBR from glucocorticoid-activated genes, classical GRE sequences were highly represented. AP-1 and HNF3α, two binding motifs that have been shown to act with GR for maximal activation of transcription (31, 32), also scored highly. The binding site of HNF3α is similar to that of FoxO1 and FoxO3, which perform similar metabolic functions to GR in myotubes, as they promote proteolysis, reduce protein synthesis, and reduce glucose utilization (33). Therefore, GR and FoxO may act together to transcriptionally regulate genes involved in these physiological processes. The classical GRE sequence is also highly represented in GBR of genes repressed by glucocorticoids, but the mechanism is unclear. The AP-1 element, which mediates glucocorticoid repression (34), was highly represented in the GBR of glucocorticoid-repressed genes. Most motifs identified in GBR of glucocorticoid-regulated genes have not been linked to transcriptional repression by GR.

Gene ontology analysis recognized some GR primary targets involved in the regulation of apoptosis. In myotubes, glucocorticoids were shown to potentiate apoptosis (35). This analysis also identified gene groups involved in muscle organ development and cytoskeletal organization, suggesting that glucocorticoids may modulate mechanical properties of muscle, a concept that has not been extensively studied. Genes involved in blood vessel development were also highly represented. Many of these genes regulate angiogenesis, which plays an important role in modulating skeletal muscle health (36). The role of glucocorticoids in angiogenesis has been described (37), but the impact of this function on skeletal muscle is not entirely clear.

We focused on gene clusters that modulate insulin/IGF1 receptor tyrosine kinase signaling because glucocorticoids decrease insulin-stimulated glucose utilization and protein synthesis and increase proteolysis. In skeletal muscle, glucocorticoids affect multiple steps in the insulin/IGF1-signaling pathway. Therefore, it is conceivable that glucocorticoids induce a group of genes to mediate these effects. We focused on elucidating the role of p85α, the regulatory subunit of PI3K, in glucocorticoid-inhibited insulin signaling. Excess p85α can compete with PI3K (a heterodimer of p85α and the catalytic subunit of PI3K) to interact with IRS-1 (23, 38), resulting in a decrease in insulin response. In contrast, reducing the expression of p85α improves insulin sensitivity (39). Moreover, the induction of p85α gene expression by glucocorticoids and the functional interaction between GR and the p85α /PI3K pathway were previously described (40–42). We demonstrated that p85α is a GR primary target by identifying a GRE in the *p85α* GBR. We used RNAi to decrease p85α expression in C2C12 cells to analyze its role in glucocorticoid responses. The levels of pSer473-Akt and pThr389-S6K were a little lower in EtOH-treated sh-p85α cells compared with EtOH-treated sh-scr cells (Fig. 4*B*), suggesting that the reduction of p85α expression decreased the activity of Akt and p70S6K. However, previous studies indicated that Pik3r2, another regulatory subunit of PI3K, can compensate for p85α function in skeletal muscle-specific p85α knockout mice (43). In our sh-p85α myotubes, Pik3r2 and the remaining p85α should have been enough to support downstream activities. Therefore, the reduced suppressive effect of glucocorticoids was unlikely due to the lack of activity in insulin/IGF1 signaling.

Our results from p85α RNAi experiments raise several interesting points. First, p85α reduction limited the ability of Dex to decrease IRS-1 protein expression; however, IRS-1 gene expression was unchanged after 6 or 24 h of Dex treatment according to microarray analysis. Therefore, Dex likely reduced IRS-1 protein stability, but the mechanism of p85α in glucocorticoid-promoted IRS-1 degradation is unclear. Second, p85α reduction decreased Dex-induced phosphorylation of IRS-1 at serine 307. Several kinases, including IκB kinase β (IKKβ), p70S6K, c-Jun N-terminal kinases (JNK), and PKCθ, have been shown to phosphorylate IRS-1 at serine 307 (16). To our knowledge, there are no reports that glucocorticoids can increase IKKβ activity. Because glucocorticoids decrease p70S6K activity, p70S6K is unlikely to mediate this event. Interestingly, in obese and type 2 diabetic patients, p85α protein expression correlates with the activity of JNK, PKCθ, and pSer307-IRS-1 (44). Establishing the link between glucocorticoids, p85α, JNK, and PKCθ requires further study.

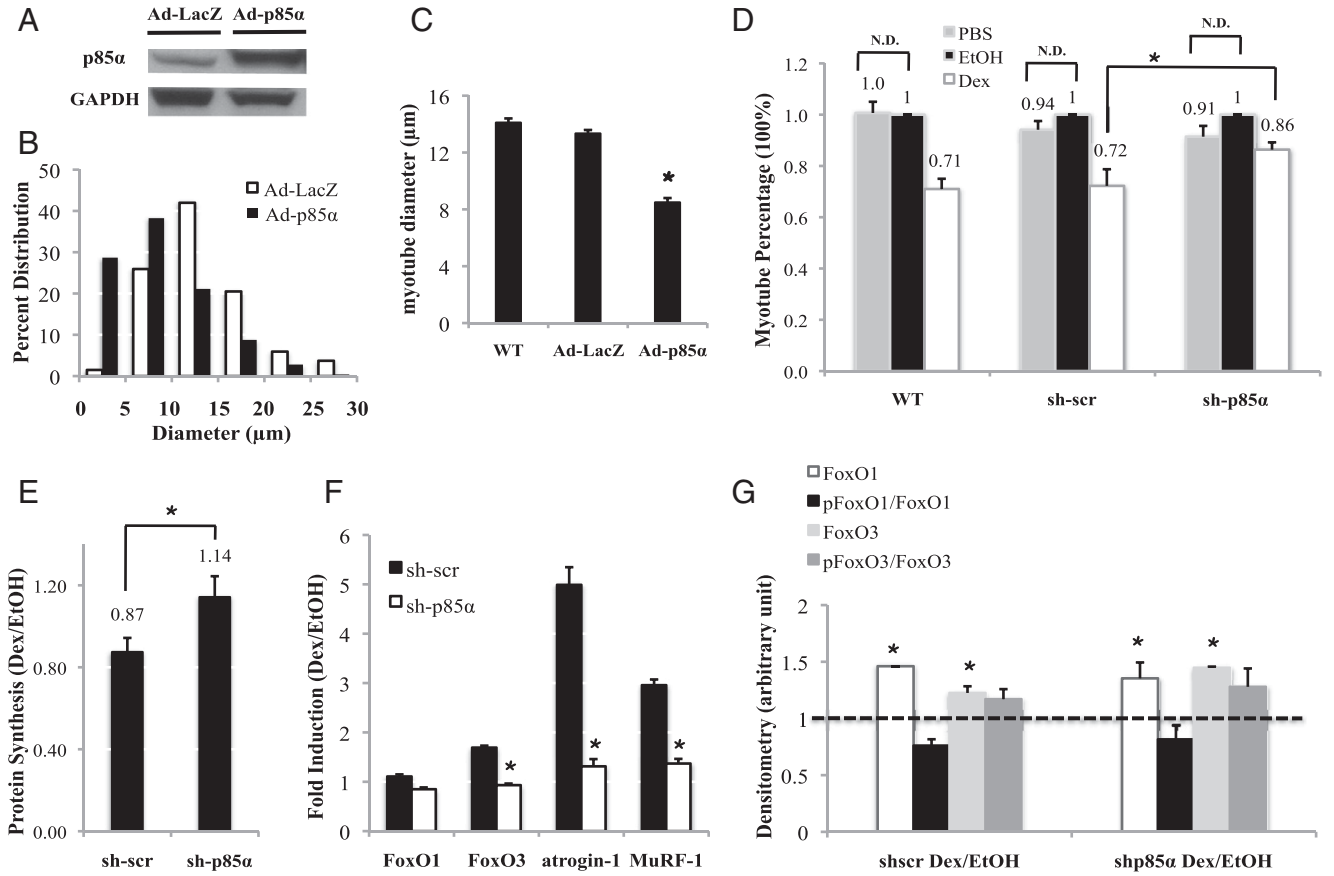

Fig. 5. Effect of p85α overexpression and knock-down on C2C12 myotube cell diameters. (*A*) Immunoblot was performed in Ad-LacZ and Ad-p85α myotubes to detect p85α protein levels. (*B*) The distribution of cell diameters in Ad-LacZ and Ad-p85α myotubes. (*C*) The average cell diameter of WT, Ad-LacZ, and Ad-p85α myotubes. (*D*) WT, sh-scr, and sh-p85α myotubes were treated with Dex, EtOH, or PBS for 72 h; EtOH-treated WT, sh-scr, and sh-p85α myotube diameters were set as 1 (100%) for Dex-treated or PBS-treated WT, sh-scr, and sh-p85α myotubes, respectively. N.D. specifies "no difference." (*E*) Protein synthesis level was measured for sh-scr and sh-p85α myotubes, with the EtOH-treated sh-scr and sh-p85α myotube protein synthesis level set as 1 for Dex-treated sh-scr and sh-p85α myotubes, respectively. (*F*) FoxO1, FoxO3, *atrogin-1*, and MuRF-1 gene expressions in sh-scr and sh-p85α myotubes. Rpl19 primer was the internal control. (*G*) Protein levels of phosphorylated and total FoxO1 and FoxO3 are shown for sh-scr and sh-p85α myotubes. (*C*–*G*) $*P < 0.05$. The error bars represent the SE for diameters. These results are averaged from at least three independent experiments.

Our studies have shown that p85α is involved in glucocorticoid-induced atrophy and glucocorticoid-inhibited protein synthesis in C2C12 myotubes. Dex treatment resulted in a 50% smaller reduction of myotube diameter in sh-p85α cells than in control cells. The remaining Dex-induced reduction of diameter in sh-p85α myotubes may be due to residual p85α. Alternatively, other GR-regulated genes might contribute to the Dex effect. Supporting this alternative, a study showed that reducing Ddit4 expression attenuates glucocorticoid-inhibited protein synthesis in L6 myotubes (15). This study suggests that additional genes, such as the remaining six GR primary targets, may also have a nonredundant effect and could mediate glucocorticoid-induced muscle atrophy by suppressing insulin/IGF1 signaling.

The ability of Dex to decrease cell diameters in sh-p85α myotubes may be due to Dex-induced protein degradation, as the inhibitory effect of Dex on protein synthesis was abolished in these cells. Glucocorticoids have been shown to increase the expression of MuRF-1 and atrogin-1, two ubiquitin E3 ligases implicated as causes of muscle atrophy (40). In mice lacking MuRF1, the ability of glucocorticoids to induce muscle atrophy is compromised (3). The previously identified *MuRF1* GRE (45) was not found in our ChIPseq; however, it is possible that our GR antibody did not recognize the conformation of GR while bound to the *MuRF1* GRE. FoxO1 is required for maximal glucocorticoid-activated *MuRF1* gene transcription. Although we did not find any GBR near or within the *atrogin-1* gene, its transcription is activated by FoxO1 and FoxO3 (11). In agreement with previous reports, we observed a reduced ratio of pFoxO1 to total FoxO1 upon Dex treatment (29). Also, we found a decreased ratio of pFoxO3 to total FoxO3. However, these ratios were similar between sh-scr and sh-p85α myotubes, despite the reduced ability of Dex to suppress Akt activity in the latter. Because Dex increased total FoxO1 and FoxO3 proteins, it added another layer of complexity for the calculation and comparison between their phosphorylation status in sh-scr and sh-p85α cells. The immunoblotting might not be sensitive enough to consistently detect the difference. Upon 72 h Dex treatment, FoxO3, MuRF-1, and atrogin-1 gene expressions were reduced in sh-p85α myotubes, but levels of total FoxO3 protein in sh-scr and sh-p85α myotubes were similar. A longer Dex treatment could be required to observe a change in FoxO3 protein level. Nonetheless, the fact that p85α is involved in Dex-activated atrogene expression suggests that it has a role in glucocorticoid-induced protein degradation.

In summary, we have identified GR-controlled transcriptional networks in myotubes and focused on one that can modulate insulin/IGF1 signaling. We highlighted the role of p85α in this crosstalk between glucocorticoid and insulin action. Future studies will test other GR primary targets to complete the picture of glucocorticoid-induced insulin resistance and muscle atrophy in skeletal muscle.

Materials and Methods

Cell Culture. The protocol for cell culture is shown in *SI Materials and Methods*.

Animals. The protocol is described in *SI Materials and Methods*. The Office of Laboratory Animal Care at the University of California, Berkeley (#R306-0111) approved all animal experiments reported in this article.

ChIPseq. The protocol of ChIP, the preparation of the genomic DNA library, the analyses of sequencing data, annotation of genes, motif research, and gene ontology analysis are described in *SI Materials and Methods*.

Microarray and Data Analysis. The protocols are presented in *SI Materials and Methods*. The microarray data are available at the Gene Expression Omnibus Web site (http://www.ncbi.nlm.nih.gov/geo/) under accession no. GSE28840.

RNA Isolation and Quantitative PCR. Protocols are described in *SI Materials and Methods*. Primer sequences are listed in Dataset S5.

Plasmids, Transfection, and Luciferase Reporter Assay. Protocols are described in *SI Materials and Methods*. Primer sequences are listed in Dataset S5.

Lentiviral Infection and Western Blot. The protocol is presented in *SI Materials and Methods*.

Muscle Atrophy Assay. The protocol is shown in *SI Materials and Methods*.

Protein Synthesis Assay. The protocol is described in *SI Materials and Methods*.

ACKNOWLEDGMENTS. This work is supported by National Institutes of Health Grant R01DK083591 and Muscular Dystrophy Association Grant 186068. T.K. is supported by a Dissertation Award Fellowship from the University of California Tobacco-Related Diseases Research Program.

1. Hu Z, Wang H, Lee IH, Du J, Mitch WE (2009) Endogenous glucocorticoids and impaired insulin signaling are both required to stimulate muscle wasting under pathophysiological conditions in mice. *J Clin Invest* 119:3059–3069.
2. Auclair D, Garrel DR, Chaouki Zerouala A, Ferland LH (1997) Activation of the ubiquitin pathway in rat skeletal muscle by catabolic doses of glucocorticoids. *Am J Physiol* 272:C1007–C1016.
3. Baehr LM, Furlow JD, Bodine SC (2011) Muscle sparing in muscle RING finger 1 null mice: Response to synthetic glucocorticoids. *J Physiol* 589:4759–4776.
4. Shimizu N, et al. (2011) Crosstalk between glucocorticoid receptor and nutritional sensor mTOR in skeletal muscle. *Cell Metab* 13(2):170–182.
5. Morgan SA, et al. (2009) 11beta-hydroxysteroid dehydrogenase type 1 regulates glucocorticoid-induced insulin resistance in skeletal muscle. *Diabetes* 58:2506–2515.
6. Dimitriadis G, et al. (1997) Effects of glucocorticoid excess on the sensitivity of glucose transport and metabolism to insulin in rat skeletal muscle. *Biochem J* 321:707–712.
7. Weinstein SP, Wilson CM, Pritsker A, Cushman SW (1998) Dexamethasone inhibits insulin-stimulated recruitment of GLUT4 to the cell surface in rat skeletal muscle. *Metabolism* 47(1):3–6.
8. Ohshima K, Shargill NS, Chan TM, Bray GA (1989) Effects of dexamethasone on glucose transport by skeletal muscles of obese (ob/ob) mice. *Int J Obes* 13(2):155–163.
9. Menconi M, Gonnella P, Petkova V, Lecker S, Hasselgren PO (2008) Dexamethasone and corticosterone induce similar, but not identical, muscle wasting responses in cultured L6 and C2C12 myotubes. *J Cell Biochem* 105:353–364.
10. Stitt TN, et al. (2004) The IGF-1/PI3K/Akt pathway prevents expression of muscle atrophy-induced ubiquitin ligases by inhibiting FOXO transcription factors. *Mol Cell* 14: 395–403.
11. Sandri M, et al. (2004) Foxo transcription factors induce the atrophy-related ubiquitin ligase atrogin-1 and cause skeletal muscle atrophy. *Cell* 117:399–412.
12. Gathercole LL, Bujalska IJ, Stewart PM, Tomlinson JW (2007) Glucocorticoid modulation of insulin signaling in human subcutaneous adipose tissue. *J Clin Endocrinol Metab* 92:4332–4339.
13. Schakman O, Gilson H, Thissen JP (2008) Mechanisms of glucocorticoid-induced myopathy. *J Endocrinol* 197(1):1–10.
14. Lee YH, White MF (2004) Insulin receptor substrate proteins and diabetes. *Arch Pharm Res* 27:361–370.
15. Wang H, Kubica N, Ellisen LW, Jefferson LS, Kimball SR (2006) Dexamethasone represses signaling through the mammalian target of rapamycin in muscle cells by enhancing expression of REDD1. *J Biol Chem* 281:39128–39134.
16. Gual P, Le Marchand-Brustel Y, Tanti JF (2005) Positive and negative regulation of insulin signaling through IRS-1 phosphorylation. *Biochimie* 87(1):99–109.
17. Song IH, Buttgereit F (2006) Non-genomic glucocorticoid effects to provide the basis for new drug developments. *Mol Cell Endocrinol* 246(1-2):142–146.
18. Nakao R, et al. (2009) Ubiquitin ligase Cbl-b is a negative regulator for insulin-like growth factor 1 signaling during muscle atrophy caused by unloading. *Mol Cell Biol* 29:4798–4811.
19. Wu WL, et al. (2011) Over-expression of NYGGF4 (PID1) inhibits glucose transport in skeletal myotubes by blocking the IRS1/PI3K/AKT insulin pathway. *Mol Genet Metab* 102:374–377.
20. Wick KR, et al. (2003) Grb10 inhibits insulin-stimulated insulin receptor substrate (IRS)-phosphatidylinositol 3-kinase/Akt signaling pathway by disrupting the association of IRS-1/IRS-2 with the insulin receptor. *J Biol Chem* 278:8460–8467.
21. Barbour LA, et al. (2005) Increased P85alpha is a potent negative regulator of skeletal muscle insulin signaling and induces in vivo insulin resistance associated with growth hormone excess. *J Biol Chem* 280:37489–37494.
22. Ueki K, et al. (2003) Positive and negative roles of p85 alpha and p85 beta regulatory subunits of phosphoinositide 3-kinase in insulin signaling. *J Biol Chem* 278:48453–48466.
23. Draznin B (2006) Molecular mechanisms of insulin resistance: Serine phosphorylation of insulin receptor substrate-1 and increased expression of p85alpha: the two sides of a coin. *Diabetes* 55:2392–2397.
24. Budanov AV, Karin M (2008) p53 target genes sestrin1 and sestrin2 connect genotoxic stress and mTOR signaling. *Cell* 134:451–460.
25. Peterson TR, et al. (2009) DEPTOR is an mTOR inhibitor frequently overexpressed in multiple myeloma cells and required for their survival. *Cell* 137:873–886.
26. Lesniewski LA, et al. (2007) Bone marrow-specific Cap gene deletion protects against high-fat diet-induced insulin resistance. *Nat Med* 13:455–462.
27. Luisi BF, et al. (1991) Crystallographic analysis of the interaction of the glucocorticoid receptor with DNA. *Nature* 352:497–505.
28. Bodine SC, et al. (2001) Identification of ubiquitin ligases required for skeletal muscle atrophy. *Science* 294:1704–1708.
29. Zhao W, et al. (2009) Dependence of dexamethasone-induced Akt/FOXO1 signaling, upregulation of MAFbx, and protein catabolism upon the glucocorticoid receptor. *Biochem Biophys Res Commun* 378:668–672.
30. Yu CY, et al. (2010) Genome-wide analysis of glucocorticoid receptor binding regions in adipocytes reveal gene network involved in triglyceride homeostasis. *PLoS ONE* 5: e15188.
31. Wang JC, Strömstedt PE, O'Brien RM, Granner DK (1996) Hepatic nuclear factor 3 is an accessory factor required for the stimulation of phosphoenolpyruvate carboxykinase gene transcription by glucocorticoids. *Mol Endocrinol* 10:794–800.
32. Miner JN, Yamamoto KR (1991) Regulatory crosstalk at composite response elements. *Trends Biochem Sci* 16:423–426.
33. Gross DN, van den Heuvel AP, Birnbaum MJ (2008) The role of FoxO in the regulation of metabolism. *Oncogene* 27:2320–2336.
34. De Bosscher K, Vanden Berghe W, Haegeman G (2003) The interplay between the glucocorticoid receptor and nuclear factor-kappaB or activator protein-1: Molecular mechanisms for gene repression. *Endocr Rev* 24:488–522.
35. Lee MC, Wee GR, Kim JH (2005) Apoptosis of skeletal muscle on steroid-induced myopathy in rats. *J Nutr* 135:1806S–1808S.
36. Hudlicka O, Brown M, Egginton S (1992) Angiogenesis in skeletal and cardiac muscle. *Physiol Rev* 72:369–417.
37. Logie JJ, et al. (2010) Glucocorticoid-mediated inhibition of angiogenic changes in human endothelial cells is not caused by reductions in cell proliferation or migration. *PLoS ONE* 5:e14476.
38. Barbour LA, et al. (2004) Human placental growth hormone increases expression of the p85 regulatory unit of phosphatidylinositol 3-kinase and triggers severe insulin resistance in skeletal muscle. *Endocrinology* 145:1144–1150.
39. Mauvais-Jarvis F, et al. (2002) Reduced expression of the murine p85alpha subunit of phosphoinositide 3-kinase improves insulin signaling and ameliorates diabetes. *J Clin Invest* 109(1):141–149.
40. Zheng B, Ohkawa S, Li H, Roberts-Wilson TK, Price SR (2010) FOXO3a mediates signaling crosstalk that coordinates ubiquitin and atrogin-1/MAFbx expression during glucocorticoid-induced skeletal muscle atrophy. *FASEB J* 24:2660–2669.
41. Fujita T, Fukuyama R, Enomoto H, Komori T (2004) Dexamethasone inhibits insulin-induced chondrogenesis of ATDC5 cells by preventing PI3K-Akt signaling and DNA binding of Runx2. *J Cell Biochem* 93:374–383.
42. Andrade MV, Hiragun T, Beaven MA (2004) Dexamethasone suppresses antigen-induced activation of phosphatidylinositol 3-kinase and downstream responses in mast cells. *J Immunol* 172:7254–7262.
43. Luo J, et al. (2006) Loss of class IA PI3K signaling in muscle leads to impaired muscle growth, insulin response, and hyperlipidemia. *Cell Metab* 3:355–366.
44. Bandyopadhyay GK, Yu JG, Ofrecio J, Olefsky JM (2005) Increased p85/55/50 expression and decreased phosphotidylinositol 3-kinase activity in insulin-resistant human skeletal muscle. *Diabetes* 54:2351–2359.
45. Waddell DS, et al. (2008) The glucocorticoid receptor and FOXO1 synergistically activate the skeletal muscle atrophy-associated MuRF1 gene. *Am J Physiol Endocrinol Metab* 295:E785–E797.

Chapter 2

Transcriptional Regulation of FoxO3 Gene by Glucocorticoids

Abstract

Glucocorticoids and FoxO3 exert similar metabolic effects in skeletal muscle. FoxO3 gene expression was increased by dexamethasone (Dex), a synthetic glucocorticoid, in mouse C2C12 myotubes and *gastrocnemius* muscle. In C2C12 myotubes the increased expression is due to, at least in part, the elevated rate of FoxO3 gene transcription. In the mouse FoxO3 gene we identified three glucocorticoid receptor (GR) binding regions (GBRs): one in upstream of the transcription start site, -17kbGBR; and two in introns, +45kbGBR and +71kbGBR Together, these three GBRs contain 4 glucocorticoid response elements (GREs). Micrococcal nuclease (MNase) assay showed that 30 min Dex treatment increased the sensitivity to MNase in the GRE of +45kbGBR, but not in +71kbGBR. Upon 60 min Dex treatment; however, the sensitivity to MNase was elevated in +71kbGBR, but not in +45kbGBR. Dex treatment for 30 and 60 min did not affect the chromatin structure of the -17kbGBR whose GRE was located in a linker region, whereas the GREs of +45kbGBR and +71kbGBR were located on nucleosomes. Dex treatment for 30 min also increased the levels of acetylated histone H3 and H4 in all three GBRs. Finally, using chromatin conformation capture assay, we showed that Dex treatment increased the interaction between the -17kbGBR and two genomic regions: one located around +500 bp and the other located around +73 kb. Overall, our results indicate that glucocorticoids activated FoxO3 gene transcription through multiple GREs. Each GRE was regulated by distinct mechanisms, and DNA looping is likely involved in this transcriptional activation process.

Introduction

Glucocorticoids play a critical role in the regulation of skeletal muscle physiology. Glucocorticoids inhibit glucose utilization and protein synthesis, and promote protein degradation in skeletal muscle. Inhibiting glucose utilization preserves plasma glucose, the primary energy source for brain, and promoting protein degradation and repressing protein synthesis produce free amino acids, which can be used as the substrates for hepatic gluconeogenesis. These effects are important metabolic adaptation for the survival of mammals during stress conditions, such as fasting and starvation. However, chronic or excess glucocorticoid treatment can cause severe metabolic disorders, such as muscle atrophy and insulin resistance in skeletal muscle (1-3).

Glucocorticoids perform their biological functions by binding to an intracellular receptor, the glucocorticoid receptor (GR). Upon binding to glucocorticoids, GR is recruited to genomic glucocorticoid response elements (GRE) to regulate the transcription of nearby genes. These primary target genes then trigger glucocorticoid-regulated physiological responses. Our previous chromatin immunoprecipitation sequencing (ChIPseq) experiments identified 4 GR binding regions (GBR) in or near the mouse FoxO3 gene (Kuo and Wang, manuscript in revision). The induction of FoxO3 mRNA and protein levels by glucocorticoids has been shown previously both *in vitro* and *in vivo* (4-6). The FoxO3 gene encodes a transcription factor that plays a vital role in skeletal muscle protein and glucose metabolism (7,8). First, the transcription factor inhibits glucose oxidation by activating the transcription of pyruvate dehydrogenase kinase 4 (PDK4) (9). Interestingly, glucocorticoids also induce PDK4 gene transcription (9). In the human PDK4 gene promoter, the binding of both FoxO3 and FoxO1, another member of the FoxO transcription factor family, are necessary for the maximum level of glucocorticoid-induced PDK4 transcription (9). Second, like glucocorticoids, the FoxO3 transcription factor stimulates the transcription of genes that activate protein degradation, such as MuRF1 and atrogin-1; and genes that suppress protein synthesis; such as Eif4ebp1 (10,11). Constitutively active FoxO3 has been shown to be sufficient to induce muscle atrophy, whereas dominant negative Foxo3 has been shown to prevent the muscle atrophy caused by either disuse or glucocorticoids (10,11). Furthermore, the dominant negative form of FoxO3 suppresses glucocorticoid-induced atrogin-1 gene expression (10,11). Overall, these results strongly suggest that glucocorticoid-regulated glucose and protein metabolism require the participation of FoxO3.

Because of the important role of FoxO3 in glucocorticoid action, we systematically examine the mechanisms of glucocorticoid-regulated FoxO3 gene expression in this report. With nuclear run-on assay, we examined whether the FoxO3 gene was transcriptionally regulated by glucocorticoids. We characterized the four GBRs in the FoxO3 gene identified by ChIPseq, and further identified 15-bp GREs that mediate the glucocorticoid response within these GBRs. The acetylation status of histone H3 and H4 surrounding these GBRs was checked. Moreover, we mapped the position of nucleosomes wrapped by these GBRs, and studied the effect of glucocorticoid treatment on their chromatin structures. Finally, we used chromatin conformation capture (3C) assay to test the potential interactions between GBRs and the genomic region near the transcription start site (TSS).

Results

Glucocorticoids increase the expression of FoxO3 gene in vitro and in vivo

C2C12 myotubes were treated with vehicle control ethanol (EtOH) or dexamethasone (Dex), a synthetic glucocorticoid, for 2, 6, 24 or 48h. Although 2h Dex treatment had no significant effect on FoxO3 gene expression (Fig. 1A), treatment for 6, 24, and 48 h markedly increased its expression (Fig. 1A). To study the glucocorticoid effect on FoxO3 gene expression in vivo, wild type (WT) mice were injected with control PBS or Dex (5 mg/kg/day body weight) for 4 days. FoxO3 gene expression was 2.5 fold higher in the gastrocnemius muscle from Dex-injected WT mice than that from PBS-treated ones (Fig. 1B). Next, we utilized transgenic mice overexpressing corticotropin-releasing hormone (CRH, CRH-Tg) to examine long-term glucocorticoid effects on FoxO3 gene expression. These transgenic mice have chronically elevated levels of CRH, which stimulates the secretion of adrenocorticotropin hormone (ACTH). ACTH further increases the secretion of corticosterone to circulation. We found that FoxO3 gene expression was about 1.8 fold higher in gastrocnemius muscles from CRH-Tg mice than those from WT ones (Fig. 1C). Overall, these experiments demonstrated that the expression of FoxO3 was induced by glucocorticoids both *in vitro* and *in vivo*.

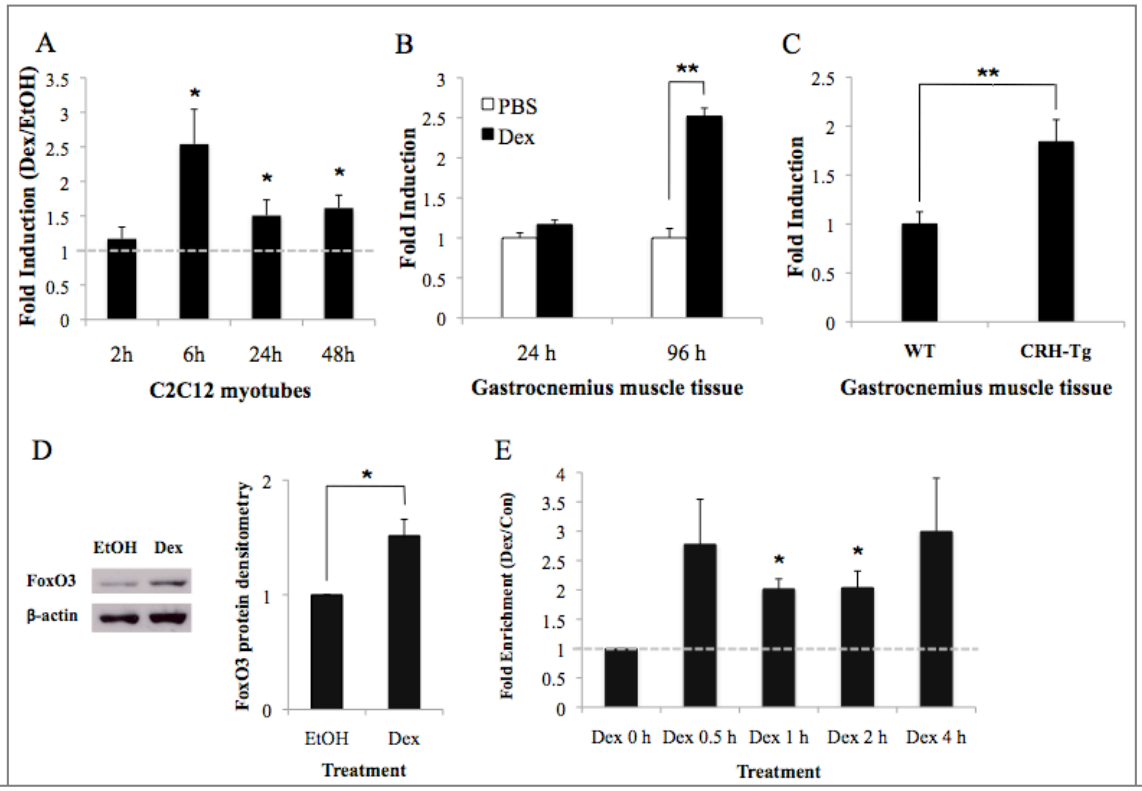

Fig. 1. Induction of FoxO3 gene expression by glucocorticoids *in vitro* and *in vivo*.
A) C2C12 myotubes were treated with 1 μM Dex or control EtOH for 2, 6, 24 or 48 h. B) C57BL/6 mice were injected with 5mg/kg/day of Dex or control PBS for 1 day (24 h) or 4 days (96 h). Their gastrocnemius muscles were isolated. C) Gastrocnemius muscles were collected from wild type and CRH-Tg mice. For A, B and C, primers specific to the FoxO3 and the Rpl19 (internal control) genes were used in qPCR. Fold induction was calculated by normalizing to Rpl19, and taking the ratio of Dex over EtOH. D) C2C12 myotubes were treated with 1 μM Dex or control EtOH for 24 h, and FoxO3 protein levels were measured. Densitometry result is from at least three independent immunoblottings. E) Nuclear run-on assay for monitoring FoxO3 in *in vitro* transcription. C2C12 myotubes were untreated or treated with 1 μM Dex for 0, 0.5, 1, 2 or 4 h. Primers specific to FoxO3 (across exon 1 and intron 1) and Rpl19 (internal control) were used in qPCR. For A, B, C, D, and E, Error bars indicate standard error. *$p < 0.05$, **$p < 0.01$.

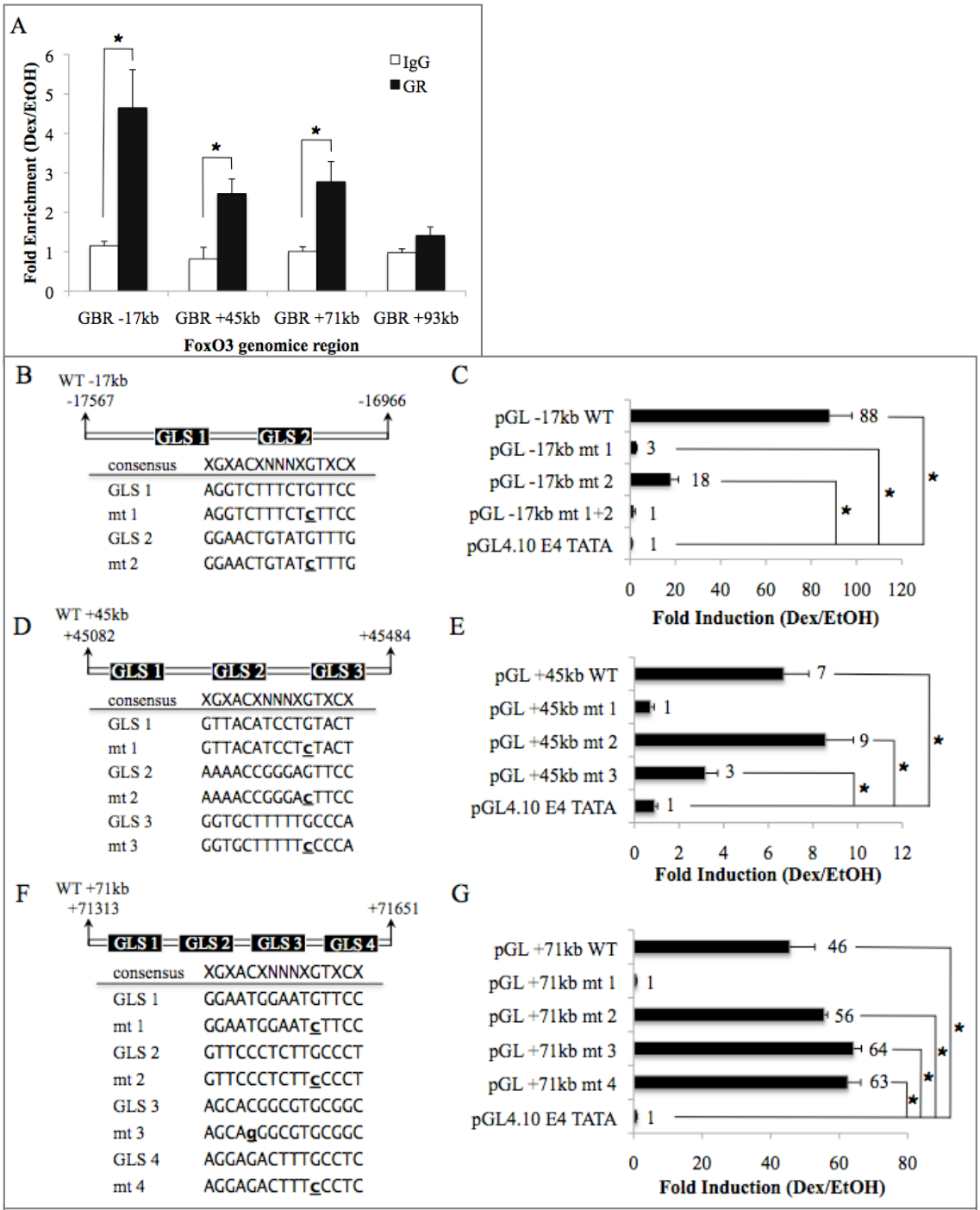

Fig. 2. The identification of the GREs in FoxO3 GBRs.
A) ChIP to confirm GR recruitment to GBRs identified from ChIPseq. C2C12 myotubes were treated with 1 μM Dex or control EtOH for 1 h. Primers flanking the -17kbGBR, the +45kbGBR, the +71kbGBR, the +93kbGBR and Rpl19 (internal control) were used in qPCR. Error bars represent the SEM of the fold enrichment from five independent experiments. For 2B, 2D and 2F, the location of each GBR, the sequence of consensus GRE, the sequence of GLSs, and each mutated nucleotide are shown. For 2C, 2E and 2G, reporter plasmids described in 2B, 2D and 2F were cotransfected with a human GR expression vector and a Renilla internal control plasmid in C2C12 myoblasts, and their luciferase activities are shown in 2C, 2E and 2G, respectively. B) The -17kbGBR genomic region. C) Reporter assay for Fig. 2B. D) The -45kbGBR genomic region. E) Reporter assay for Fig. 2D. F) The +71kbGBR genomic region. G) Reporter assay for Fig. 2F. Fold induction was calculated by taking the ratio of luciferase activity in Dex-treated samples over EtOH-treated ones. Error bar represents SEM. *$p < 0.001$, T test is calculated comparing each reporter plasmid to pGL4.10 E4TATA vector.

Next, we performed nuclear run-on assay to test the induction of FoxO3 gene in transcriptional level by glucocorticoids. Since transcriptional activation of the FoxO3 gene by Dex should occur prior to the observation of its mRNA increase, we chose time points earlier than 6h for the nuclear run-on assay. Fig. 1D shows that the FoxO3 transcription was induced by glucocorticoids at all time points we tested: 30 min, 1h, 2h and 4h. It indicates that the increased FoxO3 gene expression was due to, at least in part, the induction of its transcription, as early as 30 min after Dex treatment.

Identification of GBRs in the genomic region of FoxO3 gene

Previously, our ChIPseq identified 4 potential GBRs in or nearby FoxO3 gene genomic region. These include the genomic region between -17455 to -17126 (relative to the TSS, referred to as the -17kbGBR), between +45231 and +45317 (called the +45kbGBR), between +71380 and +71565 (called the +71kbGBR) and between +98640 and +98777 (called the +93kbGBR). The +45kbGBR and the +71kbGBR were located in introns, whereas the +93kbGBR was located in the 3' untranslated region. We conducted conventional ChIP to verify the recruitment of GR to these GBRs in C2C12 myotubes. We found that GR was recruited to the -17kbGBR, the +45kbGBR and the +71kbGBR, but not the +93kbGBR, upon 1h treatment of Dex (Fig. 2A). We individually inserted each GBR upstream of the TATA box in a luciferase reporter, pGL4.10-E4TATA and performed reporter assay. For C2C12 myoblasts transfected with reporters containing the -17kbGBR, the +45kbGBR or the +71kbGBR, Dex-treated cells gave a significantly higher luciferase activity than EtOH-treated ones (Fig. 2C, 2E, 2G). These results indicate that the -17kbGBR, the +45kbGBR and the +71kbGBR contain functional GREs that confer glucocorticoid responses.

Next, we searched for sequences resembling the consensus GRE identified from our ChIPseq (12), RGXACAnnnTGTXCY, in the -17kbGBR, the +45kbGBR and the +71kbGBR. We mutated position 11 of this consensus GRE from a G to a C residue, or position 5, from C to G (Fig. 2B, 2D, 2F). These residues have been previously shown to make direct contact with the GR. In the -17kbGBR, two GRE-like sequences (GLSs) were found (Fig. 2B). Mutation of GLS1 resulted in more than a 95% decrease in response to Dex, whereas mutation of GLS2 caused about 80% reduction of Dex response. Double mutation of GLS1 and 2 completely abolished its response to Dex (Fig. 2C). These results suggested that both GLS1 and 2 are required to confer a complete response to glucocorticoids in -17kbGBR, while GLS1 plays a more prominent role. In this regard, the sequence of GLS1, but not the sequence of GLS2, is highly conserved in human and rat FoxO3 gene (Table 1), further suggesting its important role in evolution.

For the +45kbGBR, three GLSs were located (Fig. 2D). Mutation of GLS2 had no effect on Dex response, whereas mutation of GLS3 gave a 57% decrease in response to Dex (Fig. 2E). Furthermore, mutation of GLS1 completely eliminated its response to Dex (Fig. 2E). These results indicated that GLS1 plays a primary role, and GLS3 plays an accessory role in mediating glucocorticoid response. Notably, the GLS1 sequence is also highly conserved in human and rat FoxO3 genes (Table 1).

For the +71kbGBR, four GLSs were found (Fig. 2F). Mutation of GLS2, 3 or 4 had no effect on the Dex response (Fig. 2G). However, mutation in GLS1 completely removed its response to

Dex (Fig. 2G). Therefore, GLS1 alone conferred a complete glucocorticoid response in the +71kbGBR, and its sequence is also conserved in human and rat FoxO3 genes (Table 1).

Glucocorticoids increase the level of acetylated histones in FoxO3 genomic region surrounding GBRs

Histone hyperacetylation is highly associated with transcription activation. We monitored the level of acetylated histone H3 and H4 (AcH3 and AcH4, respectively) and total H3 and H4 in genomic regions containing a GRE as well as regions located upstream or downstream from each GRE. When considering the level of histone acetylation, overall density of histone H3 and H4 should be taken into account. Therefore, the change in histone acetylation can be reflected more accurately by the ratios of AcH3/H3 and AcH4/H4. For the -17kbGBR, the +45kbGBR and the +71kbGBR, we found that Dex treatment did not induce hyperacetylation of H3 or H4 in the GRE regions (Fig. 3A, B, C). However, the level of AcH3/H3 and AcH4/H4 were markedly increased in the genomic regions upstream and downstream from the GRE in the -17kbGBR

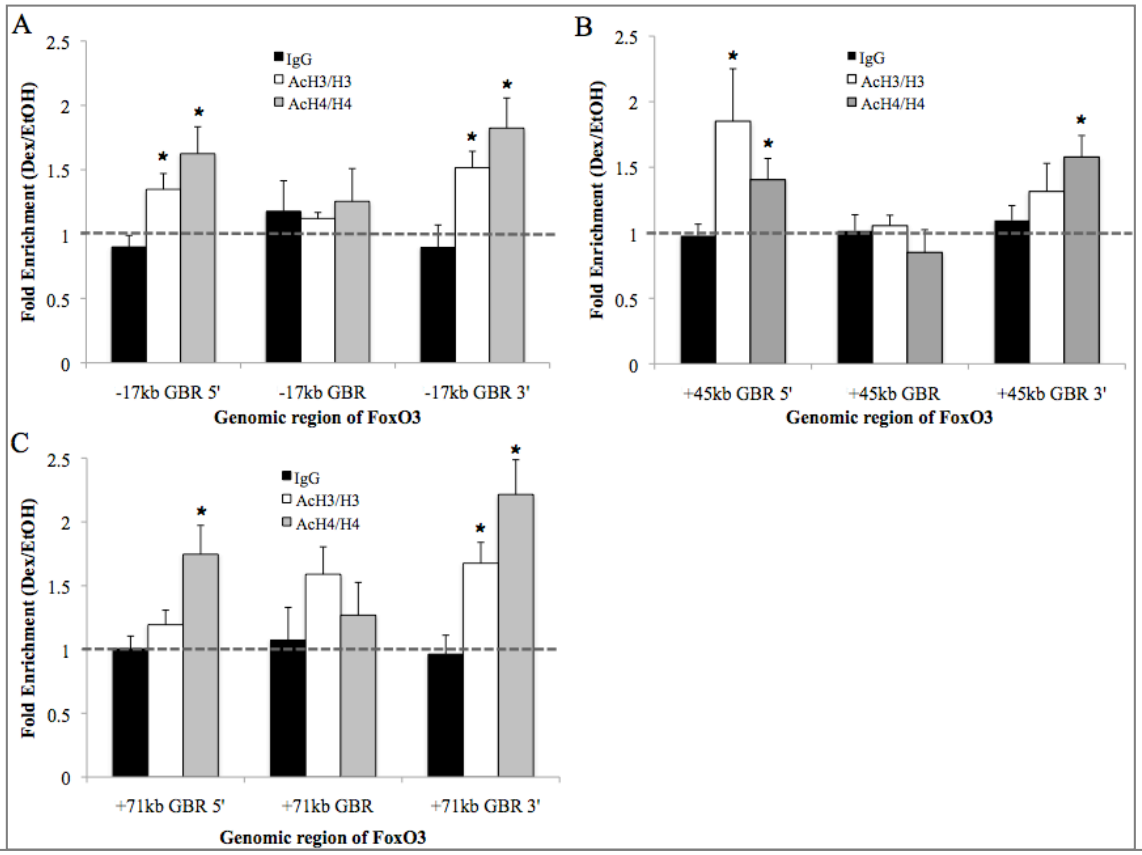

Fig. 3. Assessment of histone H3 and H4 acetylation near the GRE of the FoxO3 gene.
C2C12 myotubes were treated with 1 μM Dex or control EtOH for 30 min. ChIP was performed with antibodies recognizing total histone H3 (H3) and H4 (H4), and multiple acetylated lysines on histone H3 (AcH3) and H4 (AcH4). A) The -17kb GBR primer marks FoxO3 genomic region of -17308 to -17184; the -17kb GBR 5' primer, -17678 to -17570; and the -17kb GBR 3' primer, -16909 to -16786. B) The +45kb GBR primer defines FoxO3 genomic region of +45219 to +45302; the +45kb GBR 5' primer, +44853 to +44929, and the +45kb GBR 3' primer, +45631 to +45683. C) The +71kb GBR primer identifies FoxO3 genomic region of +71443 to +71555; the +71kb GBR 5' primer, +71290 to +71381; and the +71kb GBR 3' primer, +72129 to +72215. Error bars represent SEM of fold enrichment (Dex-treated samples divided by EtOH-treated samples and then further normalized by total histone levels) from at least three independent experiments. *$p < 0.05$.

(Fig. 3A). For the +45kbGBR, the level of AcH3/H3 and AcH4/H4 were increased in the genomic region upstream from its GRE, but only H4 was hyperacetylated in the region downstream from it (Fig. 3B). Finally, for the +71kbGBR, the level of AcH4/H4 was elevated in the genomic region upstream from its GRE, while both H3 and H4 were hyperacetylated in the region downstream from it (Fig. 3C). These results indicate that glucocorticoids increase the histone acetylation surrounding, but not within, each GRE. Furthermore, different patterns of H3 and H4 hyperacetylation in each GBR suggest that distinct set of histone acetylatransferases (HATs) could be involved in the regulation of histone acetylation in these 3 GBRs.

Glucocorticoid treatment differentially induce chromatin structural changes in GBRs

Treatment of glucocorticoids has been shown to disrupt nucleosome assembly or change the position of nucleosome in the genome. We used micrococcal nuclease (MNase) to map the position of nucleosomes surrounding the three FoxO3 GBRs.

For the -17kbGBR, three nucleosomes were detected: -17550 to -17400, -17400 to -17250, and -17200 to -17050. Dex treatment did not affect the position of these three nucleosomes, as their sensitivity to MNase was similar between EtOH-treated and Dex-treated cells. Interestingly, the major GRE (-17231 to -17217) in the -17kbGBR is located in a linker region between nucleosome 2 and 3 (Fig. 5A, 5B).

For the +45kbGBR, two nucleosomes were observed: +44850 to +45050 and +45250 to +45450. These nucleosomes appeared to cover more than 146 bp of DNA, probably due to the lack of overlapping primer sets in certain GC-rich regions. Nonetheless, the effect of glucocorticoids on these nucleosomes is apparent. Dex treatment for 30 min markedly increased the sensitivity to MNase of both nucleosomes (Fig. 4C). This increase of sensitivity, however, was not seen in cells treated with Dex for 60 min (Fig. 4D). Thus, the density of chromatin structure of these two nucleosomes in the +45kbGBR region was reduced upon 30 min Dex treatment, and it was transient.

For the +71kbGBR region, three nucleosomes were detected: +71300 to +71420, +71420 to +71560, and +71560 to +71700. Dex treatment for 30 min did not affect the position or sensitivity to MNase of these nucleosomes (Fig. 5E). However, 60 min treatment significantly increased the sensitivity to MNase of the 2nd nucleosome, where its nucleosome position is un-recognizable in the 60 min Dex-treated sample. This result strongly suggests total nucleosomal disruption in the region of +71420 to +71560. Interestingly, this region harbors the highly conserved +71kb GLS1 sequence.

Overall, these results show that glucocorticoids differentially modulate the chromatin structure of the three GBRs in the FoxO3 genomic region, suggesting that distinct mechanisms are adapted by these GBRs to participate in GR-activated FoxO3 gene transcription.

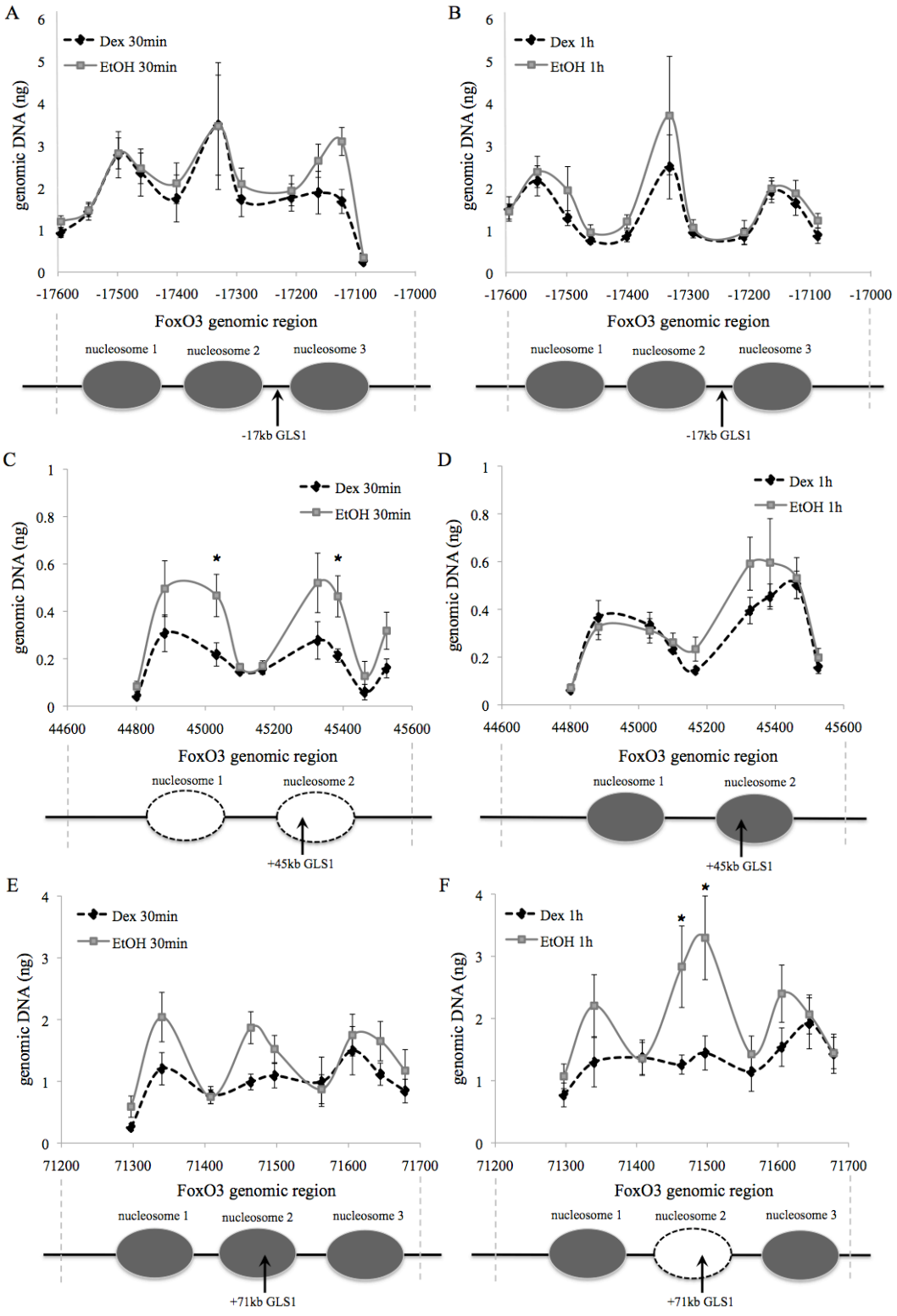

Fig. 4. Nucleosome mapping of the FoxO3 GBRs.
C2C12 myotubes were treated 1 μM Dex or control EtOH. Nucleosome positions were analyzed with MNase digestion, followed by qPCR with primers spanning FoxO3 GBRs. For 4A and 4B, nucleosome mappings between -17600 and -17100 of the FoxO3 gene are shown for 30 min and 1 h treatment, respectively. 11 primers were used to span this region. For 4C and 4D, nucleosome mappings between +44800 and +45600 of the FoxO3 gene are shown for 30 min and 1 h treatment, respectively. 9 primers were used to span this region. For 4E and 4F, nucleosome mappings between +71300 and +71700 of the FoxO3 gene are shown for 30 min and 1 h, respectively. 9 primers were used to span this region. For Fig. 4, the positions of nucleosomes are drawn. Error bars represent SEM of the genomic DNA amount from an average of at least five independent experiments. *$p < 0.05$.

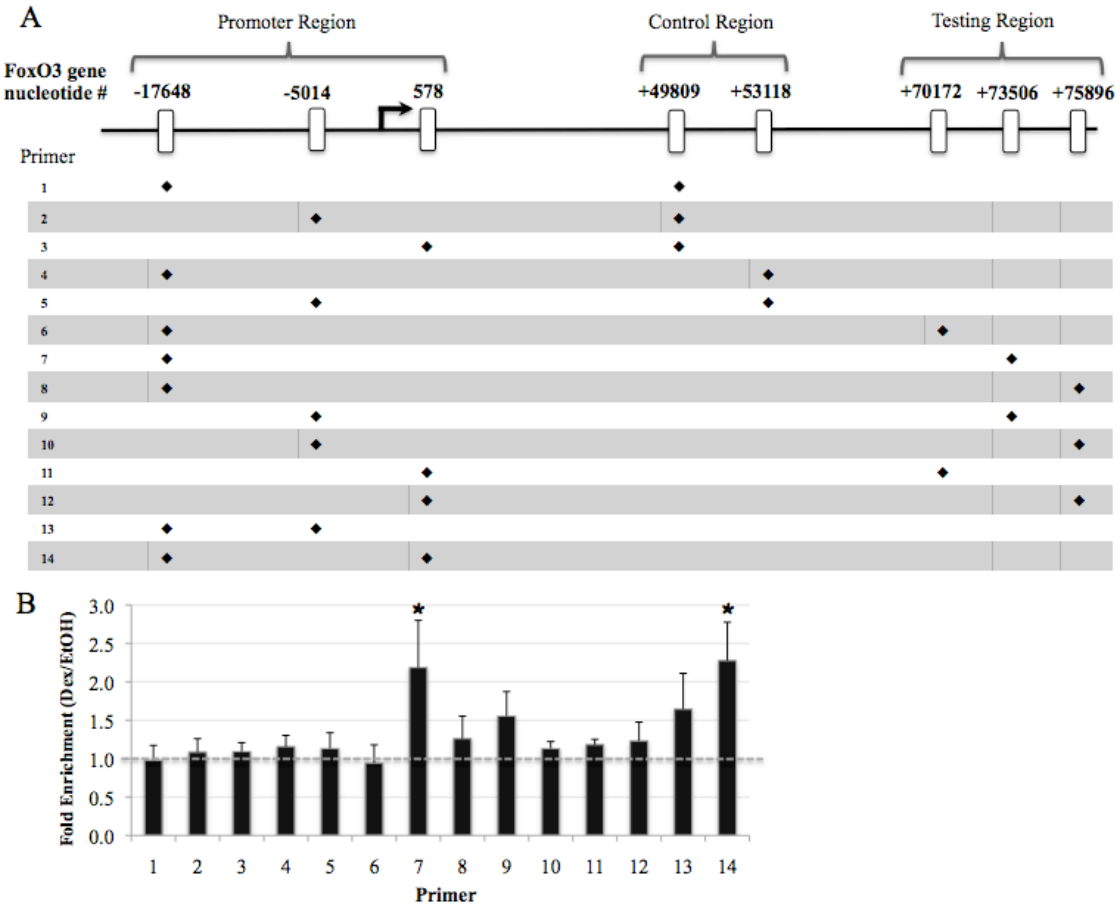

Fig. 5. Chromatin Conformation Capture (3C) identified potential physical interaction between genomic regions near GBRs and TSS of FoxO3 gene.
A) A schematic diagram of the position of Bgl II sites in the promoter region, the control region and the testing region of the FoxO3 gene. C2C12 myotubes were treated with 1 μM Dex or control EtOH. DNA was digested with Bgl II and re-ligated, and qPCR was used to detect the amount of ligation products obtained with each individual primer set pairing the promoter region (-17648, -5014, -578), the control region (+49809, +53118) and the testing region (+70172, +73506, +75896). The nucleotide positions represent the mid-point of each primer set. 14 primer sets showed a significant amount of PCR product. B) PCR amplification results of primer set 1-14. Error bars represent SEM of fold enrichment from seven independent experiments. A bacterial artificial clone (BAC, RP24-177H14), harboring the entire FoxO3 genomic region, was used as control for random chromatin interaction. The data shown all have higher amount of ligated products in Dex and EtOH-treated samples than in BAC control. $^{*}p < 0.05$.

The potential interactions between FoxO3 GBRs and TSS

All three FoxO3 GBRs are located far away from the TSS. Thus, to stimulate FoxO3 transcription, they may need to interact with the genomic region near the TSS. We performed chromatin conformation capture (3C) to examine the potential interaction between GBRs and TSS genomic regions. C2C12 myotubes were treated with control EtOH or Dex for 30 min or 60 min, cross-linked, followed by nuclei isolation. The samples were digested with restriction enzyme, Bgl II, and then diluted for intracellular re-ligation. With primers pairing between each GBR and TSS, qPCR was used to assess the fold induction of the ligated product comparing Dex-treated to EtOH-treated samples. We tested more than a hundred primer pairs, and most of them did not detect any PCR products. Nevertheless, we were able to find fourteen primer pairs that produce significant levels of PCR products (Fig. 5A). Interestingly, the level of ligated

product from two primer pairs was consistently increased by Dex treatment for 60 min (Fig. 5B), but levels were not increased by treatment for 30 min (data not shown). One product was between the primer pair from +73506 (the number represents the midpoint of the primer) and the -17648 region; the other was between -17648 and +578. Thus, Dex treatment induced DNA looping in a time-dependent manner, which resulted in an increased interaction between the 3' end of the +71kbGBR and the -17kbGBR, and between the -17kbGBR and the genomic region near TSS.

Discussion

Glucocorticoids and FoxO3 play similar roles in the regulation of protein and glucose metabolism in skeletal muscle. Therefore, the induction of FoxO3 gene expression by glucocorticoids has an important physiological implication. Here, we extensively studied the mechanism of glucocorticoid-activated FoxO3 gene expression. We first showed that glucocorticoids activated the transcription of the FoxO3 gene in C2C12 myotubes. We identified three GBRs in or near the FoxO3 gene, and the functional GREs within the GBRs. Interestingly, these three GBRs are far away from the TSS. Several lines of evidence suggest that they all play a role in glucocorticoid-activated FoxO3 gene transcription.

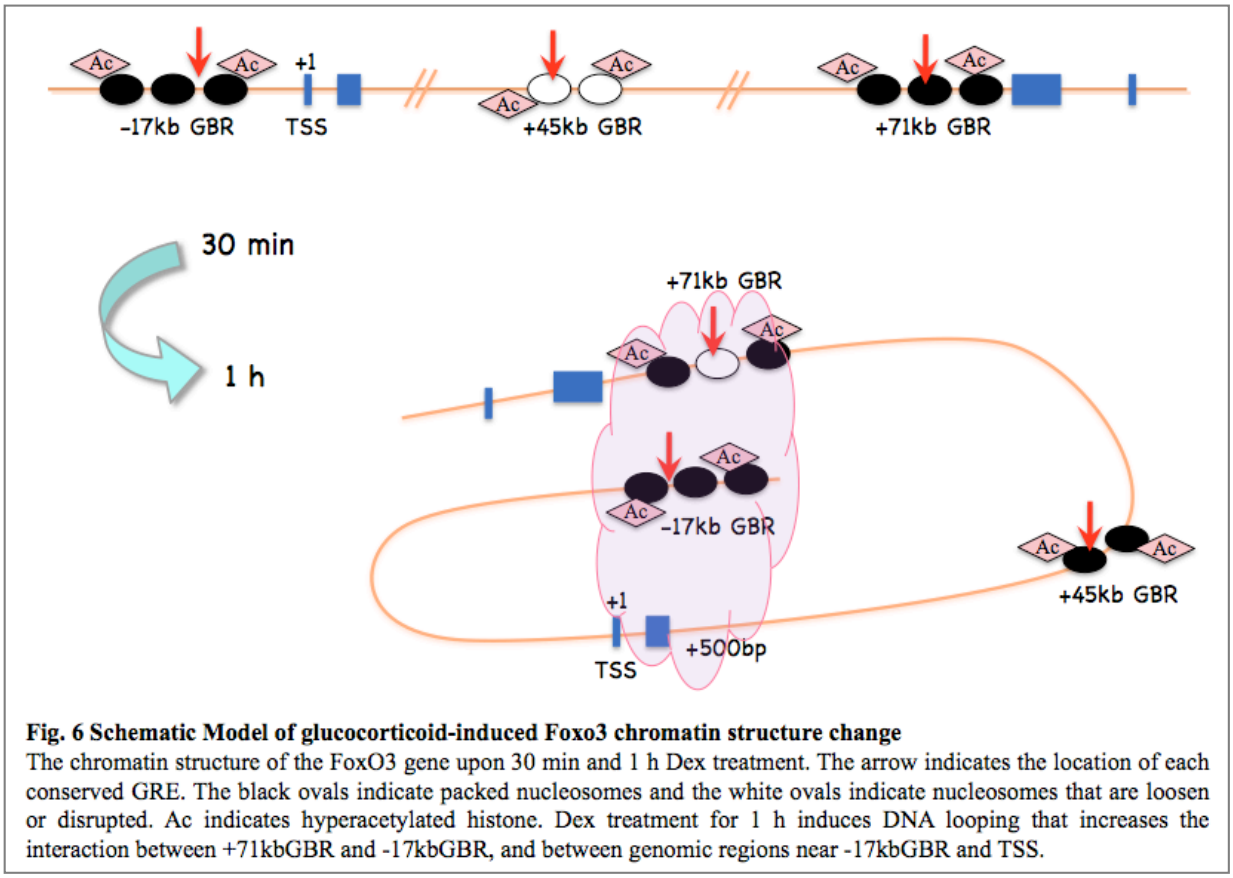

Fig. 6 Schematic Model of glucocorticoid-induced Foxo3 chromatin structure change
The chromatin structure of the FoxO3 gene upon 30 min and 1 h Dex treatment. The arrow indicates the location of each conserved GRE. The black ovals indicate packed nucleosomes and the white ovals indicate nucleosomes that are loosen or disrupted. Ac indicates hyperacetylated histone. Dex treatment for 1 h induces DNA looping that increases the interaction between +71kbGBR and -17kbGBR, and between genomic regions near -17kbGBR and TSS.

First, all three GBRs can confer a glucocorticoid response when individually inserted into a reporter gene. In these GBRs, a total of four GREs were identified. Intriguingly, the sequences of three out of the four GREs (one from each GBR) are highly conserved in human and rat FoxO3 genes (Table 1), suggesting that these three GRE sequences in humans and rats may also play a role in glucocorticoid-regulated FoxO3 gene transcription.

Second, we observed the change of chromatin structure surrounding two GBRs. An increase of sensitivity to MNase was observed in the nucleosome that contains the GRE in the +45kbGBR upon 30 min glucocorticoid treatment. At the same time point; however, there is no significant change in the chromatin structure of the +71kbGBR. Instead, its structure was disrupted upon 60

min glucocorticoid treatment. Furthermore, at the 30 min glucocorticoid treatment time point, while histone H4 was hyperacetylated both immediately upstream and downstream of both the +45kbGBR and the +71kbGBR, H3 is hyperacetylated only upstream of the +45kbGBR and only downstream of the +71kbGBR. These results indicate that these GBRs likely respond to glucocorticoid treatment with different mechanisms for participation in stimulating FoxO3 gene transcription. Previous studies have shown that the nucleotide sequence of a GRE plays a central role in modulating GR function (13,14), as distinct GRE sequences were shown to induce different conformational change of GR (15). This is likely to affect the ability of GR to associate with transcriptional coregulators. Furthermore, the genomic sequence surrounding a GRE might harbor binding sites for other transcription factors, as GR frequently acts with other factors to stimulate the transcription of genes (14,16). As the sequences of the GREs in the +45kbGBR and the +71kbGBR as well as their surrounding genomic sequences are different, it is not surprising that distinct mechanisms are employed in these two GBRs.

Table 1. The Conservation of GREs in FoxO3 GBRs

-17kbGBR1 GLS1 (-17217 to -17231)		
Mouse	(chr 10, 42013775-42013789)	GGAACAGAAAGACCT
Human	(chr 6, 108971185-108971199)	GGAACAGAAAGACCT
Rat	(chr 20, 426775094-426775108)	GGAACTGAATGCCCT
+45kbGBR GLS1 (+45252 to +45266)		
Mouse	(chr 10, 41951283-41951297)	AGTACAGGATGTAAC
Human	(chr 6, 109049036-109049050)	AGTACAGAATGTGCC
Rat	(chr 20, 42618757-42618771)	AGTACAGGACGTACC
+71kbGBR GLS1 (+71478 to +71492)		
Mouse	(chr 10, 41925057-41925071)	GGAACATTCCATTCC
Human	(chr 6, 109082126-109082140)	AGAACATTCCATTCC
Rat	(chr 20, 46192439-46192453)	GGAACATTCCATCC

* The genomic location of mouse GREs and its conserved counterparts in human and rat genome are shown.

To add another layer of complexity, the -17kbGBR appears to employ a totally different mechanism from those of the +45kbGBR and the +71kbGBR. The chromatin structure surrounding the -17kbGBR was not affected by either 30 or 60 min glucocorticoid treatment, and its GRE is located in the linker region between two nucleosomes. Thus, unlike the GREs in the +45kbGBR and the +71kbGBR, which are located within a nucleosome, the chromatin structure of the -17kbGBR probably does not need to change to expose GREs for more GR binding. Markedly, both histone H3 and H4 were hyperacetylated in genomic regions immediately upstream and downstream of the GRE upon glucocorticoid treatment. This hyperacetylation around the -17kbGBR may allow other transcription factors binding close to the GRE to act with GR to modulate FoxO3 gene transcription.

Third, in 3C experiments, we found that Dex treatment for 60 min potentially increases interactions between genomic regions near GBRs and TSS. These include the interaction between genomic regions around the +73 kb and the -17kbGBR, and between the -17kbGBR and the genomic region around +578 bps. Based on these results, we contemplate a model for FoxO3 genomic configuration upon GR activation (Fig. 6). In this model, the -17kbGBR is drawn to the +578 bp genomic region upon glucocorticoid treatment to interact with the TSS. The communication between the +71kbGBR and the -17kbGBR could reinforce the interface between the -17kbGBR and the TSS. If we consider these interactions in a three-dimensional

geometry, the +71kbGBR could also be close to the TSS through its communication with the -17kbGBR (Fig. 6). The interaction between genomic regions around +73kb and +578bp was not affected by glucocorticoid treatment, suggesting that the +71kbGBR and the TSS do not interact directly; the possibility of the -17kbGBR bringing the +71kbGBR closer to the TSS cannot be excluded.

It is important to note that we did not observe these interactions upon 30 min of Dex treatment. At this time point, Dex had already increased the transcription of the FoxO3 gene based on the nuclear run-on assay. We cannot exclude the possibility that DNA looping occurs within 30 min of Dex treatment. It is possible that we did not monitor the genomic regions that have an increase in interactions. This is somewhat limited by the restriction enzyme chosen for 3C experiments. However, it is also possible that DNA looping is not required for the stimulation of FoxO3 gene transcription by 30 min of Dex treatment. In some cases, although steroid receptor binding sites located far away from the TSS, DNA looping is not observed (17). We did not observe increased interaction between the +45kbGBR and the other genomic regions tested. However, this does not exclude the possibility of the +45kbGBR being drawn to the TSS upon glucocorticoid treatment at some other time points, and does not exclude the possibility that the genomic region close to +45kbGBR may interact with the genomic locations we did not test.

The induction of DNA looping by glucocorticoids has been shown in other examples (18,19). But the mechanism of glucocorticoid-induced DNA looping is not entirely clear. One DNA binding protein that can induce DNA looping is CTCF (20,21). Cohesin has been shown to act with CTCF to induce DNA looping (22,23). Based on CTCF ChIP sequencing results from the UCSC genome browser, there are multiple CTCF binding sites in the FoxO3 genomic region. However, the binding of CTCF to these sites is independent of glucocorticoid treatment. Glucocorticoid treatment must initiate processes that facilitate the looping. Some transcription cofactors may participate in a DNA looping event. It has been shown that Mediators form a complex with cohesin to participate in the induction of DNA looping (24). SWI/SNF chromatin remodeling complex has also been shown to induce chromatin looping (25). It is well established that GR can recruit Mediator (26,27) and SWI/SNF complexes (28,29). The role of these cofactors and Dex-induced DNA looping in the FoxO3 gene needs further study.

In summary, in this report we have shown that glucocorticoids employ a novel mechanism in regulating FoxO3 gene transcription, where three GBRs with a total of four GREs, are involved in the transcriptional activation process. These three GBRs are regulated by distinct mechanisms and layered interactions between GBRs and the TSS are likely employed. Further study of these transcriptional regulatory mechanisms is not only important in the understanding of glucocorticoid action in skeletal muscle, but will also provide a valuable model for elucidating the complex mechanisms of GR-regulated gene transcription.

Material and Method

Cell culture: Mouse C2C12 cells were purchased from the Cell and Tissue Culture Facility at the University of California, Berkeley. They were maintained in Dulbecco's modified Eagle's medium (DMEM; Mediatech) containing 10% fetal bovine serum (FBS; Tissue Culture Biologicals) and incubated at 37°C with 5% CO_2. Upon reaching 95~100 % confluence, C2C12 myoblasts were differentiated into myotubes with 2% horse serum (J.R. Scientific) in DMEM. The C2C12 cells were maintained in 2% horse serum-containing DMEM, changed every 2 days, until fully differentiated into myotubes, taking approximately 4-6 days. For all cell culture experiments, C2C12 myotubes were treated with 1 μM Dex or an equal volume (0.05% v/v of media) of vehicle control ethanol (EtOH).

Animals: Male 8-week-old C57BL/6 mice were purchased from Charles River. Mice were injected with 5 mg/kg Dex (Sigma) or PBS for 1 or 4 days. After the treatment, gastrocnemius muscles were isolated from mice. Transgenic mice overexpressing corticotropin-releasing hormone (CRH) were provided by Mary Stenzel-Poore (30). The Office of Laboratory Animal Care at the University of California, Berkeley (Approval number R306-0111) approved all animal experiments conducted in this paper.

Nuclear run-on: C2C12 myotubes were untreated or treated with 1 μM Dex for 30min, 1h, 2h or 4h. Cells were then washed once with PBS, and 3ml of lysis buffer (10 mM Tris-HCl pH 7.4, 3 mM $MgCl_2$, 10 mM NaCl, 150 mM sucrose and 0.5% NP40) was added to each plate, followed by incubation at 4°C for 10-15 min. Cell lysate was collected and spun at 170x g at 4°C for 5 min to pellet the nuclei. Nuclei were washed once with lysis buffer w/o NP40, and resuspended in freezing buffer (50 mM Tris-HCl at pH 8.3, 40% glycerol, 5 mM $MgCl_2$ and 0.1 mM EDTA). The total number of nuclei from each of the untreated and Dex-treated samples was counted, and $1x10^6$ nuclei were used for in vitro transcription. Two aliquots from each sample were used, one sample was incubated in 100 μl of 2x *in vitro* transcription buffer (200 mM KCl, 20 mM Tris-HCl pH 8.0, 5 mM $MgCl_2$, 4 mM dithiothreitol (DTT), 4 mM each of ATP, GTP and CTP, 200 mM sucrose and 20% glycerol) with 8 μl biotin-UTP (Roche, or equal amount from Epicentre), and the other sample was incubated in 100 μl 2x in vitro transcription buffer with 8 μl UTP (negative control) for 60 min at 30°C. Then, 6 μl of 250 mM CaCl2 and 6 μl of RNAse-free DNase (Roche) (10 U/ml) were added to stop the reactions. Total RNA was isolated using the Nucleospin RNA II kit (Macherey-Nagel).

Dyna beads M-280 (Invitrogen) were washed twice in solution A (0.1 mM NaOH, 0.5 M NaCl) for 5 min, once in solution B (0.1 M NaCl) for 5 min, and then resuspended in binding/wash buffer (10 mM Tris-HCl pH 7.5, 1 mM EDTA and 2 M NaCl) with 1 μl (40 units) RNasin per 100 μl of beads. Then, 50 μl of beads were added to total RNA isolated, incubated at 42°C for 30 min, followed by vigorous shaking on a shaker at room temperature for 3h. The beads were precipitated with magnets and centrifugation, and supernatant was discarded. The beads were then washed once for 15 min with 500 μl 15% formamide with 2x saline-sodium citrate (SSC) buffer, twice for 5 min with 1 ml 2x SSC buffer, then resuspended in 30 μl RNase- and DNase-free water. Finally, 10 μl of beads were used for each reverse transcription (RT) reaction prior to real-time PCR (qPCR). These primers were used in qPCR: mFOXO3_runon_F, ACT CCC GTC

TTT TCC TCT CC; mFOXO3_runon_R, GGA AGT GAT CTT GGC AGG TC; mRPL19_cDNA_F, ATG GAG CAC ATC CAC AAG C; and mRPL19_cDNA_R, TCC TTG GTC TTA GAC CTG CG.

RNA isolation and quantitative PCR: Total RNA was isolated from mouse gastrocnemius muscles using TRI Reagent® RT (Molecular Research Center, Inc.). To synthesize randomly primed cDNA, 0.5 μg of total RNA, 4 μl of 2.5 mM dNTP and 2 μl of 15 μM random primers (New England Biolabs) were mixed at a volume of 16 μl, and incubated at 70°C for 10 min. Then, a 4-μl cocktail containing 25 units of Moloney Murine Leukemia Virus (M-MuLV) Reverse Transcriptase (New England Biolabs), 10 units of RNasin (Promega) and 2 μl of 10x reaction buffer (New England Biolabs) was added, and samples were incubated at 42°C for 1h and then at 95°C for 5 min. The cDNA was diluted and used to perform real-time quantitative PCR (qPCR) using the EVA QPCR SuperMix Kit (Biochain), following manufacturer's protocol. qPCR was performed in either a 7900HT, 7500HT or StepOne PCR System (Applied Biosystems) and analyzed with the ΔΔ-Ct method, as supplied by the manufacturer (Applied Biosystems). *Rpl19* gene expression was used for internal normalization. Primer sequences are listed in Supplemental Material S1.

Plasmids, transfection, and luciferase reporter assay: pGL4.10-E4TATA reporter plasmid was generated by insertion of a 50-bp minimal *E4* TATA promoter sequence (Lin et al. 1988) into the *Bgl* II to *Hind* III sites of vector pGL4.10 to drive luciferase expression (Bolton et al. 2007). Each chosen GBR fragment, extending 100-150 bp upstream and downstream of the GBR, was amplified from genomic C2C12 DNA (primer sequences are listed in Supplemental Material S1), using the Expand Long Template PCR System (Roche Applied Science) and cloned into the pGL4.10-E4TATA vector with *Kpn* I/*Xho* I sites. The QuikChange Lightning mutagenesis kit (Stratagene) was used to make site-directed mutations per the manufacturer's instructions. Lipofectamine 2000 (Invitrogen) was used to transfect C2C12 myoblast according to the technical manual. Twenty-four hours post-transfection, cells were treated with either 1 μM Dex or control EtOH in differentiation media for 16-20 h. Cells were then harvested and their luciferase activities were measured with the Dual-Luciferase Reporter Assay kit (Promega) according to procedures in the technical manual.

Chromatin immunoprecipitation (ChIP): Fully differentiated C2C12 myotubes were treated with 1 μM Dex or control EtOH for 1h, cross-linked in 2% formaldehyde for 3 min at 37°C. The reactions were quenched with 0.125 M glycine. The cells were then washed with 1x PBS, and the cells were scraped and lysed in cell lysis buffer (50 mM HEPES-KOH at pH 7.4, 1 mM EDTA, 150 mM NaCl, 10% glycerol, 0.5% Triton X-100), supplemented with protease inhibitor cocktails (Calbiochem). The cell lysate was incubated for 1h at 4°C, and the crude nuclear extract was collected by centrifugation at 600xg for 5 min at 4°C. The nuclei were resuspended in 1 mL of ice-cold RIPA buffer (10 mM Tris-HCL at pH 8.0, 1 mM EDTA, 150 mM NaCl, 5% glycerol, 1% Triton X-100, 0.1% sodium deoxycholate, 0.1% SDS, supplemented with protease inhibitor). The chromatin was fragmented with a Branson Sonifier 250 sonicator (13 min total, 20 sec pulse at 35% power followed by 40 sec pause). To remove insoluble components, we centrifuged the samples at 13,000 rpm for 15 min at 4°C and recovered the supernatant. For GR ChIP, 1 μg of rabbit polyclonal anti-GR antibody (N499, provided by Keith R. Yamamoto laboratory, UCSF) was added to the supernatant to immunoprecipitate GR-bound chromatin at

4°C overnight. For histone modification ChIP, the following antibodies were used: anti-histone H3 (ab1791, abcam), anti-acetyl histone H3 (ab47915, abcam), anti-histone H4 (05-858, Millipore) and anti-acetyl histone H4 (06-866, Millipore). Normal rabbit IgG antibody (sc-2027, Santa Cruz Biotechnology) was used as negative control for all ChIP. The next day, 100 µl of 50% protein A/G (GR ChIP, Santa Cruz Biotechnology) or protein A (histone modification ChIP, Upstate) bead slurry, containing 100 µg/ml salmon sperm DNA, was added into each immunoprecipitation and nutated at 4°C for 2h. The beads were then washed twice with RIPA buffer, three times with RIPA buffer containing 500 mM NaCl, twice with LiCl buffer (20 mM Tris at pH 8.0, 1 mM EDTA, 250 mM LiCl, 0.5% NP-40, 0.5% sodiumdeoxycholate) and one time with RIPA buffer, all supplemented with protease inhibitor. After removing the remaining wash buffer, 75 µl of proteinase K solution (TE pH 8.0, 0.7% SDS, 200 µg/ml proteinase K) was added to each IP reaction, followed by incubation at 55°C for 3h and 65°C for overnight to reverse formaldehyde cross-linking. ChIP DNA fragments were purified with QIAquick PCR purification kit (Qiagen), eluting in 60 µl of Qiagen Elution Buffer.

Micrococcal nuclease (MNase) assay: C2C12 myotubes were treated with 1 µM Dex or an equal volume (0.05% v/v of media) of vehicle control ethanol (EtOH) for 30 min or 60 min. Cells were cross-linked with 1% formaldehyde for 3 min at 37°C, and the reaction was quenched by the addition of glycine to a final concentration of 0.125 M. Cells were then washed once with PBS and scraped in ice-cold MNase NP-40 lysis buffer (10 mM Tris pH 7.4, 10 mM NaCl, 3 mM MgCl2, 0.5% NP-40, 0.15 mM spermine, 0.5 mM spermidine). After shaking for 3-5h at 4°C in MNase lysis buffer, nuclei were collected by centrifugation and washed in ice-cold MNase digestion buffer w/o $CaCl_2$ (10 mM Tris at pH 7.4, 15 mM NaCl, 60 mM KCl, 0.15 mM spermine, 0.5 mM spermidine). Samples were then resuspended in ice-cold MNase digestion buffer with $CaCl_2$ (10 mM Tris at pH 7.4, 15 mM NaCl, 60 mM KCl, 0.15 mM spermine, 0.5 mM spermidine, 1 mM $CaCl_2$). Nuclei were treated with 1 unit of MNase (Nuclease micrococcal from Staphylococcus aureus, Sigma-Aldrich, N5386-200UN) for 60-90 min at 25°C. Reactions were stopped by the addition of 80 µl MNase digestion buffer with $CaCl_2$, 20 µl MNase stop buffer (100 mM EDTA, 10 mM EGTA), 75 µg Proteinase K, and 20 µl 10% SDS, and then cells were incubated at 65°C overnight. Samples were run on 1.5% agarose gel, and single nucleosome-wrapped DNA (about 150 bp) was purified with Qiagen gel extraction kit. The concentration of the samples was measured and diluted to 0.3 ng/µl for use in qPCR. The qPCR primers were designed to span approximately 500-bp regions, covering the identified GREs in each of the GBRs. When there were gaps between primers, the gaps were no more than 20 bps long. These primers are listed in Supplemental Material S1.

Chromatin conformation capture (3C): Two 15-cm plates of C2C12 myotubes were used: one treated with 1 µM Dex, the other with control EtOH for 1 h. After treatment, cells were fixed in 2% formaldehyde and incubated at 37°C for 3 min. Glycine was added to a final concentration of 0.125 M at room temperature for 5 min to quench the cross-linking. Cells were then washed with ice-cold PBS and resuspended in 5 ml of ice-cold PBS. The cells were transferred through a 40 µm nylon cell strainer (BD Falcon 352340) and centrifuged at 320 x g (100 rpm) at 4°C for 7 min. The pellet was then resuspended in 20 ml ice-cold lysis buffer (10 mM Tris-HCl at pH 8.0, 10 mM NaCl, 0.2% NP-40 and complete protease inhibitor) and rotated at 4°C for at least 1h. Samples were centrifuged at 15,000 to 18,000 rpm at room temperature for 5 min and resuspended in 2 ml of 1.1x Bgl II restriction enzyme buffer, 60 µl of 10% SDS (final

concentration 0.3%), 200 µl of 20% Triton X-100 (final concentration 1.8%) and shaken at 37^{o}C for 1h. Then, 1,600 units of Bgl II restriction enzyme were added to each sample and incubated at 37^{o}C overnight. The next day, 320 µl of 10% SDS (final concentration 1.3%) was added and incubated at 65^{o}C for 30 min, followed by the addition of 1.5 ml of 20 % Triton X-100 (final concentration 1%), 2.8 ml of 10x T4 DNA ligase buffer (NEB) and up to 28 ml of de-ionized water, followed by incubation at 37^{o}C for 1h. Then, 1 µl of T4 DNA ligase (400 u) was added to each sample, and samples were kept at 4^{o}C overnight. The next day, 60 µl of proteinase K (20 mg/ml, Fermentas) were added, and samples were incubated at 65^{o}C overnight. The next morning, 120 µl of RNase A (10 mg/ml, Fermentas) were added, followed by 45 min incubation at 37^{o}C. Four rounds of phenol/chloroform extraction were used to clear SDS, and aqueous phase was recovered. Then, DNA was precipitated with 0.1 volumes of 3 M sodium acetate at pH 4.8 and 2 volumes of 100% ethanol in -80^{o}C overnight. Followed by centrifugation at 4000 rpm at 4^{o}C for 60 min, the DNA pellets were washed with 70% ethanol and spun at 4000 rpm at 4^{o}C for 10 min. The DNA pellets were dissolved in 500 µl of TE buffer, pH 8.0. Forward and reverse primers for qPCR are designed to flank the junction of Bgl II restriction enzyme site, and paired according to Fig. 6. A list of primers is included in Supplemental material S1.

Acknowledgement

We thank Dr. Hei Sook Sul for the comments on the manuscript. This work is supported by the NIH (R01DK083591) and the Muscular Dystrophy Association (186068). T.K. is supported by the Dissertation Award Fellowship from the University of California Tobacco-Related Diseases Research Program.

References

1. Pivonello, R., De Leo, M., Vitale, P., Cozzolino, A., Simeoli, C., De Martino, M. C., Lombardi, G., and Colao, A. (2010) *Neuroendocrinology* **92 Suppl 1**, 77-81
2. Schakman, O., Gilson, H., and Thissen, J. P. (2008) *J Endocrinol* **197**, 1-10
3. Morgan, S. A., Sherlock, M., Gathercole, L. L., Lavery, G. G., Lenaghan, C., Bujalska, I. J., Laber, D., Yu, A., Convey, G., Mayers, R., Hegyi, K., Sethi, J. K., Stewart, P. M., Smith, D. M., and Tomlinson, J. W. (2009) *Diabetes* **58**, 2506-2515
4. Zheng, B., Ohkawa, S., Li, H., Roberts-Wilson, T. K., and Price, S. R. (2010) *Faseb J* **24**, 2660-2669
5. Nishimura, M., Mikura, M., Hirasaka, K., Okumura, Y., Nikawa, T., Kawano, Y., Nakayama, M., and Ikeda, M. (2008) *J Biochem* **144**, 717-724
6. Waddell, D. S., Baehr, L. M., van den Brandt, J., Johnsen, S. A., Reichardt, H. M., Furlow, J. D., and Bodine, S. C. (2008) *American journal of physiology. Endocrinology and metabolism* **295**, E785-797
7. Nakae, J., Oki, M., and Cao, Y. (2008) *FEBS Lett* **582**, 54-67
8. Gross, D. N., van den Heuvel, A. P., and Birnbaum, M. J. (2008) *Oncogene* **27**, 2320-2336
9. Kwon, H. S., Huang, B., Unterman, T. G., and Harris, R. A. (2004) *Diabetes* **53**, 899-910
10. Sandri, M., Sandri, C., Gilbert, A., Skurk, C., Calabria, E., Picard, A., Walsh, K., Schiaffino, S., Lecker, S. H., and Goldberg, A. L. (2004) *Cell* **117**, 399-412
11. Stitt, T. N., Drujan, D., Clarke, B. A., Panaro, F., Timofeyva, Y., Kline, W. O., Gonzalez, M., Yancopoulos, G. D., and Glass, D. J. (2004) *Mol Cell* **14**, 395-403
12. Yu, C. Y., Mayba, O., Lee, J. V., Tran, J., Harris, C., Speed, T. P., and Wang, J. C. (2010) *PloS one* **5**, e15188
13. Lefstin, J. A., and Yamamoto, K. R. (1998) *Nature* **392**, 885-888
14. Starr, D. B., Matsui, W., Thomas, J. R., and Yamamoto, K. R. (1996) *Genes Dev* **10**, 1271-1283
15. Meijsing, S. H., Pufall, M. A., So, A. Y., Bates, D. L., Chen, L., and Yamamoto, K. R. (2009) *Science* **324**, 407-410
16. Lucas, P. C., and Granner, D. K. (1992) *Annu Rev Biochem* **61**, 1131-1173
17. Magee, J. A., Chang, L. W., Stormo, G. D., and Milbrandt, J. (2006) *Endocrinology* **147**, 590-598
18. Hakim, O., John, S., Ling, J. Q., Biddie, S. C., Hoffman, A. R., and Hager, G. L. (2009) *J Biol Chem* **284**, 6048-6052

19. Hakim, O., Sung, M. H., Voss, T. C., Splinter, E., John, S., Sabo, P. J., Thurman, R. E., Stamatoyannopoulos, J. A., de Laat, W., and Hager, G. L. (2011) *Genome research* **21**, 697-706
20. Ling, J. Q., Li, T., Hu, J. F., Vu, T. H., Chen, H. L., Qiu, X. W., Cherry, A. M., and Hoffman, A. R. (2006) *Science* **312**, 269-272
21. Splinter, E., Heath, H., Kooren, J., Palstra, R. J., Klous, P., Grosveld, F., Galjart, N., and de Laat, W. (2006) *Genes Dev* **20**, 2349-2354
22. Degner, S. C., Verma-Gaur, J., Wong, T. P., Bossen, C., Iverson, G. M., Torkamani, A., Vettermann, C., Lin, Y. C., Ju, Z., Schulz, D., Murre, C. S., Birshtein, B. K., Schork, N. J., Schlissel, M. S., Riblet, R., Murre, C., and Feeney, A. J. (2011) *Proc Natl Acad Sci U S A* **108**, 9566-9571
23. Dorsett, D. (2011) *Curr Opin Genet Dev* **21**, 199-206
24. Kagey, M. H., Newman, J. J., Bilodeau, S., Zhan, Y., Orlando, D. A., van Berkum, N. L., Ebmeier, C. C., Goossens, J., Rahl, P. B., Levine, S. S., Taatjes, D. J., Dekker, J., and Young, R. A. (2010) *Nature* **467**, 430-435
25. Kim, S. I., Bresnick, E. H., and Bultman, S. J. (2009) *Nucleic Acids Res* **37**, 6019-6027
26. Chen, W., and Roeder, R. G. (2007) *Nucleic Acids Res* **35**, 6161-6169
27. Chen, W., Rogatsky, I., and Garabedian, M. J. (2006) *Mol Endocrinol* **20**, 560-572
28. John, S., Sabo, P. J., Johnson, T. A., Sung, M. H., Biddie, S. C., Lightman, S. L., Voss, T. C., Davis, S. R., Meltzer, P. S., Stamatoyannopoulos, J. A., and Hager, G. L. (2008) *Molecular cell* **29**, 611-624
29. Trotter, K. W., and Archer, T. K. (2007) *Mol Cell Endocrinol* **265-266**, 162-167
30. Stenzel-Poore, M. P., Cameron, V. A., Vaughan, J., Sawchenko, P. E., and Vale, W. (1992) *Endocrinology* **130**, 3378-3386

Chapter 2: Supplemental Material S1

Primer sequence

Gene expression

mRPL19_cDNA_F	ATGGAGCACATCCACAAGC
mRPL19_cDNA_R	TCCTTGGTCTTAGACCTGCG
mFOXO3_cDNA_F	TTCAACAGTACCGTGTTTGGAC
mFOXO3_cDNA_R	AGTGTGACACGGAAGAGAAGGT

Nuclear run-on

mRPL19_cDNA_F	ATGGAGCACATCCACAAGC
mRPL19_cDNA_R	TCCTTGGTCTTAGACCTGCG
mFOXO3_runon_F	ACTCCCGTCTTTTCCTCTCC
mFOXO3_runon_R	GGAAGTGATCTTGGCAGGTC

ChIP

mRPL19_cDNA_F	ATGGAGCACATCCACAAGC
mRPL19_cDNA_R	TCCTTGGTCTTAGACCTGCG
mFoxO3_ChIP_-17kbGBR5'_F	ACTGGAACCCAGGAAGTGTG
mFoxO3_ChIP_-17kbGBR5'_R	GAGGCCCTCTAGGTCAATCC
mFoxO3_ChIP_-17kbGBR_F	CTCCCCAACGCACTTGTACT
mFoxO3_ChIP_-17kbGBR_R	CCACTACCCAGGAAGCTCTG
mFoxO3_ChIP_-17kbGBR3'_F	GCATGTTCTGAAAGCTGCAA
mFoxO3_ChIP_-17kbGBR3'_R	ATCTTTGCAAAATGGCCAAC
mFoxO3_ChIP_+45kbGBR5'_F	CATGGGCAGCTTATTGCTTA
mFoxO3_ChIP_+45kbGBR5'_R	AGCTCTGTGGCTCTCCTCAC
mFoxO3_ChIP_+45kbGBR_F	AGCTTCCCAAGTGCTAATGG
mFoxO3_ChIP_+45kbGBR_R	GGGTTTATGAAATTGGAATGGA
mFoxO3_ChIP_+45kbGBR3'_F	CTAGGTGGCAACCTTTGACC
mFoxO3_ChIP_+45kbGBR3'_R	GAATGTGCTGGGATAAAGGAA
mFoxO3_ChIP_+71kbGBR5'_F	AGGCCTCACACTTCCCACT
mFoxO3_ChIP_+71kbGBR5'_R	AACCTGCTCTGTGGAGGAGA
mFoxO3_ChIP_+71kbGBR_F	ATTGGTTTTTCACCGAGCTG
mFoxO3_ChIP_+71kbGBR_R	CTGCCAGGGATCTGTGTGT
mFoxO3_ChIP_+71kbGBR3'_F	CTCACCTGCATTCATCTCCA
mFoxO3_ChIP_+71kbGBR3'_R	GGGTTAGGCTCTGACACTCG
mFoxO3_ChIP_+93kb_F	GAGGTAGGGCCAGGCTAGAG
mFoxO3_ChIP_+93kb_R	GACCCACAGCTGCCTTAGAC

Luciferase reporter

Luc_mFoxO3_-17kbGBR_KpnI_F	gctgcaggtaccTGGCTTGACCTGATGACATC
Luc_mFoxO3_-17kbGBR_XhoI_R	cgctctctcgagATGAATGACAAGCAGAAAGATG
Luc_mFoxO3_-17GBR_mtGLS1_sense	CTTCCTCAGAGGTCTTTCTcTTCCCTTCTGC
Luc_mFoxO3_-17GBR_mtGLS1_antisense	GCAGAAGGGAAgAGAAAGACCTCTGAGGAAG
Luc_mFoxO3_-17GBR_mtGLS2_sense	GAGCAATGTAATGGAAgTGTATGTTTGAGCCTTCC
Luc_mFoxO3_-17GBR_mtGLS2_antisense	GGAAGGCTCAAACATACAcTTCCATTACATTGCTC
Luc_mFoxO3_+45kbGBR_KpnI_F	gctgcaggtaccTGGCTTGACCTGATGACATC
Luc_mFoxO3_+45kbGBR_XhoI_R	cgctctctcgagATGAATGACAAGCAGAAAGATG
Luc_mFoxO3_+45kbGBR_mtGLS1_sense	gagtatataattggttacatcctCtactgcttagtcacc

Luc_mFoxO3_+45kbGBR_mtGLS1_antisense	ggtgactaagcagtaGaggatgtaaccaattatatactc
Luc_mFoxO3_+45kbGBR_mtGLS2_sense	gcctgaaaaaccgggaCttccagtgaggg
Luc_mFoxO3_+45kbGBR_mtGLS2_antisense	ccctcactggaaGtcccggtttttcaggc
Luc_mFoxO3_+45kbGBR_mtGLS3_sense	ctctgggtgctttttCcccatgagttgccttg
Luc_mFoxO3_+45kbGBR_mtGLS3_antisense	caaggcaactcatgggGaaaaagcacccagag
Luc_mFoxO3_+71kbGBR_KpnI_F	gctgcaGGTACCCTCATGAGAGAGGGAAACAATTTGA
Luc_mFoxO3_+71kbGBR_XhoI_F	cgctctCTCGAGCTCTGGAAGCATGTTCTACGTTGT
Luc_mFoxO3_+71kbGBR_mtGLS1_sense	ctggaaggaatggaatCttccctcttgccc
Luc_mFoxO3_+71kbGBR_mtGLS1_antisense	gggcaagagggaaGattccattccttccag
Luc_mFoxO3_+71kbGBR_mtGLS2_sense	ggaatgttccctcttCccctccaagagcag
Luc_mFoxO3_+71kbGBR_mtGLS2_antisense	ctgctcttggagggGaagagggaacattcc
Luc_mFoxO3_+71kbGBR_mtGLS3_sense	gaaagcccacagcaGggcgtgcggcagc
Luc_mFoxO3_+71kbGBR_mtGLS3_antisense	gctgccgcacgccCtgctgtgggctttc
Luc_mFoxO3_+71kbGBR_mtGLS4_sense	cactaaggagactttCcctccctgcgagg
Luc_mFoxO3_+71kbGBR_mtGLS4_antisense	cctcgcagggaggGaaagtctccttagtg

Mnase

The -17kbGBR

mFOXO3A/-17622/FO_1	T C T T G G C C T C T C C C T G T T A G
mFOXO3A/-17568/RE_1	G A G G C C C T C T A G G T C A A T C C
mFOXO3A/-17573/FO_2	G C C T C G A G T T G T G G G T A A A T
mFOXO3A/-17524/RE_2	G G T T C C C T C A G A T G A A C G A G
mFOXO3A/-17526/FO_3	A C C T T C A T G G C A T T G T G T G A
mFOXO3A/-17471/RE_3	C T T T C C A A T G G A C C A G G A T G
mFOXO3A/-17490/FO_4	A T C C T G G T C C A T T G G A A A G A
mFOXO3A/-17432/RE_4	C C T G A T G G G G A C A C T C A G A C
mFOXO3A/-17432/FO_5	G G C A G G T T A A G G G T C C T G T T
mFOXO3A/-17370/RE_5	C A G C T G C T T C T C A G C A A C T T C
mFOXO3A/-17363/FO_6	G C C A G T C A G C C A A C C A G
mFOXO3A/-17299/RE_6	G T T G G G G A G G G T G A C C T T A
mFOXO3A/-17318/FO_7	G T A A G G T C A C C C T C C C C A A C
mFOXO3A/-17266/RE_7	G C T C A A G A C A C C A A G A A A C C A
mFOXO3A/-17243/FO_8	G A G C C T T C C T C A G A G G T C T T T
mFOXO3A/-17173/RE_8	C C A C T A C C C A G G A A G C T C T G
mFOXO3A/-17192/FO_9	T G G G T A G T G G C C A A G A G G T A
mFOXO3A/-17134/RE_9	C T A G T G T C C G T C C T G G T A A G C
mFOXO3A/-17155/FO_10	A G G C T T A C C A G G A C G G A C A C
mFOXO3A/-17092/RE_10	C T G T G A C C C C C A G A A C A A C T
mFOXO3A/-17112/FO_11	AGT TGT TCT GGG GGT CAC AG
mFOXO3A/-17062/RE_11	GGA GAG AGC ACC ACA GTT GC

The +45kbGBR

mFOXO3/+44755/F_1	t a g g a g g c c a t c a a g g t g t t
mFOXO3/+44843/R_1	c a g c g g c t a c t g g c t a a g a g
mFOXO3/+44845/F_2	c a t g g g c a g c t t a t t g c t t a
mFOXO3/+44920/R_2	a g c t c t g t g g c t c t c c t c a c
mFOXO3/+44952/F_3	t t g a t g c a g c c t c a t g g a t a
mFOXO3/+45113/R_3	g c a g a g t c c t g a g g g t g a g a
mFOXO3/+45072/F_4	g c a g a a a g a t g a a a a t g c c t g t
mFOXO3/+45129/R_4	t c c t t t t g g a g g t g a a a a t a t g a

mFOXO3/+45118/F_5	c c t c c a a a a g g a a t a t t g a g g a
mFOXO3/+45215/R_5	a a a c c c a a t t t c a c a a g a a c a
mFOXO3/+45294/F_6	c a t t a g c a c t t g g g a a g c t g
mFOXO3/+45358/R_6	c a c t g g a a c t c c c g g t t t t
mFOXO3/+45346/F_7	g g a g t t c c a g t g a g g g a g a g
mFOXO3/+45423/R_7	a a c t c a t g g g c a a a a a g c a c
mFOXO3/+45433/F_8	g c t c c c t g c t g t t t t g a g t c
mFOXO3/+45492/R_8	g a a g t c c t t g g c t t g a c c t g
mFOXO3/+45484/F_9	a a g g a c t t c c t t g c t c a t t c a
mFOXO3/+45568/R_9	c t g g a t g c t g c c t t g a g a a t
The +71kbGBR	
mFOXO3A/71271/FO_1	GCT GTG GTC TAA CCT GCT CTG
mFOXO3A/71323/RE_1	GCC ACA GGT ACC CAG TTC AC
mFOXO3A/71310/FO_2	c t g g g t a c c t g t g g c t g t t t
mFOXO3A/71370/RE_2	c t c a c a c t t c c c a c t c c a c a
mFOXO3A/71377/FO_3	g g a g c a g g g g a g g a a g a g
mFOXO3A/71439/RE_3	g c a g c c t c g c a c c t c t g
mFOXO3A/71435/FO_4	c t g c c a g g g a t c t g t g t g t
mFOXO3A/71493/RE_4	g g a a c a t t c c a t t c c t t c c a
mFOXO3A/71472/FO_5	g c t g g a a g g a a t g g a a t g t t
mFOXO3A/71522/RE_5	a g c t g c t t c t g c t c t t g g a g
mFOXO3A/71530/FO_6	g c t c g g t g a a a a a c c a a t g t
mFOXO3A/71595/RE_6	g g g c t t t c t a g c g t g g a c t t
mFOXO3A/71580/FO_7	c a c g c t a g a a a g c c c a c a g
mFOXO3A/71631/RE_7	g t g g a g g c a g c c a g c a t
mFOXO3A/71648/FO_8	c t c c c t g c g a g g a t t g t c t
mFOXO3A/71710/RE_8	c c c t c g c c t g t c t t a g g t a g
mFOXO3A/71617/FO_9	CTG GCT GCC TCC ACA CTA AG
mFOXO3A/71672/RE_9	GGC CGA GGA GAC AAT CCT
3C	
3C_mFoxO3_-17648_F	CCC CAT GAG AAA CAC TGG AAC CCA
3C_mFoxO3_-17648_R	CAAGAGGGCCTGGCTCAGTGG
3C_mFoxO3_-5014_F	TGG ACA GGA GGC CTG ACA GAG TG
3C_mFoxO3_-5014_R	GCCAGCGTTTTAAAGAAAAGAGGTTTACCTG
3C_mFoxO3_+578_F	CCT GGA AGG GGG CGG AGG
3C_mFoxO3_+578_R	AGAGAGAGGGCCGACCCCG
3C_mFoxO3_+49809_F	CCC ATG AAC AGC AGT GGA GAC CTG
3C_mFoxO3_+49809_R	ACTGCTGGGTTCGTGGGGAGC
3C_mFoxO3_+53118_F	CCC AGC AAC CAC ATG GTG GCT C
3C_mFoxO3_+53118_R	GTCTTCAGACACACCAGAAGAGGC
3C_mFoxO3_+70172_F	G C G C C A A G G T T T G T T A C T T G
3C_mFoxO3_+70172_R	G G A G A T A G C A C A T G C T G A C G
3C_mFoxO3_+73506_F	C G C C C T C T C A C C T T T T G A
3C_mFoxO3_+73506_R	C T G T G A T G G G G A C C T C A A C T
3C_mFoxO3_+75896_F	G G G C T G T G C T G T T T C A T A T C T
3C_mFoxO3_+75896_R	G A C A G A T C C C A A G C T T C T G C

Chapter 3

Transcriptional Regulation of Angiopoietin-like 4 (Angptl4) gene by Glucocorticoids and Insulin

Abstract

Glucocorticoids are important regulators of lipid homeostasis; however, chronically elevated glucocorticoid levels can induce hypertriglyceridemia and hepatic steatosis. The occupied glucocorticoid receptor (GR) functions as a transcription factor, although genes regulated by GR and involved in lipid metabolism are not fully understood. Angiopoietin-like 4 (ANGPTL4) is a secreted protein inhibiting extracellular lipoprotein lipase. It is synthesized and secreted during fasting and under elevated glucocorticoid level conditions to promote adipocyte intracellular lipolysis. Here, I show that dexamethasone (a synthetic glucocorticoid) treatment increased *Angptl4* mRNA levels in mouse primary hepatocytes and rat H4IIE hepatoma cells, and elevated the transcriptional rate of *Angptl4* in H4IIE cells. Using bioinformatics and chromatin immunoprecipitation (ChIP), a glucocorticoid receptor (GR) binding site was identified within the rat *Angptl4* gene. I further confirmed that this glucocorticoid response element (GRE) with mutagenesis and reporter assay. Dex treatment also increased histone H4 acetylation and DNase I accessibility around the GRE genomic regions. In *Angptl4-/-* total knockout mice, glucocorticoid-induced hypertriglyceridemia and hepatic steatosis were significantly reduced; suggesting glucocorticoid-promoted flux of triglyceride from white adipose tissue to liver requires Angptl4. Notably, hypertriglyceridemia is frequently associated with insulin resistance. I found that insulin suppressed Dex-induced Angptl4 gene expression in mouse primary hepatocytes and H4IIE cells. Using compounds inhibiting distinct molecules in the insulin signlaling pathway, PI3K, Akt, and GSK-3 are involved in the suppression effect of insulin. Moreover, mutating a *FOX* transcription factor binding site, located ~40 base pair downstream from the *Angptl4 GRE*, compromised glucocorticoid-induced luciferase activity. In addition to GR, both FoxO1 and FoxA2 proteins are recruited to the *Angptl4* GR binding region in ChIP assay. When treating the cells with insulin, GR recruitment was abolished. Finally, reducing FoxO1 expression by RNA interference in H4IIE cells decreased Dex-induced Angptl4 gene expression, mimicking the insulin response. These data suggest that FoxO1 is involved in insulin suppression of glucocorticoid-induced Angptl4 gene expression. In summary, my study established that 1) *Angptl4* is a direct GR target and participates in glucocorticoid-regulated triglyceride metabolism 2) the transcription of Angptl4 is under the control of both insulin and glucocorticoids, where insulin can suppress glucocorticoid-induced Angptl4.

Introduction

Angiopoietin-like 4 (Angptl4, also called as Fasting-induced adipose factor, FIAF) encodes a secreted protein that inhibits lipoprotein lipase (LPL) activity (1-3). LPL hydrolyzes triglycerides in lipoproteins, including those found in chylomicrons and very low-density lipoproteins (VLDL), into two free fatty acids and one monoacylglycerol. Angptl4-induced adipose tissue lipolysis is also observed in several studies (1-4). The importance of Angptl4 in the regulation of lipid homeostasis is highlighted by several genetic and physiological studies (2, 5). First, mice lacking Angptl4 gene (*Angptl4*$^{-/-}$) are hypolipidemic and have lower plasma free fatty acid levels than those of wild type mice (6, 7). When fed with high-fat diet, *Angptl4*$^{-/-}$ become obese faster than wild type mice (6). Second, mice overexpressing Angptl4 gene in distinct tissues develop different lipid disorders. Overexpression of Angptl4 gene in muscle and fat increases plasma triglyceride (TG) levels and displays a mild insulin resistance symptom (8). Adenoviral-mediated overexpression of *Angptl4* in liver also causes hyperlipidemia and fatty liver. Surprisingly, these mice also showed an improved glucose tolerance (9). Third, injecting *Angptl4* recombinant proteins rapidly increase plasma TG and free fatty acids (FFA) levels (5, 10). Finally, population-based sequencing of Angptl4 gene uncovered genetic variations that may contribute to a reduced level of plasma triglyceride (TG) (11). Overall, these data suggest that modulation of Angptl4 gene expression can result in a significant effect on lipid homeostasis.

As the name suggested, Angptl4 (a.k.a. FIAF) gene expression is induced during fasting (12). Interestingly, Angptl4 gene transcription is activated by peroxisome proliferatior-activated receptor alpha and gamma (PPAR**α** and PPAR**γ**) in hepatocytes and adipocytes, respectively (13, 14). PPAR**α** has been shown to play an important role in metabolic adaptation to fasting in liver by increasing the expression of genes involved in various pathways of lipid metabolism (15). The induction of Angptl4 gene expression during fasting; however, is not affected in mice lacking PPAR**α** (13). It suggests that other signaling pathways regulate the expression of Angptl4 gene in fasting state. Our previous gene expression analysis found that Angptl4 gene is induced by glucocorticoids, whose circulating levels are increased during fasting, in A549 human lung epithelial cells (16). But the regulation of Angptl4 gene by glucocorticoids in metabolic tissues, such as liver and fat, has not been explored. Several lines of evidence further support the potential connection between glucocorticoids and Angptl4 in metabolic tissues. Excess glucocorticoids have been implicated in the development of metabolic syndrome, a constellation of metabolic risk factors that include insulin resistance and abnormal lipid metabolism, such as hyperlipidemia, fatty liver and increased plasma FFA levels (17-19). A recent report showed that treating A^{y}/a;LDLR$^{-/-}$ mice with an inhibitor of 11b-hydroxysteroid dehydrogenase type I, which encodes an enzyme that can convert intracellular inactive glucocorticoids to active hormones and highly expressed in adipocytes and hepatocytes, resulted in an increased plasma TG clearance and a decreased liver TG synthesis (20). Notably, mice lacking Angptl4 gene displayed these two phenotypes (6, 21). Likely, Angptl4 gene expression is regulated by glucocorticoids in metabolic tissues, which in turn contributes to both physiological and pathophysiological responses of glucocorticoids. In this chapter, I present the data for the regulation of Angptl4 gene by glucocorticoid in rat H4IIE hepatoma cells.

The role of endogenous glucocorticoids is to increase glucose level in plasma for survival. To increase circulating glucose, glucocorticoids increase hepatic glucose production through gluconeogenesis (22), decrease peripheral glucose uptake into muscle and adipose tissues (23, 24), increase substrates for gluconeogenesis by breaking down muscle and adipose tissues (25, 26), and inhibit insulin release from pancreatic beta cells (27, 28). Chronic endogenous or exogenous glucocorticoid exposure can lead to increased insulin secretion to compensate for the excess glucose. This compensation ultimately can result in severe insulin resistance and metabolic dysfunction. Notably. Insulin resistance is highly associated with hyperlipidemia and an elevated adipocyte lipolysis (29), two physiological functions exerted by Angptl4. This raised a question whether Angptl4 gene expression is regulated by insulin. Indeed, the repression of Angptl4 gene expression by insulin is reported in adipocytes (30). The crosstalk between glucocorticoids and insulin has long been an important area of research, as glucocorticoids and insulin have opposite physiological effects. One of the joins between these two pathways is the forkhead family of transcription factors, such as FoxO1. Glucocorticoids have been shown to upregulate FoxO1 protein (31), and insulin can inhibit the activity of FoxO1 (32). Insulin activates Akt/PKB which phosphorylates FoxO1 on serines 256 and 319 and threonine 29, leading to the nuclear exclusion of FoxO1 (33-35). In this Chapter of my thesis, I will show that Angptl4 is a direct target of GR, and FoxO1 is required for glucocorticoid-induced Angptl4 expression.

Result

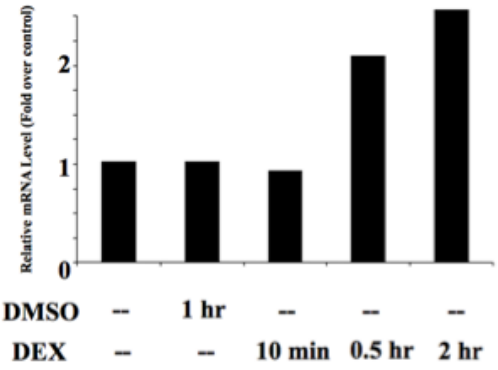

Fig. 1. Dex treatment increases the rate of *Angptl4* gene transcription in H4IIE cells. H4IIE cells were untreated, treated with DMSO for 120 min, or with Dex (0.5 μM) for 10, 30, or 120 min as shown. Nuclei from these cells were used for in vitro transcription with biotin UTP. Newly synthesized RNA was isolated on streptavidin beads. cDNA was then synthesized and qPCR performed to monitor for changes in transcription rates using primers specific to Angptl4 and β-actin (control). Shown is the fold-induction in transcription of DEX-treated samples (DEX/untreated) from one of two independent experiments showing similar results.

Glucocorticoids Increase the Rate of Rat Angptl4 Transcription

We investigated whether the elevation of Angptl4 mRNA by glucocorticoid treatment is due to an increase in the rate of *Angptl4* transcription in H4IIE cells by using nuclear run-on assays. Cells were treated with dexamethasone (Dex), a synthetic glucocorticoid, for 10 min, 0.5 h, or 2 h. Control cells were either untreated or treated with DMSO alone for 2 h. Afterward, nuclear extracts were prepared from these cells, and *in vitro* transcription was performed by adding biotin-UTP. Newly synthesized RNA was then isolated on streptavidin beads. After randomly primed cDNA was synthesized, qPCR was performed to detect changes in transcription rates using *Angptl4* specific primers. No effect was seen after 10 min of Dex treatment (Fig. 1). However, both treatments of 0.5 h and 2 h markedly increased the rate of *Angptl4* transcription (Fig. 1). These results demonstrate that glucocorticoids can regulate *Angptl4* at the transcriptional level.

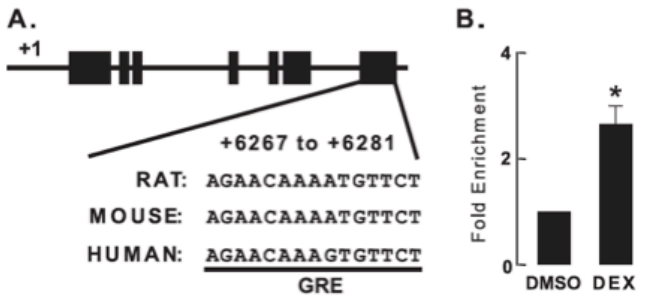

Fig. 2. Identification of an *Angptl4 GRE*.

A) schematic diagram of rat Angptl4, including the location of the predicted GR binding site. Black boxes represent exons, and lines connecting them represent introns. The predicted GR binding site sequences (AGAACATTTTGTTCT) and their conserved counterparts in human and mouse genome are shown.
B) ChIP experiments confirming the recruitment of GR to its predicted binding site. H4IIE cells were treated with either DMSO or DEX (0.5 M) for 30 min, after which they were harvested for ChIP as described ("Experimental Procedures"). Shown is the fold-enrichment of GR binding by DEX treatment (DEX/DMSO) from three independent experiments (* $p < 0.05$). The error bars represent the S. E. for the fold enrichment.

Identification of a Rat Angptl4 GRE

To investigate whether transcription of *Angptl4* is directly regulated by the GR, we sought to identify GR binding sites within the *Angptl4* genomic sequence. We applied a bioinformatic approach (BioProspector motif), with which we identified specific sequences within 64 kb of rat *Angptl4* (which extended 32 kb upstream and downstream of the transcriptional start site) that were highly similar (width of the first motif block was set at 14) to 79 previously identified GR binding sites (36). Because many important transcriptional regulatory regions within genes are conserved between multiple species, we next employed a BLAST search of the

University of California Santa Cruz genome browser to filter and isolate sequences conserved across the rat, mouse, and human genomes. This comparison yielded a single species-conserved palindromic sequence (AGAACATTTTGTTCT) located at the 3' untranslated region of *Angptl4* between 6267 and 6281 bp downstream of the transcriptional start site (Fig. 2A). We used chromatin immunoprecipitation (ChIP) assay to investigate GR recruitment to this putative GR binding site in H4IIE cells. Cells were treated for 1 h with Dex and then harvested for ChIP. Using a control IgG antibody for ChIP, the number of genomic DNA fragments precipitated in the predicted GR binding site was similar between control DMSO and Dex-treated samples. By contrast, using a GR-specific antibody for ChIP, Dex treatment resulted in a ~2.3-fold enrichment of genomic DNA fragments precipitated from the predicted GR binding site (Fig. 2B). This finding indicates that GR occupancy of this palindromic sequence occurs in a Dex-dependent manner, suggesting that this sequence may be a functional GRE.

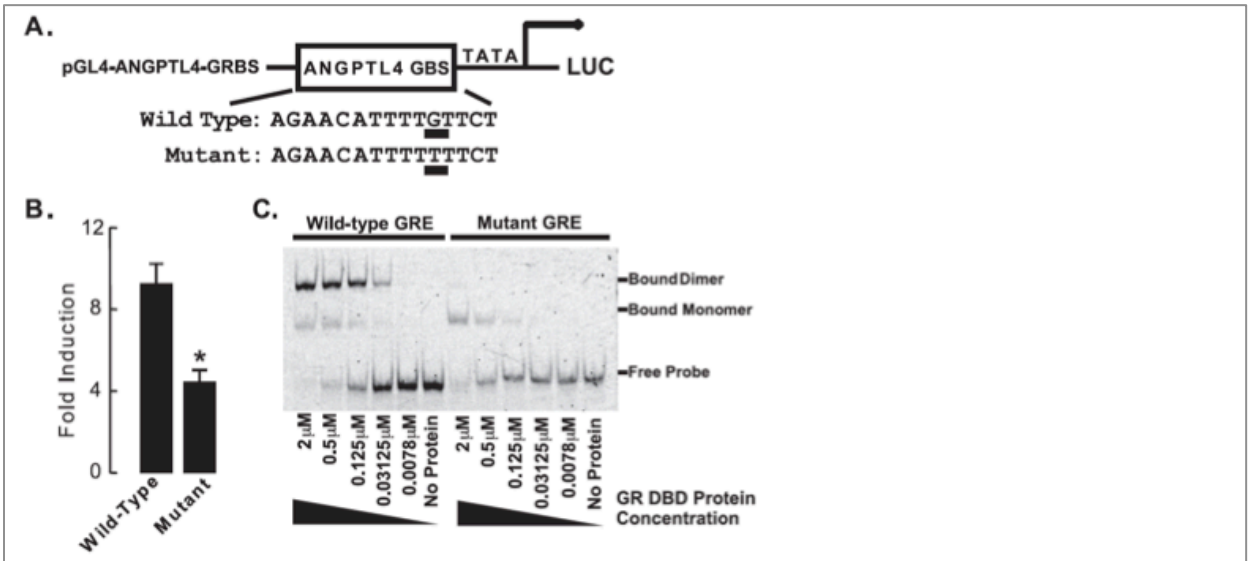

Fig. 3. The GR binding region of Angptl4 confers glucocorticoid responsiveness. A) a sequence containing either the wild-type or a mutated *Angptl4* GR binding site was inserted into the pGL4-TATA reporter to create pGL4-ANGPTL4-GRBS (mutation from Gly to Thr underlined). B) glucocorticoid responsiveness of GR binding sites in rat Angptl4. Reporter plasmids and wild-type or mutant pGL4-ANGPTL4-GRBS (75 ng) were cotransfected with pcDNA3-hGR (150 ng) and pRL (100 ng) into H4IIE cells in a 24-well plate (n=4 per group). pRL plasmid provided Renilla luciferase expression to document transfection efficiency. Transfected cells were left overnight, then washed with PBS and treated with 0.5 M DEX for an additional 16–20 h. Cells were then lysed and assayed for firefly and Renilla luciferase activities. Shown is the fold-induction of luciferase activity (DEX-treated/ethanol-treated) in cells from at least three experiments (* $p<0.05$). The error bars represent the S. E. for the fold induction. C) EMSA on mixtures of purified GR DBD and Cy5 end-labeled oligonucleotides containing either wild-type or mutant *Angptl4 GRE*, confirming direct binding of GR to the GRE. Reactions lasted 30 min and the mixtures were then run on 8% native gels and scanned by a phosphorimager. The concentration of GR DBD protein mixed with wild-type or mutant GREs ranged from 0 (no protein) to 2 μM, as shown. Data are representative of two independent experiments.

To test whether this identified genomic GR binding site is sufficient to mediate cellular responsiveness to glucocorticoids, we inserted the rat *Angptl4* genomic DNA containing this sequence into a reporter plasmid that drove expression of the firefly luciferase gene (*pGL4-ANGPTL4-GRBS*, Fig. 3A). This plasmid was transfected into H4IIE cells, and 24 h later, cells were treated with either control DMSO or Dex overnight. Treatment with Dex strongly induced luciferase activity in transfected H4IIE cells (Fig. 3B), indicating that this predicted GRE confers

glucocorticoid response. To test the specificity of this sequence in mediating the glucocorticoid response, we made a single nucleotide mutation within it (Fig. 3A, the mutated nucleotide is *underlined*). This nucleotide was chosen for mutation as previous studies demonstrated that it directly contacts GR and is an important mediator of glucocorticoid responses (37, 38). Mutation of this nucleotide reduced the glucocorticoid response by more than 50% (Fig. 3B), consistent with this sequence being a functional GRE.

Finally, we performed EMSA to confirm the direct binding of GR to the *Angptl4* GRE. We found that 0.03125 μM purified GR DBD was able to bind efficiently to Cy5-labeled *Angptl4* GRE and that this binding increased with the concentration of GR DBD protein in the reaction mixture, until, by 2 μM, it bound all of the labeled GRE (Fig. 3C). Notably, most GR DBD bound to the *Angptl4* GRE as a dimer (Fig. 3C), a requirement for transactivation. Mutant *Angptl4* GRE, which contains a single nucleotide change in one of the two GRE half-sites (Fig. 3A), had a compromised interaction with GR DBD (Fig. 3C). Although GR monomers could bind to mutant GRE, presumably at the wildtype half-site, GR dimers could not, consistent with decreased transactivation of mutant *Angptl4* GRE by GR (Fig. 3B). Even 2 μM GR DBD only bound to mutant GRE as a monomer (Fig. 3C). Together these findings confirm that GR binds directly and specifically to the identified *Angptl4* GRE.

Glucocorticoids Increase DNase I Accessibility and Histone Acetylation in Genomic Regions Near the Angptl4 GRE

Chromatin architecture can control eukaryotic gene expression *in vivo* by modulating the accessibility of genomic sequences to transcriptional activation machinery (39). Changes in the structure of chromatin are detectable by the way they alter the sensitivity of DNA to cleavage by DNase I (40, 41). Increased accessibility to DNase I cleavage indicates a relatively open chromatin conformation, whereas protection from cleavage by DNase I points to a more compact chromatin structure. The former is associated with transcriptional activation and the latter with repression.

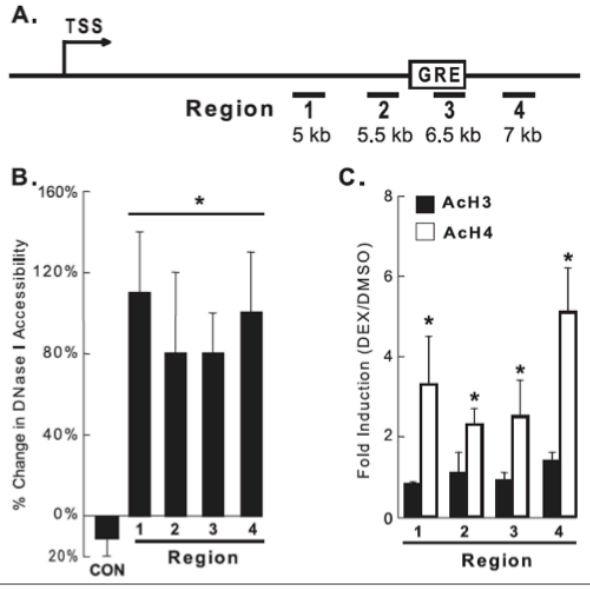

Fig. 4. Dex treatment increases DNase I accessibility and histone H4 acetylation in rat *Angptl4*.
A) schematic diagram of rat Angptl4, with TSS indicating the transcriptional start site, amplified genomic regions are underlined and numbered (1–4), and the position of the GRE shown. B) H4IIE cells were treated with DMSO or Dex (0.5 μM) for 30 min, and DNase I accessibility was analyzed as described ("Experimental Procedures"), showing increased cleavage of DNA in Dex-treated cells. C) H4IIE cells (n=4 per group) were treated with DMSO or Dex (0.5 μM) for 30 min, and the levels of acetylated histones H3 and H4 were measured in regions 1–4 by ChIP. The fold-enrichment (Dex/DMSO) was used to show increased enrichment of AcH4 but not AcH3 in DEX-treated cells (* $p<0.05$). Data in B and C were normalized to a control genomic region in rat Rpl19, and each experiment was done at least 3 times. The error bars represent the S. E. for the percent change and the fold induction.

We tested whether glucocorticoid treatment affects DNase I accessibility of genomic regions near the identified *Angptl4* GRE. H4IIE cells were treated with either control DMSO or Dex for 0.5 h, the earliest time point at which Dex increased the rate of *Angptl4* transcriptional activation in nuclear run-on assays. After Dex treatment, nuclei were isolated and treated with DNase I. Total DNA was then purified, and qPCR was performed to monitor for cleavage of specific genomic sequences by DNase I. Dex treatment markedly increased the accessibility of the *Angptl4* GRE (region 3) and surrounding genomic regions to DNase I (Fig. 4B). These results suggest that glucocorticoid treatment opens up the structure of chromatin in the vicinity of the *Angptl4* GRE, consistent with the observed increase in transcription activation. Nucleosomes form the fundamental repeating units of eukaryotic chromatin and include a core particle of DNA (~147 bp) wrapped in an octamer consisting of two copies each of the core histones H2A, H2B, H3, and H4. Increased histone acetylation, especially H3 and H4, correlates well with transcriptional activation (42). We therefore investigated whether glucocorticoids affect the acetylation status of rat *Angptl4*. H4IIE cells were treated with Dex for 30 min, after which ChIP was performed to monitor levels of acetylated histone H3 (AcH3) and histone H4 (AcH4) in genomic regions of *Angptl4*. Treatment with Dex for 30 min greatly increased levels of AcH4 in all 4 genomic regions tested, including region 3, which contained the GRE (Fig. 4A and C). Interestingly, in contrast to those of AcH4, the levels of AcH3 were not affected by Dex treatment. Overall, these results suggest that glucocorticoids specifically induce acetylation of histone H4 in activating *Angptl4* transcription.

Effects of Glucocorticoids on Lipid Metabolism Are Impaired in Angptl4-/-Mice

Plasma TG levels in mice are elevated by transgenic overexpression of *Angptl4* (8) and by injection of mice with recombinant ANGPTL4 protein (5, 10). In the liver, adenoviral overexpression of *Angptl4* results in both hyperlipidemia and hepatic steatosis (9). These features are also seen in states of chronic glucocorticoid excess, such as Cushing syndrome. We therefore investigated whether ANGPTL4 participates in the effects of glucocorticoids on lipid metabolism in mice genetically lacking ANGPTL4 (*Angptl4*-/-) (6). *Angptl4*-/- mice and wild-type littermates were treated with either PBS or 40 mg/kg Dex daily for 4 days. On day

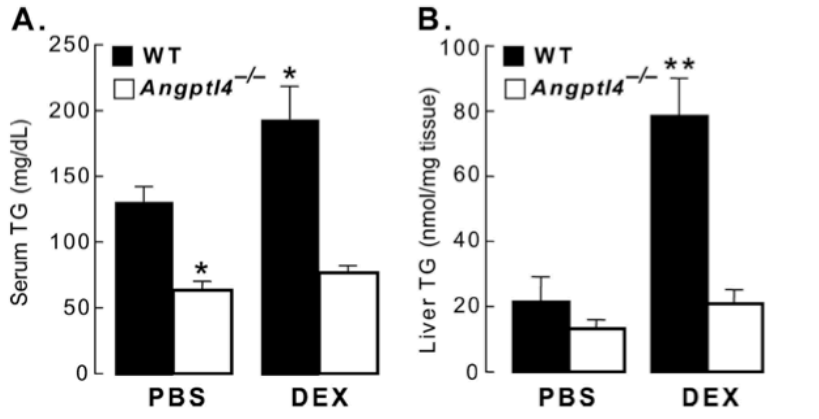

Fig. 5. The Dex-stimulated increase in serum and liver TG is impaired in Angptl4-/- mice.
A) wild-type and Angptl4-/- mice were treated daily with PBS (control; n=4–5 per group) or Dex (n=5 per group) for 4 days as described ("Experimental Procedures"), after which serum TG levels were measured. Shown is the fold-increase in serum TG of DEX-treated mice (* $p<0.05$ versus WT PBS) for both wild-type and Angptl4/ mice. B) liver TG content measured by TLC from the same mice as in A (** $p<0.05$ versus WT PBS). The error bars represent the S. E. for the TG concentration.

5, their blood and livers were collected to measure TG levels. As expected, Dex treatment of wild-type mice increased serum TG levels by ~50% (Fig. 5A). On the other hand, serum TG levels in *Angptl4*-/- mice were lower at baseline and were much less responsive to Dex treatment (Fig. 5A), indicating a requirement for ANGPTL4 in this aspect of glucocorticoid-mediated lipid metabolism. Dex treatment also increased liver TG levels ~4 fold in wild-type mice (Fig. 5B). In *Angptl4*-/- mice, however, Dex-induced accumulation of hepatic TG was minimal (Fig. 5B). Thus, *Angptl4*-/- livers were protected from the pro-steatotic effects of glucocorticoids. Overall, these experiments establish ANGPTL4 as an important participant in glucocorticoid-regulated lipid homeostasis *in vivo*.

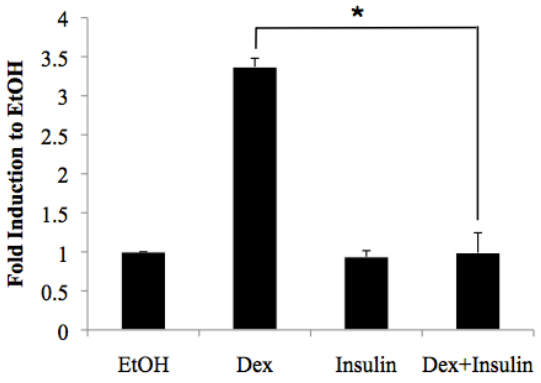

Fig. 6. Insulin represses Dex-induced Angptl4 gene expression in mouse primary hepatocytes. Primary hepatocytes were treated with control ethanol (EtOH), 0.5 μM dexamethasone (Dex), 1 nM insulin, or Dex+insulin for 5 h. RNA isolation and RT-qPCR were followed. Primers specific to rat Angptl4 and Rpl19 (internal control) gene were used in qPCR. Fold induction was calculated by normalizing to Rpl19, and taking the ratio of treatment over EtOH. Error bars indicate standard error. * $p < 0.05$.

Insulin suppressed glucocorticoid-induced Angptl4 gene expression

We treated rat primary hepatocytes with 0.5 μM of dexamethasone (Dex), a synthetic glucocorticoid, or vehicle control ethanol (EtOH) for 5 h. Followed by RNA isolation and RT-qPCR, Angptl4 gene expression was induced about 3.4 fold comparing Dex to EtOH (Fig. 6). To determine the effect of insulin on Dex-induced Angptl4 gene expression, primary hepatocytes were treated with a combination of 1 nM of insulin and 0.5 μM of Dex for 5 h. Glucocorticoid-induced Angptl4 gene expression is completely abolished with insulin treatment (Fig. 6). It is important to note that insulin treatment alone did not decrease Angptl4 gene expression.

Identification of signaling molecules in insulin signaling pathway required to inhibit glucocorticoid-induced Angptl4 gene transcription

To determine the insulin signaling molecule(s) that are required for insulin-repressed glucocorticoid-induced Angptl4, various inhibitors were used (Fig. 7). GDC-09410 was used to inhibit p110, the catalytic subunit of phosphatidylinositol 3-kinase (PI3K). API-2 was applied to inhibit Akt. MK-8669 blocked mTOR, and rapamycin inhibited S6 kinase (S6K). In addition, glycogen synthase kinase-3β (GSK-3β) inhibitor SB-216763 treatment mimicked insulin effect, as Akt inhibits GSK-3β. We treated rat H4IIE hepatoma cells with control EtOH, 0.5 μM Dex, or a combination of Dex and 1 nM insulin, followed by RNA collection and RT-qPCR. The same effect was observed in H4IIE cell line and primary hepatocytes, as insulin completed repressed glucocorticoid-induced Angptl4 (Fig. 7). With MK-8669 and rapamycin, there is no change, while adding GDC-09410 or API-2 to Dex and insulin-treated H4IIE cells relieved the repression of insulin from 1.1 fold to 2.7 or 28.7 fold, respectively (Fig. 7). As a result,

inhibiting mTOR or S6K has no change, while blocking p110 and Akt compromised the repression of insulin. Moreover, treating H4IIE cells with Dex and SB-216763 reduced glucocorticoid-induced Angptl4 from 18.9 to 6.5 fold (Fig. 7). As a result, inhibiting GSK-3β mimicked the repression of insulin on glucocorticoid-induced Angptl4 gene expression.

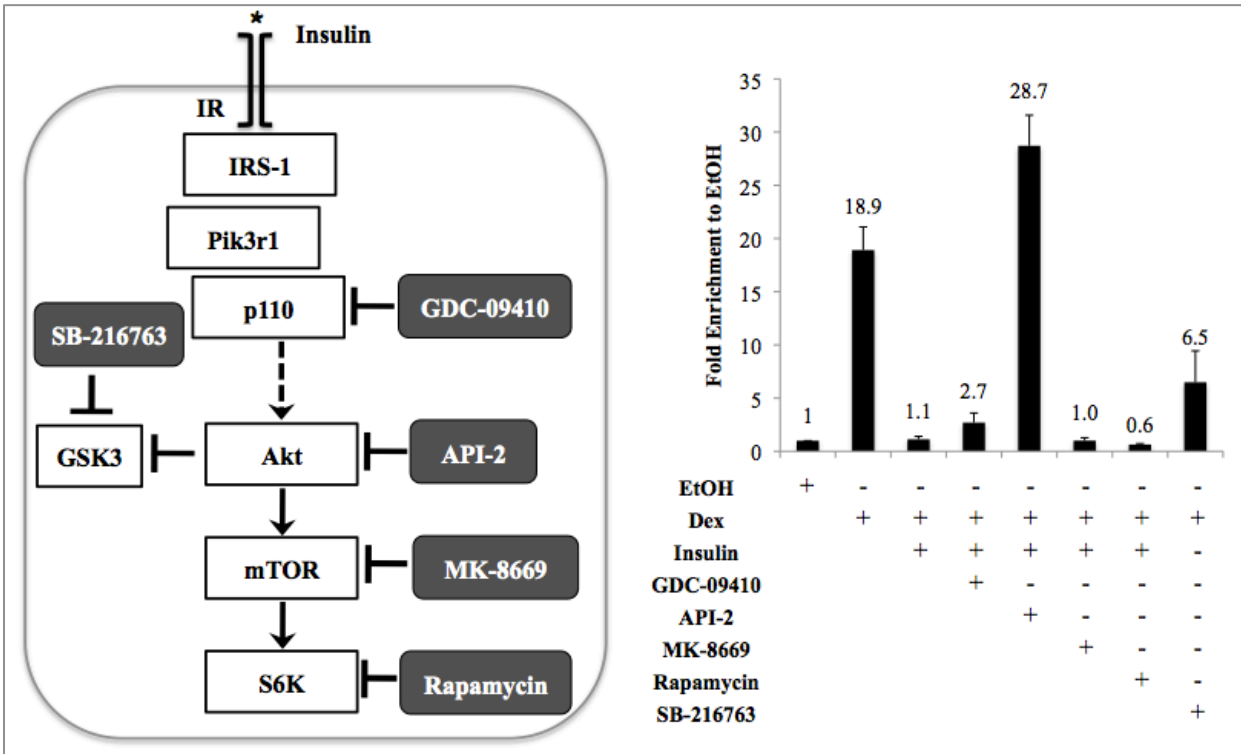

Fig. 7. The inhibitors of PI3K, Akt and GSK3 compromise the ability of insulin to suppress Dex-induced Angptl4 gene expression. H4IIE cells were treated for 5 h with control EtOH, 0.5 μM Dex, 1 nM Insulin (Ins), and in combination with one of the following inhibitors: 10 μM p110 inhibitor GDC-09410, 5 μM Akt inhibitor API-2, 0.5 nM mTOR inhibitor MK-8669, 200 nM S6K inhibitor rapamycin, or 5 μM GSK3 inhibitor SB-216763. RNA isolation and RT-qPCR were followed. Primers specific to Angptl4 and Rpl19 (internal control) gene were used in qPCR. Fold induction was calculated by normalizing to Rpl19, and taking the ratio of treatment over EtOH. Error bars indicate standard error.

Insulin suspended GR recruitment for Angptl4

To figure how insulin represses glucocorticoid-induced Angptl4 gene expression, we looked at whether GR recruitment at the GR binding region of Angptl4 is affected. H4IIE cells were treated with control EtOH, 0.5 μM Dex, or a combination of 0.5 μM Dex and 1 nM insulin for 30 min. Followed with chromatin immunoprecipitation (ChIP), primer specific to previously determined *Angptl4* GR binding region (43) was used in qPCR to figure GR recruitment. Compared to EtOH, Dex treatment induced GR recruitment by 6 fold (Fig. 8). On the contrary, insulin eliminated Dex-induced 6-fold GR recruitment to 1.2 fold (Fig. 8).

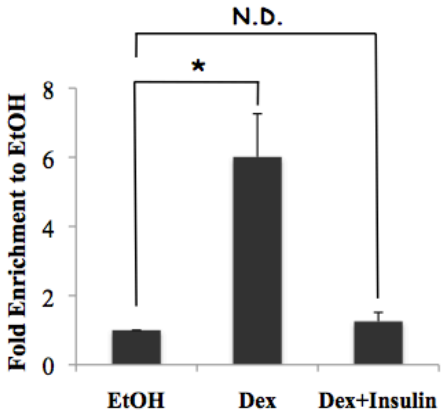

Fig. 8. Insulin treatment diminishes GR occupancy at the *Angptl4 GRE*. The 15-bp GRE of *Angptl4* is located at chr17: 33,911,836 to 33,911,850, equivalent to nucleotide (nt) position +6229 to +6243 relative to *Angptl4* transcription start site. Primer used here marks nt +6541 and +6654 relative to *Angptl4* transcription start site. Fold induction was calculated by normalizing to Rpl19, and taking the ratio of treatment over EtOH. Error bars indicate standard error. N.D. specifies no difference, and * indicates $p < 0.05$.

***FOX* binding required for maximal glucocorticoid-induced *Angptl4* transcription**

The 500 base pair (bp) GR binding region of rat *Angptl4*, from nucleotide (nt) position 6030 to 6529 relative to its transcription start site, was inserted upstream of a luciferase reporter plasmid, pGL4.10-E4 TATA (44, 45). Denoted as pWT_6030~6529 (Fig. 9A), it confers glucocorticoid response, as its Dex-induced luciferase activity was up 12 folds compared to EtOH (Fig 9B). Moreover, insulin was able to suppress Dex-induced luciferase activity from 12 fold to 1.6 fold. To narrow the region for insulin response element (IRE), we deleted part(s) of pWT_6030~6529 and obtained plasmids pDel#1_6181~ 6376, pDel#2_6181~6529, and pDel#3_6181~6376, followed by reporter assay. Surprisingly, insulin was able to suppress glucocortcoid response even with the smallest region, suggesting that nt 6181 to 6376 region harbors IRE.

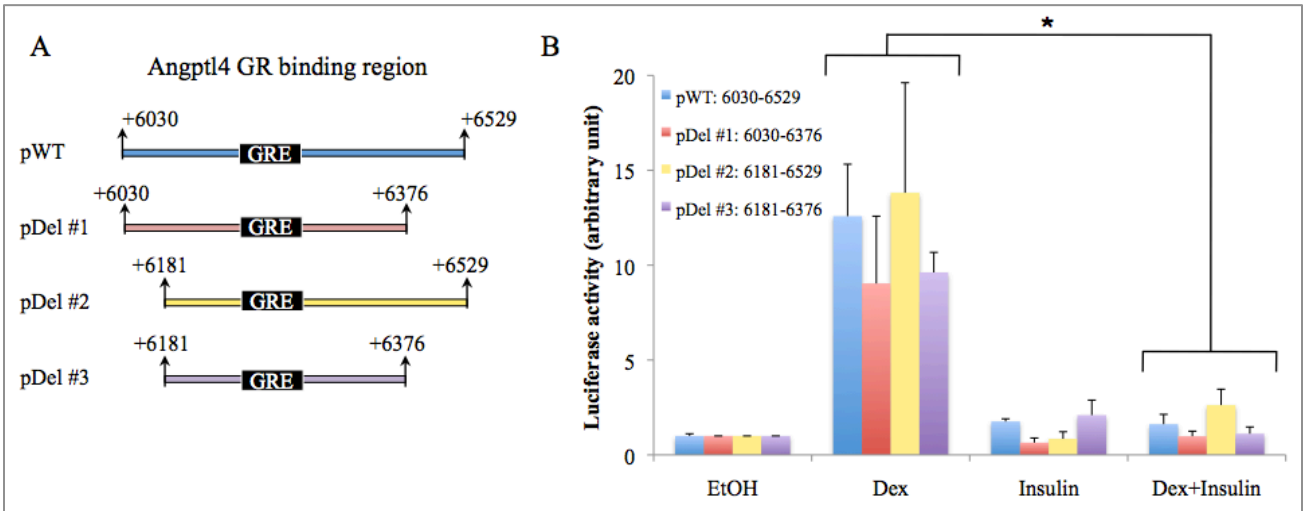

Fig. 9. Genomic region between nucleotide +6181 to +6376 of rat *Angptl4* gene contains both insulin and glucocorticoid response elements. A) Wild type (WT) GR binding region, nucleotide (nt) +6030 to +6529 relative to rat Angptl4 transcription start site, is inserted upstream of a luciferase gene in reporter plasmid pGL4.10 E4TATA. It is noted as pWT. Deletions of WT GR binding region give the following reporter plasmids: pDel #1 (nt +6030 to +6529), pDel #2 (nt +6181 to +6529), pDel #3 (nt +6181 to +6376). B) Reporter plasmids (250 ng) described in A) were co-transfected with a human GR expression vector (150 ng) and a Renilla internal control plasmid (50 ng) into H4IIE cells. Twenty-four h post-transfection, cells were treated with control EtOH, 0.5 μM Dex, 1 nM insulin, or Dex+Insulin for 20-24 h. Fold induction is calculated by taking the ratio of treatment over EtOH. Error bar represent standard error. * $p < 0.05$.

We used TFSEARCH (http://www.cbrc.jp/research/db/TFSEARCH.html) to look for binding motif within nt 6181 to 6376 region of *Angptl4* gene. Binding motifs for SRY, AML-1a, TATA, GR, HNF-3β/FoxA2, Ik-1, Ik-2, and Ik-3 passed the threshold of 85. Among them, HNF-3b/FoxA2 has a direct connection with insulin signaling. Akt protein has been reported to inactivate HNF-3β /FoxA2, as well as FoxO1 and FoxO3, by phosphorylation (32, 46). Importantly, HNF-3β /FoxA2, FoxO1 and FoxO3 all bind to the same site. For simplicity, HNF-3β /FoxA2 binding site will now be referred to as Fox response element, or FRE.

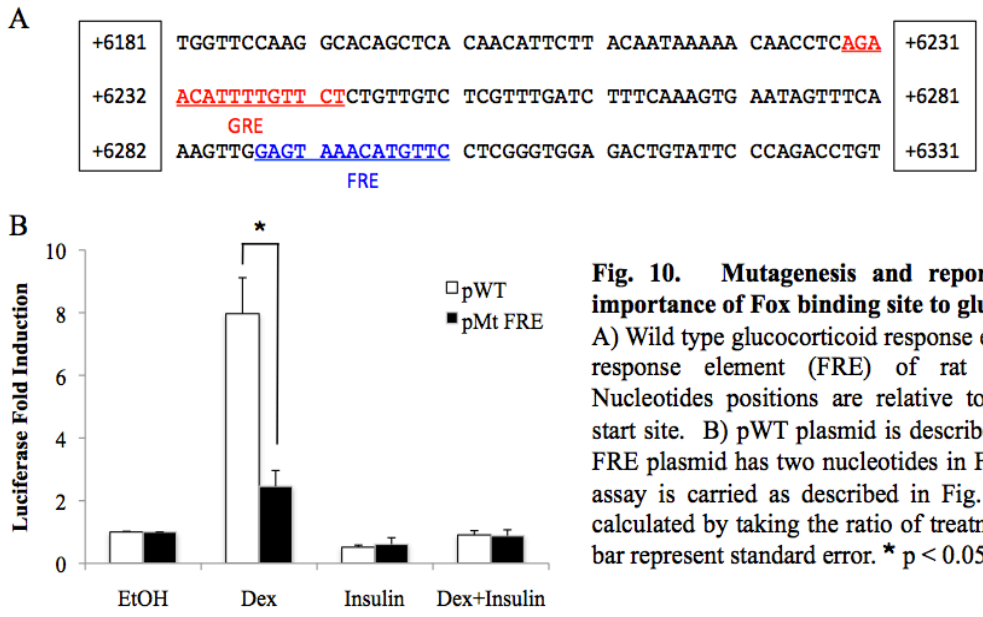

Fig. 10. Mutagenesis and reporter assay reveal the importance of Fox binding site to glucocorticoid response. A) Wild type glucocorticoid response element (GRE) and Fox response element (FRE) of rat Angptl4 are shown. Nucleotides positions are relative to Angptl4 transcription start site. B) pWT plasmid is described in Fig. 4A, and pMt FRE plasmid has two nucleotides in FRE mutated. Reporter assay is carried as described in Fig. 4B. Fold induction is calculated by taking the ratio of treatment over EtOH. Error bar represent standard error. * $p < 0.05$.

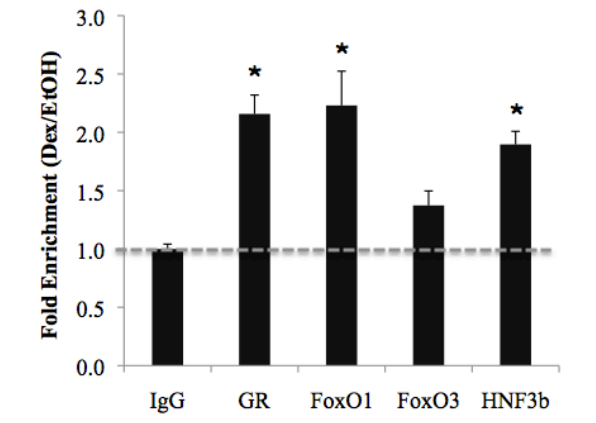

Fig. 11. Chromatin immunoprecipitation (ChIP) shows FoxO1 and HNF3b are recruited near GRE. FoxO1/HNF3b site is located at nt +6287 to +6301 relative to *Angptl4* transcription start site. H4IIE cells were treated with control EtOH or 0.5 μM Dex for 30 min. After ChIP, qPCR were followed, with primer flanking nt +6945 to +7049 relative to *Angptl4* transcription start site. Fold enrichment represents the ratio of Dex to EtOH response. Error bars indicate standard error, and * indicates $p < 0.05$.

To figure if FRE relayed the suppression of insulin on glucocorticoid-induced Angptl4 gene expression, mutagenesis was applied to the FRE (Fig. 10A). Reporter assay showed that, with mutated FRE, glucocorticoid-induced luciferase activity was significantly reduced from 8 fold to 2.5 fold (Fig. 10B). However, even with mutated FRE, insulin was able to suppress glucocorticoid-induced luciferase activity from 2.5 fold to 0.9 fold, suggesting additional element might be involved.

FoxO1 and HNF-3β /FoxA2 proteins are recruited at GR binding region of Angptl4

Since HNF-3β /FoxA2, FoxO1 and FoxO3 all can bind FRE, we performed ChIP with specific antibody to each Fox protein to determine recruitment. H4IIE cells were

treated with control EtOH or 0.5 μM Dex for 30 min. ChIP was performed followed by qPCR with primer flanking previously identified GR binding region (43). Based on ChIP, in addition to the positive control GR being in the GR binding region of *Angptl4*, FoxO1 and HNF-3β /FoxA2, but not FoxO3, are recruited (Fig. 11).

FoxO1 protein is required for glucocorticoid-induced Angptl4 gene expression

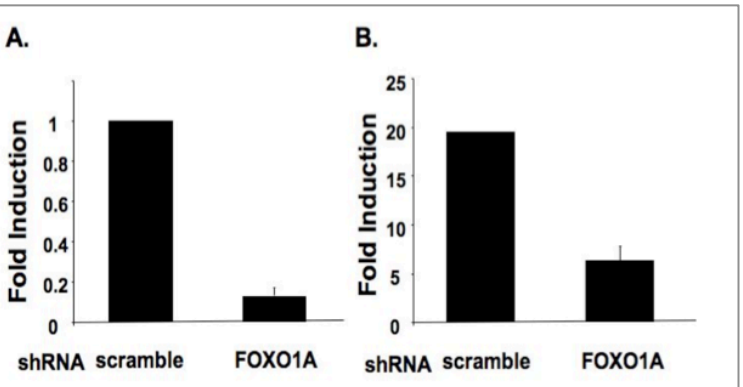

Fig. 12. FoxO1 RNA interference with shRNA reduced Dex-induced Angptl4 gene expression. A) shFoxO1 decreased the expression of FoxO1 in H4IIE cells. B) Dex-activated Angptl4 gene expression was reduced in shFoxO1 H4IIE cells compared to shscr ones.

To further test the role of FoxO1 in glucocorticoid-induced Angptl4 gene expression, we used RNA interference (RNAi) to reduce its expression in H4IIE cells. We used lentiviruses to deliver small hairpin RNA (shRNA) targeting FoxO1 into the cells. We subcloned oligonucleotides that contain specific shRNA sequences targeting FoxO1 into pLKO.1 vector. This plasmid was then be transfected into 293T cells with pMD.G (encoding the VSV-G protein) and psPAX2 (encoding the viral capsid). Scramble shRNA, which does not target any known rat gene, was used as a negative control. We infected H4IIE cells with lentiviruses that expressing FoxO1 shRNA (shFoxO1) or scramble shRNA (shscr) for 25 days. Then, shFoxO1 and shscr H4IIE cells were treated with control EtOH or 0.5 μM Dex for 5h. Total RNA was prepared and reverse transcription was performed to covert RNA to cDNA. qPCR was used to monitor the expression of FoxO1 and Angptl4 gene. As shown in Fig. 12A, compared to shscr, shFoxO1 reduced FoxO1 gene expression to 20% in H4IIE cells. Reducing FoxO1 expression resulted in decreased glucocorticoid-activated Angptl4 gene expression from 20 fold to 5 fold (Fig. 12B). These results confirmed that FoxO1 is required in the glucocorticoid response on Angptl4 gene transcription.

Discussion

In this Chapter, I presented several novel findings regarding to the transcriptional regulation of Angptl4 gene. First, Angptl4 is a direct target of GR, and GR controls Angptl4 transcription through modulating DNase I accessibility and histone acetylation within the gene. Second, Angptl4 is involved in glucocorticoid-induced increase of serum and liver TG. Third, FoxO1 binding is necessary for a maximal glucocorticoid-induced Angptl4 gene transcription.

The GRE of rat Angptl4 gene was identified at 3' untranslated region. This GRE is conserved in both mouse and human, although another GR binding region was found in human ANGPTL4 gene. Glucocorticoids increase the DNase I accessibility of genomic region surrounding the GRE, which suggests that either chromatin remodeling complex, such as Swi/Snf, or histone acetyltransferase (HAT) is involved in this process. I found that the acetylation of histone H4 was induced by Dex. Interestingly, the acetylation status of H3 was not affected. It suggests that specific HATs could be involved in this process.

The crosstalk between insulin and glucocorticoids is a physiologically important aspect in metabolism. Insulin can counteract glucocorticoid actions, or vice versa, depending on the circumstance and tissue depots. In skeletal muscles, glucocorticoids enhance protein breakdown and inhibit muscle growth, while insulin/IGF-1 signaling promote protein synthesis and growth. When C2C12 myotubes were treated with a combination of Dex, a syntheic glucocorticoid, and IGF-1, IGF-1 suppressed protein degradation and prevented Dex-induced increase in proteolysis (31). In addition, Dex seems to counteract IGF-1-suppressed protein breakdown in Dex+IGF-1 treated cells compared to IGF-1 treatment alone (31). In Chapter 1, I presented evidence, in Dex-treated myotubes, of glucocorticoids inhibiting insulin signaling through upregulating the expression of eights genes that have been shown to inhibit various signaling molecules in the insulin pathway.

Overexpression of Angptl4 results in hyperlipidemia and elevating adipocyte lipolysis, two phenotypes observed in insulin resistant patients. I therefore hypothesized that insulin has suppressive effect on glucocorticoid-induced Angptl4 gene expression. Indeed, treating H4IIE hepatoma cells with insulin resulted in a suppression of Dex-induced Angptl4 gene expression. Insulin also reduced Dex-increased GR occupancy at the *Angptl4 GRE* in ChIP experiments. Next I asked: what is the mechanism of the insulin repression? To answer this question, various inhibitors, each inhibiting a single insulin-signaling molecule, were applied with Dex treatment to H4IIE cells. I narrowed the component necessary for insulin suppression to be downstream from Akt and upstream from mTOR. Since Akt has been reported to inhibit GSK-3β, we test whether insulin suppression requires GSK-3β. Naturally, insulin inhibits GSK-3β, therefore, GSK-3β inhibitor mimics insulin signaling. Treating H4IIE cells with GSK-3β inhibitor mimicked insulin suppression on Dex-induced Angptl4 gene expression, suggesting that GSK-3β plays a role in insulin-repressed Dex-induced Angptl4 gene expression. Since a combination of insulin and Dex treatment suppressed Dex-induced Angptl4 gene expression from 18.9 fold to 1.1 fold, while a combination of GSK-3β inhibitor and Dex treatment reduced Dex-induced Angptl4 from 18.9 fold to 6.5 fold, I hypothesized that increasing the concentration of GSK-3β inhibitor can further repress Dex-induced Angptl4 to 1.1 fold, mediating the complete insulin suppression. However, this is not the case (data not shown). Even with quadruple the amount of

GSK-3β inhibitor, Dex-induced Angptl4 gene expression was still around 6 fold. This result suggests that other component(s) in the insulin signaling, in addition to GSK-3β, contribute to the insulin suppression. Alternatively, this inhibitor may not have completely inhibited GSK3β under our experimental conditions.

When inhibiting Akt, insulin suppression on Dex-induced Angptl4 gene expression was relieved entirely, if not potentiated, from 18.9 fold to 28.7 fold, indicating that Akt is essential for insulin suppression. Since Akt inhibits GSK-3β, Akt likely plays the primary role, while GSK-3β plays the secondary role, in insulin suppression. Alternatively, Akt and GSK-3β may phosphorylate a downstream target protein, which then participates in the insulin-suppressed Dex-induced Angptl4 expression.

To identify insulin response element (IRE) that mediates the suppressive effect of insulin, a reporter plasmid harboring genomic region of rat *Angptl4* gene from nt +6030 to +6529 (relative to transcription start site) were subjected to reporter assay. This 500-bp GR binding region, , contains both GRE and IRE, as insulin treatment suppressed Dex-induced luciferase activity. A putative FoxA/FoxO transcription factor binding site, which has been previously shown to act as an IRE, was identified near the GRE. By mutating this FoxA/FoxO binding site, Dex-induced luciferase activity was significantly reduced from 8 fold to 2.5 fold, even without insulin treatment. Thus, interfering FoxA/FoxO binding mimics the insulin response on Angptl4 gene. Notably, insulin treatment further suppressed Dex-induced luciferase activity from 2.5 fold to 0.9

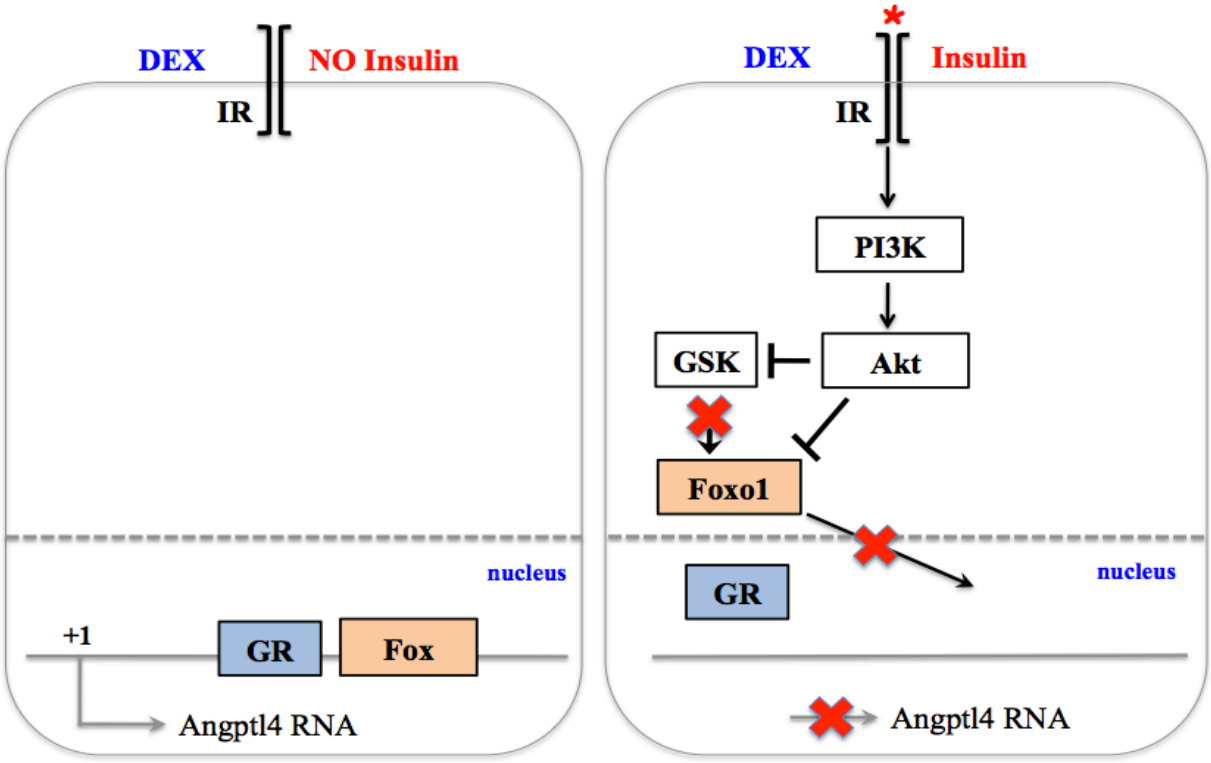

Fig. 13. Proposed mechanism of the transcription of Angptl4. A) When no insulin is present, FoxO1 can bind to the FRE of *Angptl4* and help GR to transcribe Angptl4. B) When insulin is present, Akt inactivates FoxO1 by phosphorylation, which results in the export of FoxO1 protein from the nucleus. Without FoxO1 protein, glucocorticoid-induced Angptl4 gene expression is greatly reduced.

fold, suggesting that there might be another IRE at work. With ChIP, we found FoxO1 and HNF-3β/FoxA2 proteins, but not FoxO3, are recruited with GR. It is important to note that FoxO1 and FoxA2 occupancy were observed only upon Dex treatment but not in cells treated with EtOH. With RNA interference, we knocked down 90% of FoxO1 in H4IIE cells, and observed a 70% decrease in Dex-induced Angptl4 gene expression. These data suggest that FoxO1 is required for glucocorticoid-induced Angptl4 gene expression, though the potential involvement of FoxA2 cannot be ruled out. Interestingly, it is well established that Akt can inhibit whereas GSK-3β can activate FoxO1. Thus, FoxO1 is the likely the transcription factor mediate insulin suppression of Angptl4 gene. It has been shown that the dissociation of FoxO1 from hormone response unit contributes to the insulin/IGF-1 inhibition of gene transcription in other genes (47, 48). A combined GR-FoxA2 binding site is located in the mouse G6Pase promoter overlapping two FoxO1 binding sites. Mutation of the FoxO1 binding sites reduced the effect of insulin; where as mutation of the GR/FoxA2 binding site had no effect on the insulin response (49). In mice lacking FoxO1 gene, the ability of insulin to inhibit G6Pase gene expression is abolished. Interestingly, we also observed HNF-3β/FoxA2 being recruited to the genomic region of *Angptl4 GRE*. Previous studies also showed that insulin acts through Akt to phosphorylate FoxA2 and inhibit its activity through both nuclear exclusion dependent and independent mechanism. However, the regulation of HNF-3β/FoxA2 by GSK-3β has not been reported.

Fig. 13 shows a model of insulin- and glucocorticoid-regulated Angptl4 gene transcription. Upon Dex treatment (left panel), GR occupies the GRE, and FoxO1 also was recruited to its binding site near the GRE. GR and FoxO1 cooperatively promotes Angptl4 gene transcription. When cells are treated with both Dex and insulin (right panel), PI3K/Akt pathway is activated. Akt phosphorylates FoxO1, which excludes FoxO1 from nucleus. GSK-3β has been shown to enhance Drosophila homolog of FoxO activity and also associates with FoxO1. GR occupancy is decreased upon insulin treatment. This example suggests that GR and FoxO1 require the presence of one another for maximal occupancy on this genomic region. Overall, the study of *Angptl4 GRE* genomic region presents another novel example for the crosstalk between glucocortiocids and insulin.

Material and Method

Cell Culture: H4IIE rat hepatoma cells (a gift from Dr. Daryl Granner, Vanderbilt University) were maintained in Dulbecco's modified Eagle's medium (DMEM) with 5% fetal bovine serum (FBS, tissue culture biological) and incubated at 37°C with 5% CO_2. Treatments were diluted in DMEM only and applied to cultured cells. For all cell culture experiments, H4IIE cells were grown to 95% confluence and treated with 0.5 μM Dex or an equal volume (0.05% v/v of media) of vehicle control ethanol (EtOH). Rat primary hepatocytes were purchased from SF General Hospital (San Francisco, CA).

Chromatin immunoprecipitatino (ChIP): H4IIE cells (1×10^8 to 2×10^8 cells) were treated with control EtOH, 0.5 μM Dex, or a combination of Dex and 1 nM insulin for 30 min, then cross-linked by using formaldehyde at a final concentration of 1% at room temperature for 5 min. The ChIP protocol was otherwise as previously described in Chapter one of the Thesis. Antibodies used are: anti-GRN499 (a generous gift from Dr. Keith Yamamoto, UCSF), anti-FoxO1 (sc-11350X, Santa Cruz Biotechnology), anti-FoxO3 (07-702, Millipore), anti-HNF-3ß/FoxA2 (sc-9187X, Santa Cruz Biotechnology), and normal rabbit IgG (sc-2027, Santa Cruz Biotechnology).

Nuclear Run-on: H4IIE cells were grown to confluence and treated with DMSO or Dex for different times. Cells were then harvested and incubated in lysis buffer (10 mM Tris-HCl, pH 7.4, 3 mM $MgCl_2$, 10 mM NaCl, 150 mM sucrose, and 0.5% Nonidet P-40) at 4 °C for 5 min. Nuclei were then isolated by microcentrifuge at 170 x *g* at 4 °C for 5 min. The total nuclei from each of the DMSO- or Dex-treated samples were counted, and equal numbers of nuclei were used for *in vitro* transcription. We split the samples into two aliquots. One was incubated in 100 μl of 2x *in vitro* transcription buffer (200 mM KCl, 20 mM Tris-HCl, pH 8.0, 5 mM $MgCl_2$, 4 mM dithiothreitol, 4 mM each of ATP, GTP, and CTP, 200 mM sucrose, and 20% glycerol) plus 8 μl of biotin-UTP (Roche), and the other in 100 μl of 2x *in vitro* transcription buffer plus 8 μl of UTP (negative control) for 30 min at 29 °C. 6 μl of 250 mM $CaCl_2$ and 6 μl of RNase-free DNase (Roche) (10 units/μl) were then added to stop the reactions. Total RNA was then isolated using Nucleospin RNA II (E&K). Dyna beads M-280 (Invitrogen) were washed twice in solution A (0.1 mM NaOH, 0.5 M NaCl) for 5 min, once in solution B (0.1 M NaCl) for 5 min, and then resuspended in binding/wash buffer (10 mM Tris-HCl, pH 7.5, 1 mM EDTA, and 2 M NaCl) plus 1 μl (40 units) of RNasin (Promega) per 100 μl of beads. 50 μl of beads (in binding/wash buffer) were then added to RNA, incubated at 42 °C for 20 min, and then shaken for 2 h at room temperature. Afterward, the beads were centrifuged and the supernatant discarded. The beads were then washed once (5 min) with 500 μl of 15% formamide plus 2x saline/sodium citrate buffer and twice with 1 ml of 2x saline/sodium citrate buffer. The beads were then resuspended in 30 μl of RNase- and DNase-free water. 10 μl of beads were used for each reverse transcription reaction prior to quantitative PCR (qPCR).

RNA isolation and quantitative PCR: To synthesize randomly primed cDNA, 0.5 μg of total RNA, 4 μl of 2.5 mM dNTP and 2 μl of 15 μM random primers (New England Biolabs) were mixed at a volume of 16 μl, and incubated at 70°C for 10 min. Then, a 4-μl cocktail containing 25 units of Moloney Murine Leukemia Virus (M-MuLV) Reverse Transcriptase (New England

Biolabs), 10 units of RNasin (Promega) and 2 μl of 10x reaction buffer (New England Biolabs) was added, and samples were incubated at 42 °C for 1h and then at 95°C for 5 min. The cDNA was diluted and used to perform real-time quantitative PCR (qPCR) using the EVA QPCR SuperMix Kit (Biochain), following manufacturer's protocol. qPCR was performed in either a 7900HT, 7500HT or StepOne PCR System (Applied Biosystems) and analyzed with the ΔΔ-Ct method, as supplied by the manufacturer (Applied Biosystems). *Rpl19* gene expression was used for internal normalization. Primer sequences are listed in Supplemental Material S1. Inhibitors used are as the following: p110 inhibitor GDC-09410 (Cayman), Akt inhibitor API-2 (Torcris), mTOR inhibitor deforolimus MK-8669 (Cayman), S6K inhibitor rapamycin (Cayman), and GSK inhibitor SB-216763 (Torcris).

Plasmids, transfection, and luciferase reporter assay: pGL4.10-E4TATA reporter plasmid was generated by insertion of a 50-bp minimal *E4* TATA promoter sequence (44) into the *Bgl* II to *Hind* III sites of vector pGL4.10 to drive luciferase expression (45). Each chosen GBR fragment, extending 100-150 bp upstream and downstream of the GBR, was amplified from genomic H4IIE DNA (primer sequences are listed in Supplemental Material S1), using the Expand Long Template PCR System (Roche Applied Science) and cloned into the pGL4.10-E4TATA vector with *Kpn* I/*Xho* I sites or otherwise specified in primer sequence. The QuikChange Lightning mutagenesis kit (Stratagene) was used to make site-directed mutations per the manufacturer's instructions. Lipofectamine 2000 (Invitrogen) was used to transfect H4IIE cells according to the technical manual. Twenty-four hours post-transfection, cells were treated with either 0.5 μM Dex or control EtOH in differentiation media for 16-20 h. Cells were then harvested and their luciferase activities were measured with the Dual-Luciferase Reporter Assay kit (Promega) according to procedures in the technical manual.

DNase I Accessibility Assay: Nuclei from H4IIE cells treated with control DMSO or Dex for 1 h were digested with 6.25–200 units/ml of DNase I (Qiagen) for 5 min at 22 °C. The reaction was stopped by treatment with Proteinase K for 1 h at 65 °C. DNA samples were purified using PCR purification columns (Qiagen). The samples underwent qPCR analysis to determine the relative amounts of cleaved products (primer sequences are listed in Supplemental Material S1), which were used to express the percent of DNA cleavage by DNase I.

Electrophoretic Mobility Shift Assay (EMSA): Serial dilutions of purified GR DNA binding domain (DBD) protein (provided by Dr. Miles Pufall, University of California, San Francisco) were mixed with complementary oligonucleotides (2×10^{8} M) containing either wild-type or mutant *Angptl4* GREs end-labeled with Cy5 in a solution comprised of 20 mM Tris, pH 7.5, 2 mM $MgCl_2$, 0.1 mM EDTA, 10% glycerol, 0.3 mg/ml bovine serum albumin, 4 mM dithiothreitol, and 0.1 μg/μl dI-dC. The mixtures reacted for 30 min to reach equilibrium and were then run out on 8% native gels and scanned by a Typhoon phosphorimager (Amersham Biosciences).

Animals: C57BL/6J (B6) wild-type mice were purchased from The Jackson Laboratory. *Angptl4*-/- mice were provided by the laboratories of Andras Nagy (Samuel Lunenfeld Research Institute, Mount Sinai Hospital) and Jeff Gordon (Washington University). Heterozygous mice (*Angptl4*-/-) on a mixed B6:129/Sv background were generated as described (6), and *Angptl4*-/-, *Angptl4*-/-, and *Angptl4*-/- littermates, obtained by crossing *Angptl4*-/- mice were compared. The

PCR protocols for genotyping animals were previously described (6). Mice (3–4 months old) were injected intraperitoneally daily with 40 mg/kg body weight of water-soluble Dex (Sigma) in PBS for 4 consecutive days. Twenty h after the final injection, mice were fasted for 4 h (50) and then used for blood collection and tissue harvest.

Liver and Serum TG Analyses: *Liver TG Analysis*—Liver samples were pulverized in liquid nitrogen and homogenized in a buffer consisting of 50 mM Tris-HCl, pH 7.4, 250 mM sucrose, and protease inhibitors. Lipids were extracted in chloroform/methanol (2:1) and separated by TLC on Silica Gel G-60 plates with the solvent hexane/ethyl ether/acetic acid (v/v/v, 80:20:1). The TG bands were visualized by exposure to iodine, and then scraped and analyzed as described (51), with triolein (Sigma) as a standard, and expressed per tissue weight.

Serum Analysis—Serum was isolated from whole blood immediately after collection, and a colorimetric kit (Roche Diagnostics) was used to measure serum TG levels.

Acknowledgement

We thank Dr. Sebastiaan Meijsing for EMSA assay protocol, Dr. Miles Pufall for purified GR DBD, and Dr. Donald Scott for the nuclear run-on assay protocol.

Reference

1. Hato T, Tabata M, & Oike Y (2008) The role of angiopoietin-like proteins in angiogenesis and metabolism. *Trends Cardiovasc Med* 18(1):6-14.
2. Kersten S (2005) Regulation of lipid metabolism via angiopoietin-like proteins. *Biochem Soc Trans* 33(Pt 5):1059-1062.
3. Li C (2006) Genetics and regulation of angiopoietin-like proteins 3 and 4. *Curr Opin Lipidol* 17(2):152-156.
4. Gray NE*, et al.* (2012) Angiopoietin-like 4 (Angptl4) protein is a physiological mediator of intracellular lipolysis in murine adipocytes. *The Journal of biological chemistry* 287(11):8444-8456.
5. Yoshida K, Shimizugawa T, Ono M, & Furukawa H (2002) Angiopoietin-like protein 4 is a potent hyperlipidemia-inducing factor in mice and inhibitor of lipoprotein lipase. *Journal of lipid research* 43(11):1770-1772.
6. Backhed F*, et al.* (2004) The gut microbiota as an environmental factor that regulates fat storage. *Proceedings of the National Academy of Sciences of the United States of America* 101(44):15718-15723.
7. Koster A*, et al.* (2005) Transgenic angiopoietin-like (angptl)4 overexpression and targeted disruption of angptl4 and angptl3: regulation of triglyceride metabolism. *Endocrinology* 146(11):4943-4950.
8. Mandard S*, et al.* (2006) The fasting-induced adipose factor/angiopoietin-like protein 4 is physically associated with lipoproteins and governs plasma lipid levels and adiposity. *The Journal of biological chemistry* 281(2):934-944.
9. Xu A*, et al.* (2005) Angiopoietin-like protein 4 decreases blood glucose and improves glucose tolerance but induces hyperlipidemia and hepatic steatosis in mice. *Proceedings of the National Academy of Sciences of the United States of America* 102(17):6086-6091.
10. Akiyama TE*, et al.* (2004) Peroxisome proliferator-activated receptor beta/delta regulates very low density lipoprotein production and catabolism in mice on a Western diet. *The Journal of biological chemistry* 279(20):20874-20881.
11. Romeo S*, et al.* (2007) Population-based resequencing of ANGPTL4 uncovers variations that reduce triglycerides and increase HDL. *Nat Genet* 39(4):513-516.
12. Kersten S*, et al.* (2000) Characterization of the fasting-induced adipose factor FIAF, a novel peroxisome proliferator-activated receptor target gene. *J Biol Chem* 275(37):28488-28493.
13. Mandard S*, et al.* (2004) The direct peroxisome proliferator-activated receptor target fasting-induced adipose factor (FIAF/PGAR/ANGPTL4) is present in blood plasma as a

truncated protein that is increased by fenofibrate treatment. *J Biol Chem* 279(33):34411-34420.
14. Yoon JC*, et al.* (2000) Peroxisome proliferator-activated receptor gamma target gene encoding a novel angiopoietin-related protein associated with adipose differentiation. *Mol Cell Biol* 20(14):5343-5349.
15. Desvergne B, Michalik L, & Wahli W (2006) Transcriptional regulation of metabolism. *Physiol Rev* 86(2):465-514.
16. Wang JC*, et al.* (2004) Chromatin immunoprecipitation (ChIP) scanning identifies primary glucocorticoid receptor target genes. *Proc Natl Acad Sci U S A* 101(44):15603-15608.
17. Walker BR (2006) Cortisol-cause and cure for metabolic syndrome? *Diabet Med* 23(12):1281-1288.
18. Walker BR (2007) Glucocorticoids and cardiovascular disease. *Eur J Endocrinol* 157(5):545-559.
19. Macfarlane DP, Forbes S, & Walker BR (2008) Glucocorticoids and fatty acid metabolism in humans: fuelling fat redistribution in the metabolic syndrome. *The Journal of endocrinology* 197(2):189-204.
20. Nuotio-Antar AM, Hachey DL, & Hasty AH (2007) Carbenoxolone treatment attenuates symptoms of metabolic syndrome and atherogenesis in obese, hyperlipidemic mice. *Am J Physiol Endocrinol Metab* 293(6):E1517-1528.
21. Desai U*, et al.* (2007) Lipid-lowering effects of anti-angiopoietin-like 4 antibody recapitulate the lipid phenotype found in angiopoietin-like 4 knockout mice. *Proc Natl Acad Sci U S A* 104(28):11766-11771.
22. McMahon M, Gerich J, & Rizza R (1988) Effects of glucocorticoids on carbohydrate metabolism. *Diabetes/metabolism reviews* 4(1):17-30.
23. Sakoda H*, et al.* (2000) Dexamethasone-induced insulin resistance in 3T3-L1 adipocytes is due to inhibition of glucose transport rather than insulin signal transduction. *Diabetes* 49(10):1700-1708.
24. Weinstein SP, Wilson CM, Pritsker A, & Cushman SW (1998) Dexamethasone inhibits insulin-stimulated recruitment of GLUT4 to the cell surface in rat skeletal muscle. *Metabolism: clinical and experimental* 47(1):3-6.
25. Divertie GD, Jensen MD, & Miles JM (1991) Stimulation of lipolysis in humans by physiological hypercortisolemia. *Diabetes* 40(10):1228-1232.
26. Hasselgren PO (1999) Glucocorticoids and muscle catabolism. *Current opinion in clinical nutrition and metabolic care* 2(3):201-205.
27. Vegiopoulos A & Herzig S (2007) Glucocorticoids, metabolism and metabolic diseases. *Molecular and cellular endocrinology* 275(1-2):43-61.
28. Delaunay F*, et al.* (1997) Pancreatic beta cells are important targets for the diabetogenic effects of glucocorticoids. *The Journal of clinical investigation* 100(8):2094-2098.
29. Samuel VT, Petersen KF, & Shulman GI (2010) Lipid-induced insulin resistance: unravelling the mechanism. *Lancet* 375(9733):2267-2277.
30. Yamada T, Ozaki N, Kato Y, Miura Y, & Oiso Y (2006) Insulin downregulates angiopoietin-like protein 4 mRNA in 3T3-L1 adipocytes. *Biochemical and biophysical research communications* 347(4):1138-1144.
31. Sacheck JM, Ohtsuka A, McLary SC, & Goldberg AL (2004) IGF-I stimulates muscle growth by suppressing protein breakdown and expression of atrophy-related ubiquitin

ligases, atrogin-1 and MuRF1. *American journal of physiology. Endocrinology and metabolism* 287(4):E591-601.
32. Tran H, Brunet A, Griffith EC, & Greenberg ME (2003) The many forks in FOXO's road. *Science's STKE : signal transduction knowledge environment* 2003(172):RE5.
33. Barthel A, Schmoll D, & Unterman TG (2005) FoxO proteins in insulin action and metabolism. *Trends in endocrinology and metabolism: TEM* 16(4):183-189.
34. Rena G*, et al.* (2002) Two novel phosphorylation sites on FKHR that are critical for its nuclear exclusion. *The EMBO journal* 21(9):2263-2271.
35. Zhang X*, et al.* (2002) Phosphorylation of serine 256 suppresses transactivation by FKHR (FOXO1) by multiple mechanisms. Direct and indirect effects on nuclear/cytoplasmic shuttling and DNA binding. *The Journal of biological chemistry* 277(47):45276-45284.
36. So AY, Cooper SB, Feldman BJ, Manuchehri M, & Yamamoto KR (2008) Conservation analysis predicts in vivo occupancy of glucocorticoid receptor-binding sequences at glucocorticoid-induced genes. *Proceedings of the National Academy of Sciences of the United States of America* 105(15):5745-5749.
37. Luisi BF*, et al.* (1991) Crystallographic analysis of the interaction of the glucocorticoid receptor with DNA. *Nature* 352(6335):497-505.
38. So AY, Chaivorapol C, Bolton EC, Li H, & Yamamoto KR (2007) Determinants of cell- and gene-specific transcriptional regulation by the glucocorticoid receptor. *PLoS genetics* 3(6):e94.
39. Li B, Carey M, & Workman JL (2007) The role of chromatin during transcription. *Cell* 128(4):707-719.
40. Fletcher TM*, et al.* (2000) Structure and dynamic properties of a glucocorticoid receptor-induced chromatin transition. *Molecular and cellular biology* 20(17):6466-6475.
41. John S*, et al.* (2008) Interaction of the glucocorticoid receptor with the chromatin landscape. *Molecular cell* 29(5):611-624.
42. Shahbazian MD & Grunstein M (2007) Functions of site-specific histone acetylation and deacetylation. *Annual review of biochemistry* 76:75-100.
43. Koliwad SK*, et al.* (2009) Angiopoietin-like 4 (ANGPTL4, fasting-induced adipose factor) is a direct glucocorticoid receptor target and participates in glucocorticoid-regulated triglyceride metabolism. *The Journal of biological chemistry* 284(38):25593-25601.
44. Lin YS, Carey MF, Ptashne M, & Green MR (1988) GAL4 derivatives function alone and synergistically with mammalian activators in vitro. *Cell* 54(5):659-664.
45. Bolton EC*, et al.* (2007) Cell- and gene-specific regulation of primary target genes by the androgen receptor. *Genes & development* 21(16):2005-2017.
46. Wolfrum C, Besser D, Luca E, & Stoffel M (2003) Insulin regulates the activity of forkhead transcription factor Hnf-3beta/Foxa-2 by Akt-mediated phosphorylation and nuclear/cytosolic localization. *Proceedings of the National Academy of Sciences of the United States of America* 100(20):11624-11629.
47. Vander Kooi BT*, et al.* (2003) The three insulin response sequences in the glucose-6-phosphatase catalytic subunit gene promoter are functionally distinct. *The Journal of biological chemistry* 278(14):11782-11793.
48. Puigserver P*, et al.* (2003) Insulin-regulated hepatic gluconeogenesis through FOXO1-PGC-1alpha interaction. *Nature* 423(6939):550-555.

49. Onuma H*, et al.* (2009) Insulin and epidermal growth factor suppress basal glucose-6-phosphatase catalytic subunit gene transcription through overlapping but distinct mechanisms. *The Biochemical journal* 417(2):611-620.
50. Wang JC*, et al.* (2006) Novel arylpyrazole compounds selectively modulate glucocorticoid receptor regulatory activity. *Genes & development* 20(6):689-699.
51. Snyder F & Stephens N (1959) A simplified spectrophotometric determination of ester groups in lipids. *Biochimica et biophysica acta* 34:244-245.

Chapter 3: Supplemental Material S1

Primer sequence

Gene expression

rAngptl4_cDNA_Fo	AGACCCGAAGGATAGAGTCCC
rAngptl4_cDNA_Re	CCTTCTGGAACAGTTGCTGG
mAngptl4_cDNA_Fo	AAGATGCACAGCATCACAGG
mAngptl4_cDNA_Re	ATGGATGGGAAATTGGAGC
rRPL19_cDNA_Fo	ACAAGCGGATTCTCATGGAG
rRPL19_cDNA_Re	TCCTTGGTCTTAGACCTGCG
mRPL19_cDNA_Fo	ATGGAGCACATCCACAAGC
mRPL19_cDNA_Re	TCCTTGGTCTTAGACCTGCG

ChIP

rRPL19_ChIP_Fo	ACAAGCGGATTCTCATGGAG
rRPL19_ChIP_Re	TCCTTGGTCTTAGACCTGCG
mRPL19_ChIP_Fo	ATGGAGCACATCCACAAGC
mRPL19_ChIP_Re	TCCTTGGTCTTAGACCTGCG
rAngptl4_ChIP_Region1_+5.0/+5.5kb_Fo	GTGCTCTCAGTCTGGAAAACCC
rAngptl4_ChIP_Region1_+5.0/+5.5kb_Re	GCCGTGGAATAGAGTGGAAG
rAngptl4_ChIP_Region2_+5745bp_Fo	GCTCAGCCATCAGGTAAAGG
rAngptl4_ChIP_Region2_+5838bp_Re	TGGGAGTCGGTGATCTCTTT
rAngptl4_ChIP_Region3_+6541bp_Fo	TTGACCGACTGGAGATAGGG
rAngptl4_ChIP_Region3_+6653bp_Re	ATGTTGTGAGCTGTGCCTTG
rAngptl4_ChIP_Region4_+6945bp_Fo	GGCTCCCAACCTTCACATAG
rAngptl4_ChIP_Region4_+7049bp_Re	ATAGGAGCCTGTGGAGGTCA

Luciferase assay

Luc_rAngptl4_KpnI_WT_Fo	gctgcaGGTACCgctcttgttacctgctatgtgaaggtt
Luc_rAngptl4_XhoI_WT_Re	cgctctCTCGAGtggagatgcagagggaccatttcagtcc
Luc_rAngptl4_KpnI_+6529bp	gctgcaGGTACCgctcttgttacctgctatgt
Luc_rAngptl4_XhoI_+6030bp	cgctctCTCGAGtggagatgcagagggacca
Luc_rAngptl4_KpnI_+6376bp	gctgcaGGTACCggaagctgaaatcactggga
Luc_rAngptl4_XhoI_+6181bp	cgctctCTCGAGggttccaaggcacagctca

Mutagenesis

Luc_rAngptl4_mtGRE_sense	CAACCTCAGAACATTTAGATCTCTGTTGTCTCG
Luc_rAngptl4_mtGRE_antisense	CGAGACAACAGAGATCTAAATGTTCTGAGGTTG
Luc_rAngptl4_mtFOX_sense	CAAAGTTGGAGTAAAGATGTTCCTCGGGTGGAG
Luc_rAngptl4_mtFOX_antisense	CTCCACCCGAGGAACATCTTTACTCCACACTTTG

Nuclear Run-on

B-actin_RunOn_Fo	tagccctcttttgtgccttg
B-actin_RunOn_Re	tgccactcccaaagtaaagg
rAngptl4_RunOn_Fo	gggtggtagcctgtagtgga
rAngptl4_RunOn_Re	ctgtaggtggctggtggttt

THE JOURNAL OF BIOLOGICAL CHEMISTRY VOL. 284, NO. 38, pp. 25593–25601, September 18, 2009

Angiopoietin-like 4 (ANGPTL4, Fasting-induced Adipose Factor) Is a Direct Glucocorticoid Receptor Target and Participates in Glucocorticoid-regulated Triglyceride Metabolism*[S]

Received for publication, May 26, 2009, and in revised form, July 22, 2009 Published, JBC Papers in Press, July 23, 2009, DOI 10.1074/jbc.M109.025452

Suneil K. Koliwad[‡§¶], Taiyi Kuo[‖], Lauren E. Shipp[‖], Nora E. Gray[‖], Fredrik Backhed[**], Alex Yick-Lun So[‡‡], Robert V. Farese, Jr.[‡§¶§§], and Jen-Chywan Wang[‖1]

*From the [‡]Gladstone Institute of Cardiovascular Disease, Departments of [§]Medicine, [§§]Biochemistry and Biophysics, and [‡‡]Cellular and Molecular Pharmacology, and [¶]Cardiovascular Research Institute, University of California, San Francisco, California 94143, the [‖]Department of Nutritional Science and Toxicology, University of California, Berkeley, California 94720, and the **Sahlgrenska Center for Cardiovascular and Metabolic Research/Wallenberg Laboratory and Department of Molecular and Clinical Medicine, University of Gothenburg, Gothenburg SE-41345, Sweden*

Glucocorticoids are important regulators of lipid homeostasis, and chronically elevated glucocorticoid levels induce hypertriglyceridemia, hepatic steatosis, and visceral obesity. The occupied glucocorticoid receptor (GR) is a transcription factor. However, those genes regulating lipid metabolism under GR control are not fully known. Angiopoietin-like 4 (ANGPTL4, fasting-induced adipose factor), a protein inhibitor of lipoprotein lipase, is synthesized and secreted during fasting, when circulating glucocorticoid levels are physiologically increased. We therefore tested whether the ANGPTL4 gene (*Angptl4*) is transcriptionally controlled by GR. We show that treatment with the synthetic glucocorticoid dexamethasone increased *Angptl4* mRNA levels in primary hepatocytes and adipocytes (2–3-fold) and in the livers and white adipose tissue of mice (~4-fold). We tested the mechanism of this increase in H4IIE hepatoma cells and found that dexamethasone treatment increased the transcriptional rate of *Angptl4*. Using bioinformatics and chromatin immunoprecipitation, we identified a GR binding site within the rat *Angptl4* sequence. A reporter plasmid containing this site was markedly activated by dexamethasone, indicative of a functional glucocorticoid response element. Dexamethasone treatment also increased histone H4 acetylation and DNase I accessibility in genomic regions near this site, further supporting that it is a glucocorticoid response element. Glucocorticoids promote the flux of triglycerides from white adipose tissue to liver. We found that mice lacking ANGPTL4 (*Angptl4*$^{-/-}$) had reductions in dexamethasone-induced hypertriglyceridemia and hepatic steatosis, suggesting that ANGPTL4 is required for this flux. Overall, we establish that ANGPTL4 is a direct GR target that participates in glucocorticoid-regulated triglyceride metabolism.

Glucocorticoids are steroid hormones that act as key transcriptional regulators of human metabolism during the fasted state, when their levels are physiologically increased. In particular, glucocorticoids facilitate the mobilization of triglycerides (TG)[2] from the white adipose tissue (WAT) for use by the liver in processes such as gluconeogenesis, TG synthesis, and very low density lipoporotein synthesis and secretion (1, 2). However, the full set of genes that mediate this effect via transcriptional control by glucocorticoids is not known.

Fasting also increases circulating levels of angiopoietin-like 4 (ANGPTL4, a fasting-induced adipose factor). ANGPTL4 is a protein secreted by the liver and WAT that can inhibit lipoprotein lipase (LPL) activity and stimulate WAT lipolysis (3–5). LPL hydrolyzes lipoprotein TG, promoting fatty acid storage in the WAT. This activity is counterbalanced by that of lipases, which hydrolyze stored TG, promoting fatty acid release by adipocytes. Therefore, one could predict that reducing ANGPTL4 activity would promote WAT TG storage, whereas increasing it would favor lipolysis. This prediction is consistent with the results of genetic and physiological studies. First, mice lacking ANGPTL4 (*Angptl4*$^{-/-}$) have decreased plasma TG levels and an increased capacity for weight gain (6). By contrast, mice overexpressing *Angptl4* in the WAT have a dramatically limited capacity for TG storage and increased levels of plasma TG, fatty acids, and glycerol (7). Plasma TG and fatty acid levels are similarly increased in mice by adenoviral overexpression of *Angptl4* in the liver (8) and by systemic injection of recombinant ANGPTL4 (9, 10). Finally, a recent large population-based study uncovered sequence variations in *Angptl4* that are associated with loss of function and reduced plasma TG levels in humans (11). In summary, these data suggest that transcrip-

* This work was supported by American Heart Association Beginning Grant-in-aid 0565157Y (to J. C. W.) and an A. P. Giannini Foundation Fellowship (to S. K. K.).

[S] The on-line version of this article (available at http://www.jbc.org) contains supplemental Table S1.

[1] To whom correspondence should be addressed: Morgan Hall, Rm. 315, Berkeley, CA 94720-3104. Tel.: 510-643-1039; E-mail: walwang@berkeley.edu.

[2] The abbreviations used are: TG, triglyceride; WAT, white adipose tissue; DEX, dexamethasone; LPL, lipoprotein lipase; DMSO, dimethyl sulfoxide; ChIP, chromatin immunoprecipitation; PPAR, peroxisome proliferator-activated receptor; ERK, extracellular signal-regulated kinase; qPCR, quantitative PCR; PBS, phosphate-buffered saline; EMSA, electrophoretic mobility shift assay; DBD, DNA binding domain; MAP kinase, mitogen-activated protein kinase; *Pepck*, phosphoenolpyruvate carboxykinase; GR, glucocorticoid receptor; GRE, glucocorticoid receptor element.

tional modulation of *Angptl4* expression could serve as an important regulatory mechanism in TG homeostasis.

We previously showed that *Angptl4* mRNA levels are increased by glucocorticoids in A549 lung epithelial cells, suggesting that glucocorticoids may exert transcriptional control over *Angptl4* expression (12). Several lines of evidence support this hypothesis in metabolic tissues. First, excess glucocorticoids promote hypertriglyceridemia, as also seen in models where ANGPTL4 levels are increased (1, 13, 14). Second, reducing the ratio of active to inactive glucocorticoids by pharmacologically inhibiting 11β-hydroxysteroid dehydrogenase type I increased plasma TG clearance and decreased liver TG synthesis, two components of the phenotype seen in *Angptl4*$^{-/-}$ mice (6, 15). Therefore, it is possible that both physiologic and pathophysiologic responses to glucocorticoids may involve the regulation of *Angptl4* expression in metabolic tissues. However, whether *Angptl4* expression is indeed directly regulated by glucocorticoids in the liver and WAT remains unexplored.

Given the prominent role of ANGPTL4 in systemic TG metabolism, we explored the regulation of *Angptl4* by glucocorticoids. We first examined whether glucocorticoids regulate *Angptl4* expression in primary hepatocytes and adipocytes, mouse livers and WAT, and established cell lines. We then dissected the mechanism of glucocorticoid-regulated *Angptl4* expression using a rat hepatoma cell line, H4IIE. Finally, we used *Angptl4*$^{-/-}$ mice to investigate the potential role of ANGPTL4 in glucocorticoid-regulated TG homeostasis.

EXPERIMENTAL PROCEDURES

Cell Culture

H4IIE rat hepatoma cells (a gift from Dr. Daryl Granner, Vanderbilt University) were cultured in Dulbecco's modified Eagle's medium with 5% fetal bovine serum (Invitrogen). When cells were treated with dexamethasone (DEX), Dulbecco's modified Eagle's medium with 5% charcoal stripped fetal bovine serum (J R Scientific) was used. Rat primary hepatocytes were purchased from Cambrix. Human primary adipocytes were purchased from ZenBio.

ChIP

H4IIE cells (1×10^8 to 2×10^8 cells) were cross-linked by using formaldehyde at a final concentration of 1% at room temperature for 5 or 10 min. The chromatin immunoprecipitation (ChIP) protocols were otherwise as previously described (16, 17).

Nuclear Run-on

H4IIE cells were grown to confluence and treated with DMSO or DEX for different times. Cells were then harvested and incubated in lysis buffer (10 mM Tris-HCl, pH 7.4, 3 mM $MgCl_2$, 10 mM NaCl, 150 mM sucrose, and 0.5% Nonidet P-40) at 4 °C for 5 min. Nuclei were then isolated by microcentrifuge at 170 × *g* at 4 °C for 5 min. The total nuclei from each of the DMSO- or DEX-treated samples were counted, and equal numbers of nuclei were used for *in vitro* transcription. We split the samples into two aliquots. One was incubated in 100 μl of 2× *in vitro* transcription buffer (200 mM KCl, 20 mM Tris-HCl, pH 8.0, 5 mM $MgCl_2$, 4 mM dithiothreitol, 4 mM each of ATP, GTP, and CTP, 200 mM sucrose, and 20% glycerol) plus 8 μl of biotin-UTP (Roche), and the other in 100 μl of 2× *in vitro* transcription buffer plus 8 μl of UTP (negative control) for 30 min at 29 °C. 6 μl of 250 mM $CaCl_2$ and 6 μl of RNase-free DNase (Roche) (10 units/μl) were then added to stop the reactions. Total RNA was then isolated using Nucleospin RNA II (E&K).

Dyna beads M-280 (Invitrogen) were washed twice in solution A (0.1 mM NaOH, 0.5 M NaCl) for 5 min, once in solution B (0.1 M NaCl) for 5 min, and then resuspended in binding/wash buffer (10 mM Tris-HCl, pH 7.5, 1 mM EDTA, and 2 M NaCl) plus 1 μl (40 units) of RNasin (Promega) per 100 μl of beads. 50 μl of beads (in binding/wash buffer) were then added to RNA, incubated at 42 °C for 20 min, and then shaken for 2 h at room temperature. Afterward, the beads were centrifuged and the supernatant discarded. The beads were then washed once (5 min) with 500 μl of 15% formamide plus 2× saline/sodium citrate buffer and twice with 1 ml of 2× saline/sodium citrate buffer. The beads were then resuspended in 30 μl of RNase- and DNase-free water. 10 μl of beads were used for each reverse transcription reaction prior to quantitative PCR (qPCR).

qPCR

Total RNA was isolated from cells by using QIAshredder and RNeasy kits (Qiagen). Total RNA from liver and epididymal WAT was isolated by using Tri-reagent (Molecular Research Center Inc.). To synthesize random-primed cDNA, 0.5 μg of total RNA (10 μl), 4 μl of 2.5 mM dNTP, and 2 μl of random primers (New England Biolabs) were mixed and incubated at 70 °C for 10 min. A 4-μl mixture containing 25 units of Moloney murine leukemia virus reverse transcriptase (New England Biolabs), 10 units of RNasin, and 2 μl of 10× reaction buffer (New England Biolabs) was then added and incubated at 42 °C for 1 h. The reaction was then incubated at 95 °C for 5 min.

The resultant cDNA was diluted to 200 μl, and 2.5 μl was used to perform qPCR in a 25-μl reaction containing *Taq* DNA polymerase (1.25 units; Promega), 1× reaction buffer, 1.5 mM $MgCl_2$, 0.5 mM dNTP (Invitrogen), 0.2× SYBR Green I dye (Molecular Probes), and 250 nM of each primer. Alternatively, EVA QPCR SuperMix Kit (Biochain) was used per the manufacturer's protocol. qPCR was performed in either an Opticon-2 DNA Engine (MJ Research) or a 7900HT PCR System (Applied Biosystems) and analyzed by using the δ-δ Ct method as supplied by the manufacturer. *Rpl19* expression was used for internal normalization. All primer sequences are presented in supplemental Table S1.

Western Blot

Livers and Epididymal WAT were collected, frozen in liquid nitrogen, and stored at −80 °C. Samples were thawed, suspended, and homogenized in RIPA buffer (10 mM Tris-HCl, pH 8.0, 1 mM EDTA, 150 mM NaCl, 5% glycerol, 0.1% sodium deoxycholate, 0.1% SDS, and 1% Triton X-100) supplemented with protease inhibitors. Tissue lysates were cleared by centrifugation (17,000 × *g* for 15 min at 4 °C). Lysates were then resolved by SDS-PAGE, and proteins were transferred to nitrocellulose membranes (Amersham Biosciences) using semidry transfer (Bio-Rad). Membranes were blocked for 8 h at 22 °C

with 5% (w/v) nonfat milk in TBS (50 mM Tris base, 200 mM NaCl, pH 7.5). Membranes were then incubated overnight at 4 °C in TBS with 5% milk containing primary antibody, followed by washes with TBS plus 0.5% Tween 20 at pH 7.5 (TBST). Membranes were then incubated for 2 h at 22 °C in TBS with 5% milk containing secondary antibody followed by washes with TBST. Proteins were detected by chemiluminescence (Western Lighting Plus-ECL, PerkinElmer Life Sciences). Membranes were stripped for 0.5 h at 22 °C in PBS with 7 μl/ml of β-mercaptoethanol, washed with PBS for 0.5 h, and blocked for 4 h in TBS with 10% milk before re-probing with other primary antibodies. The following antibodies were used: ANGPTL4 (Rb polyclonal antibodies to ARP4, ab2920; Abcam Inc.), β-actin (C4) mouse monoclonal IgG_1 (sc-47778; Santa Cruz Biotechnology), anti-rabbit IgG_1-horseradish peroxidase (Cell Signaling), and anti-mouse IgG_1-horseradish peroxidase (sc-2060; Santa Cruz Biotechnology).

Blots were scanned as TIFF files to Adobe Photoshop CS4 (version 11.0) and quantified using Image J software. The optical density of the ANGPTL4 band divided by that of the respective β-actin band are presented.

Cloning and Site-directed Mutagenesis

The rat *Angptl4* genomic region containing the predicted GR binding site was amplified by PCR using specific primers. The PCR fragment was restriction-digested and subcloned into the pGL4-TATA reporter. A mutagenesis kit (QuikChange) was used to make site-directed mutations per the manufacturer's instructions (Stratagene).

DNase I Accessibility Assay

Nuclei from H4IIE cells treated with vehicle or DEX for 1 h were digested with 6.25–200 units/ml of DNase I (Qiagen) for 5 min at 22 °C. The reaction was stopped by treatment with Proteinase K for 1 h at 65 °C. DNA samples were purified using PCR purification columns (Qiagen). The samples underwent qPCR analysis to determine the relative amounts of cleaved products (see supplemental Table 1 for primer sequences), which were used to express the percent of DNA cleavage by DNase I.

Transfection

Transfection in H4IIE cells was done with Lipofectamine 2000 (Invitrogen) according to the technical manual. 24 h post-transfection, cells were treated with either DMSO or 0.5 mM DEX overnight. Cells were then harvested, and luciferase activity was measured by a dual-luciferase assay kit (Promega) according to the technical manual.

Electrophoretic Mobility Shift Assay (EMSA)

Serial dilutions of purified GR DNA binding domain (DBD) protein (provided by Dr. Miles Pufall, University of California, San Francisco) were mixed with complementary oligonucleotides (2×10^{-8} M) containing either wild-type or mutant *Angptl4* GREs end-labeled with Cy5 in a solution comprised of 20 mM Tris, pH 7.5, 2 mM $MgCl_2$, 0.1 mM EDTA, 10% glycerol, 0.3 mg/ml bovine serum albumin, 4 mM dithiothreitol, and 0.1 μg/μl dI-dC. The mixtures reacted for 30 min to reach equilibrium and were then run out on 8% native gels and scanned by a Typhoon phosphorimager (Amersham Biosciences).

Animals

C57BL/6J (B6) wild-type mice were purchased from The Jackson Laboratory. *Angptl4*$^{-/-}$ mice were provided by the laboratories of Andras Nagy (Samuel Lunenfeld Research Institute, Mount Sinai Hospital) and Jeff Gordon (Washington University). Heterozygous mice (*Angptl4*$^{+/-}$) on a mixed B6:129/Sv background were generated as described (6), and *Angptl4*$^{+/+}$, *Angptl4*$^{+/-}$, and *Angptl4*$^{-/-}$ littermates, obtained by crossing *Angptl4*$^{+/-}$ mice were compared. The PCR protocols for genotyping animals were previously described (6).

Mice (3–4 months old) were injected intraperitoneally daily with 40 mg/kg body weight of water-soluble DEX (Sigma) in PBS for 4 consecutive days. 20 h after the final injection, mice were fasted for 4 h (17) and then used for blood collection and tissue harvest.

Liver and Serum TG Analyses

Liver TG Analysis—Liver samples were pulverized in liquid nitrogen and homogenized in a buffer consisting of 50 mM Tris-HCl, pH 7.4, 250 mM sucrose, and protease inhibitors. Lipids were extracted in chloroform/methanol (2:1) and separated by TLC on Silica Gel G-60 plates with the solvent hexane/ethyl ether/acetic acid (v/v/v, 80:20:1). The TG bands were visualized by exposure to iodine, and then scraped and analyzed as described (18), with triolein (Sigma) as a standard, and expressed per tissue weight.

Serum Analysis—Serum was isolated from whole blood immediately after collection, and a colorimetric kit (Roche Diagnostics) was used to measure serum TG levels.

Statistics

Data are expressed as mean ± S.E. for each group and comparisons were analyzed by Student's *t* test.

RESULTS

Glucocorticoids Increase Angptl4 Expression in Vitro and in Vivo—To determine whether *Angptl4* expression is regulated by glucocorticoids in primary rat hepatocytes and human adipocytes, we treated these cells with the synthetic glucocorticoid DEX for 5 h. After harvesting the cells to prepare total RNA, cDNA was synthesized and qPCR was performed using specific primers. We first confirmed that DEX treatment increased the expression of *Pepck* and *Per1* in hepatocytes and adipocytes, respectively (positive controls), and did not affect mRNA levels of *Angptl3* and *Abcd4*, two genes not known to be regulated by glucocorticoids (Fig. 1*A*). Interestingly, DEX treatment significantly increased *Angptl4* mRNA levels in both hepatocytes and adipocytes, indicating that *Angptl4* expression is regulated by glucocorticoids *in vitro*. (Fig. 1*A*).

We then tested whether glucocorticoids regulate *Angptl4* expression in the model rat hepatoma cell line, H4IIE, by treating these cells with DEX for 5 h. As for primary hepatocytes, DEX treatment increased *Angptl4* mRNA levels (Fig. 1*A*). We chose to conduct subsequent *in vitro* studies using H4IIE cells because the effect of DEX on *Pepck*, *Angptl3*, and *Angptl4*

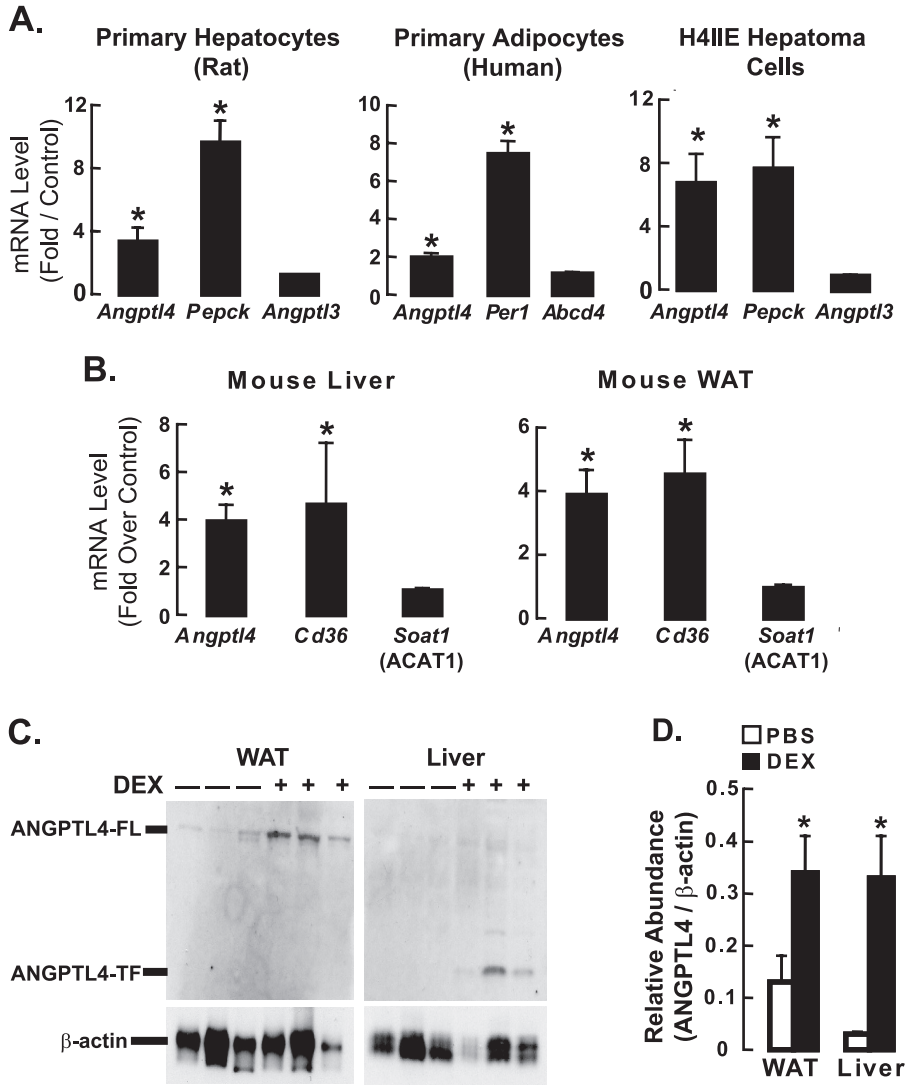

FIGURE 1. **ANGPTL4 gene and protein expression are regulated by glucocorticoids *in vivo* and *in vitro*.** *A*, rat primary hepatocytes, human primary adipocytes, and rat H4IIE hepatoma cells (n = 3–5) were treated with either DMSO or DEX (0.5 μM) for 5 h, after which mRNA levels of *Angptl4* and positive and negative control genes were measured by qPCR. Data show fold-induction of gene expression (DEX/DMSO) from at least three separate experiments (*, $p < 0.05$). *B*, mice (n = 6) were treated with either PBS or DEX (40 mg/kg) for 4 days then fasted for 4 h, after which their livers and epididymal fat (WAT) were harvested to perform qPCR as in *A* (*, $p < 0.05$). *C*, liver and WAT samples from control and DEX-treated mice in *B* were also collected for analysis of protein expression by Western blot (6.25 μg of tissue per sample run for WAT and 100 μg for liver). For each blot, the first 3 lanes are samples from individual mice treated with PBS (−), and the last 3 lanes are from DEX-treated mice (+). Full-length ANGPTL4 (*ANGPTL4-FL*) was the main band in WAT, whereas the truncated form (*ANGPTL4-TF*) predominated in the liver. β-Actin served as the internal loading control. *D*, quantification of the intensity of ANGPTL4 bands (see "Experimental Procedures") from Western blots as in *C* (n = 3). Data represent relative optical density (ANGPTL4/β-actin; *, $p < 0.05$). The error bars represent the S. E. for the fold induction and the relative abundance.

mRNA expression in these cells replicated what was seen in primary hepatocytes.

To investigate whether glucocorticoids increase *Angptl4* expression *in vivo*, we dissected the livers and epididymal WAT from C57BL6/J mice injected daily for 4 days with either DEX or PBS. We then used these tissues to prepare total RNA, synthesize cDNA, and perform qPCR to measure mRNA levels. DEX treatment increased the levels of *CD36* mRNA (positive control) but had no effect on *Soat1* (ACAT1) mRNA levels (negative control) in both liver and WAT (Fig. 1*B*). However, as it did in primary hepatocytes and adipocytes, DEX treatment of mice increased *Angptl4* mRNA levels in both the liver and WAT (Fig. 1*B*), indicating that *Angptl4* is regulated by glucocorticoids *in vivo*.

We next sought to determine whether the increase in *Angptl4* mRNA expression induced by DEX treatment is associated with an increase in ANGPTL4 protein levels. We performed Western blots on tissue lysates from control and DEX-treated mice, and found that DEX treatment for 4 days markedly elevated the levels of ANGPTL4 protein in both the WAT and liver (Fig. 1, *C* and *D*). Previous studies (19, 20) showed that the WAT mostly produces an uncleaved full-length version of ANGPTL4 (ANGPTL4-FL), whereas the liver produces more of a truncated version of ANGPTL4. Our results from the WAT and livers of DEX-treated mice agree with these observations (Fig. 1*C*).

Glucocorticoids Increase the Rate of Rat Angptl4 Transcription—We next investigated whether the elevation of *Angptl4* mRNA by glucocorticoid treatment is due to an increase in the rate of *Angptl4* transcription in H4IIE cells by using nuclear run-on assays. Cells were treated with DEX in DMSO for 10, 30, or 120 min. Control cells were either untreated or treated with DMSO alone for 120 min. Afterward, nuclear extracts were prepared from these cells, and *in vitro* transcription was performed by adding biotin-UTP. Newly synthesized RNA was then isolated on streptavidin beads. After random-primed cDNA was synthesized, qPCR was performed to detect changes in transcription rates using *Angptl4* specific primers. No effect was seen after 10 min of DEX treatment (Fig. 2). However, treatments of 30 and 120 min both markedly increased the rate of *Angptl4* transcription (Fig. 2). These results demonstrate that glucocorticoids can regulate *Angptl4* at the transcriptional level.

Identification of a Rat Angptl4 GRE—To investigate whether transcription of *Angptl4* is directly regulated by the GR, we sought to identify GR binding sites within the *Angptl4* genomic sequence. We applied a bioinformatic approach (BioProspector motif), with which we identified specific sequences within 64 kb of rat *Angptl4* (which extended 32 kb upstream and downstream of the transcriptional start site) that were highly similar

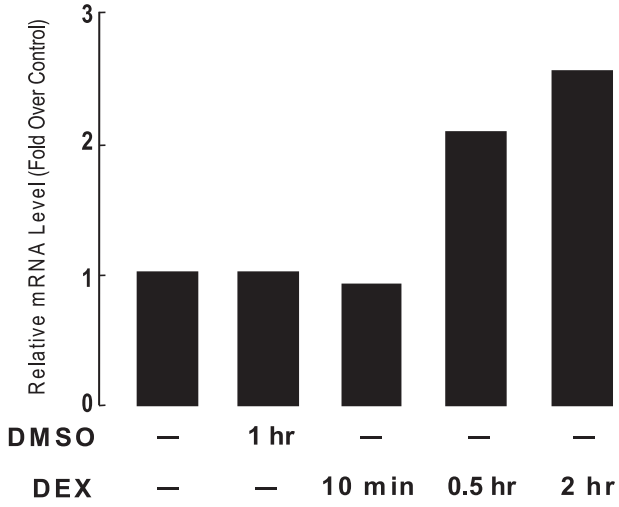

FIGURE 2. **DEX treatment increases the rate of *Angptl4* gene transcription in H4IIE cells.** H4IIE cells were untreated, treated with DMSO for 120 min, or with DEX (0.5 μM) for 10, 30, or 120 min as shown. Nuclei from these cells were used for *in vitro* transcription with biotin UTP. Newly synthesized RNA was isolated on streptavidin beads. cDNA was then synthesized and qPCR performed to monitor for changes in transcription rates using primers specific to *Angptl4* and *β-actin* (control). Shown is the fold-induction in transcription of DEX-treated samples (DEX/untreated) from one of two independent experiments showing similar results.

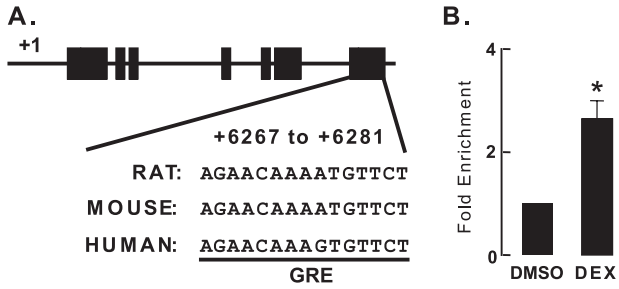

FIGURE 3. **Identification of an *Angptl4* GRE.** *A*, schematic diagram of rat *Angptl4*, including the location of the predicted GR binding site. *Black boxes* represent exons, and *lines* connecting them represent introns. The predicted GR binding site sequences (AGAACATTTTGTTCT) and their conserved counterparts in human and mouse genome are shown. *B*, ChIP experiments confirming the recruitment of GR to its predicted binding site. H4IIE cells were treated with either DMSO or DEX (0.5 μM) for 30 min, after which they were harvested for ChIP as described ("Experimental Procedures"). Shown is the fold-enrichment of GR binding by DEX treatment (DEX/DMSO) from three independent experiments (*, $p < 0.05$). The error bars represent the S. E. for the fold enrichment.

(width of the first motif block was set at 14) to 79 previously identified GR binding sites (21). Because many important transcriptional regulatory regions within genes are conserved between multiple species, we next employed a BLAST search of the University of California Santa Cruz genome browser to filter and isolate sequences conserved across the rat, mouse, and human genomes. This comparison yielded a single species-conserved palindromic sequence (AGAACATTTTGTTCT) located at the 3′-untranslated region of *Angptl4* between 6267 and 6281 bp downstream of the transcriptional start site (Fig. 3*A*). We used a ChIP assay to investigate GR recruitment to this putative GR binding site in H4IIE cells. Cells were treated for 1 h with DEX and then harvested for ChIP ("Experimental Procedures"). Using a control IgG antibody for ChIP, the number of genomic DNA fragments that were amplified in the predicted GR binding site was similar between control (DMSO) and DEX-treated samples (data not shown). By contrast, using a GR-specific antibody for ChIP, we found that DEX treatment resulted in a ~2.3-fold enrichment of genomic DNA fragments that amplified the predicted GR binding site (Fig. 3*B*). This finding indicates that GR occupancy of this palindromic sequence occurs in a DEX-dependent manner, suggesting that this sequence may be a functional GRE.

To test whether this identified genomic GR binding site is sufficient to mediate cellular responsiveness to glucocorticoids, we inserted the rat *Angptl4* genomic DNA containing this sequence into a reporter plasmid that drove expression of the firefly luciferase gene (*pGL4-ANGPTL4-GRBS*, Fig. 4*A*). This plasmid was transfected into H4IIE cells, and 24 h later, cells were treated with either DMSO (control) or DEX overnight. Treatment with DEX strongly induced luciferase activity in transfected H4IIE cells (Fig. 4*B*), indicating that this predicted GRE confers glucocorticoid responsiveness. To test the specificity of this sequence in mediating the glucocorticoid response, we made a single nucleotide mutation within it (Fig. 4*A*, the mutated nucleotide is *underlined*). This nucleotide was chosen for mutation as previous studies demonstrated that it directly contacts GR and is an important mediator of glucocorticoid responses (22, 23). Mutation of this nucleotide reduced the glucocorticoid response by more than 50% (Fig. 4*B*), consistent with this sequence being a functional GRE.

Finally, we performed EMSA to confirm the direct binding of GR to the *Angptl4* GRE. We found that 0.03125 μM purified GR DBD was able to bind efficiently to Cy5-labeled *Angptl4* GRE and that this binding increased with the concentration of GR DBD protein in the reaction mixture, until, by 2 μM, it bound all of the labeled GRE (Fig. 4*C*). Notably, most GR DBD bound to the *Angptl4* GRE as a dimer (Fig. 4*C*), a requirement for transactivation. Mutant *Angptl4* GRE, which contains a single nucleotide change in one of the two GRE half-sites (Fig. 4*A*), had a compromised interaction with GR DBD (Fig. 4*C*). Although GR monomers could bind to mutant GRE, presumably at the wild-type half-site, GR dimers could not, consistent with decreased transactivation of mutant *Angptl4* GRE by GR (Fig. 4*B*). Even 2 μM GR DBD only bound to mutant GRE as a monomer (Fig. 4*C*). Together these findings confirm that GR binds directly and specifically to the identified *Angptl4* GRE.

Glucocorticoids Increase DNase I Accessibility and Histone Acetylation in Genomic Regions Near the Angptl4 GRE—Chromatin architecture can control eukaryotic gene expression *in vivo* by modulating the accessibility of genomic sequences to transcriptional activation machinery (24). Changes in the structure of chromatin are detectable by the way they alter the sensitivity of DNA to cleavage by DNase I (25, 26). Increased accessibility to DNase I cleavage indicates a relatively open chromatin conformation, whereas protection from cleavage by DNase I points to a more compact chromatin structure. The former is associated with transcriptional activation and the latter with repression.

We tested whether glucocorticoid treatment affects DNase I accessibility of genomic regions near the identified *Angptl4* GRE. H4IIE cells were treated with either DMSO or DEX for 30 min, the earliest time point at which DEX increased the rate of *Angptl4* transcriptional activation in nuclear run-on assays.

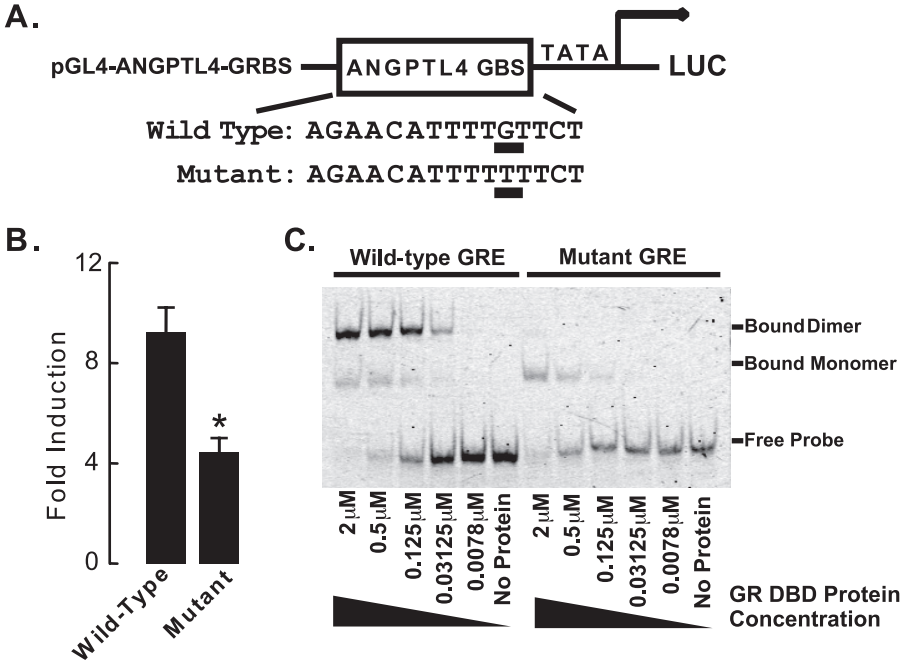

FIGURE 4. **The GR binding region of *Angptl4* confers glucocorticoid responsiveness.** *A*, a sequence containing either the wild-type or a mutated *Angptl4* GR binding site was inserted into the pGL4-TATA reporter to create pGL4-ANGPTL4-GRBS (mutation from Gly to Thr *underlined*). *B*, glucocorticoid responsiveness of GR-binding sites in rat *Angptl4*. Reporter plasmids and wild-type or mutant pGL4-ANGPTL4-GRBS (75 ng) were cotransfected with pcDNA3-hGR (150 ng) and pRL (100 ng) into H4IIE cells in a 24-well plate ($n = 4$ per group). pRL plasmid provided *Renilla* luciferase expression to document transfection efficiency. Transfected cells were left overnight, then washed with PBS and treated with 0.5 μM DEX for an additional 16–20 h. Cells were then lysed and assayed for firefly and *Renilla* luciferase activities. Shown is the fold-induction of luciferase activity (DEX-treated/ethanol-treated) in cells from at least three experiments (*, $p < 0.05$). The error bars represent the S. E. for the fold induction. *C*, EMSA on mixtures of purified GR DBD and Cy5 end-labeled oligonucleotides containing either wild-type or mutant *Angptl4* GRE, confirming direct binding of GR to the GRE. Reactions lasted 30 min, and the mixtures were then run on 8% native gels and scanned by a phosphorimager. The concentration of GR DBD protein mixed with wild-type or mutant GREs ranged from 0 (no protein) to 2 μM, as shown. Data are representative of two independent experiments.

After DEX treatment, nuclei were isolated and treated with DNase I. Total DNA was then purified, and qPCR was performed to monitor for cleavage of specific genomic sequences by DNase I. DEX treatment markedly increased the accessibility of the *Angptl4* GRE (region 3) and surrounding genomic regions to DNase I (Fig. 5*B*). These results suggest that glucocorticoid treatment opens up the structure of chromatin in the vicinity of the *Angptl4* GRE, consistent with the observed increase in transcription activation.

Nucleosomes form the fundamental repeating units of eukaryotic chromatin and include a core particle of DNA (~147 bp) wrapped in an octamer consisting of 2 copies each of the core histones H2A, H2B, H3, and H4. Increased histone acetylation, especially H3 and H4, correlates well with transcriptional activation (27). We therefore investigated whether glucocorticoids affect the acetylation status of rat *Angptl4*. H4IIE cells were treated with DEX for 30 min, after which ChIP was performed to monitor levels of acetylated histone H3 (AcH3) and histone H4 (AcH4) in genomic regions of *Angptl4*. Treatment with DEX for 30 min greatly increased levels of AcH4 in all 4 genomic regions tested, including region 3, which contained the GRE (Fig. 5, *A* and *C*). Interestingly, in contrast to those of AcH4, the levels of AcH3 were not affected by dexamethasone treatment. Overall, these results suggest that glucocorticoids specifically induce acetylation of histone H4 in activating *Angptl4* transcription.

Effects of Glucocorticoids on Lipid Metabolism Are Impaired in Angptl4$^{-/-}$ Mice—Plasma TG levels in mice are elevated by transgenic overexpression of *Angptl4* (7) and by injection of mice with recombinant ANGPTL4 protein (9, 10). In the liver, adenoviral overexpression of *Angptl4* results in both hyperlipidemia and hepatic steatosis (8). These features are also seen in states of chronic glucocorticoid excess, such as Cushing syndrome. We therefore investigated whether ANGPTL4 participates in the effects of glucocorticoids on lipid metabolism in mice genetically lacking ANGPTL4 (*Angptl4$^{-/-}$*) (6). *Angptl4$^{-/-}$* mice and wild-type littermates were treated with either PBS or 40 mg/kg DEX daily for 4 days. On day 5, their blood and livers were collected to measure TG levels. As expected, DEX treatment of wild-type mice increased serum TG levels by ~50% (Fig. 6*A*). On the other hand, serum TG levels in *Angptl4$^{-/-}$* mice were lower at baseline and were much less responsive to DEX treatment (Fig. 6*A*), indicating a requirement for ANGPTL4 in this aspect of glucocorticoid-mediated lipid metabolism. DEX treatment also increased liver TG levels ~4-fold in wild-type mice (Fig. 6*B*). In *Angptl4$^{-/-}$* mice, however, DEX-induced accumulation of hepatic TG was minimal (Fig. 6*B*). Thus, *Angptl4$^{-/-}$* livers were protected from the prosteatotic effects of glucocorticoids. Overall, these experiments establish ANGPTL4 as an important participant in glucocorticoid-regulated lipid homeostasis *in vivo*.

DISCUSSION

One important component of the physiologic response to fasting is an increase in the level of circulating glucocorticoids, which maintain levels of energy substrates in part by promoting the flux of TG from the WAT to the liver. Fasting also increases synthesis and secretion of ANGPTL4 by the WAT and liver, prompting the hypothesis that ANGPTL4 may mediate aspects of the regulatory effect of glucocorticoids on metabolism. We therefore investigated whether murine *Angptl4* is transcriptionally regulated by glucocorticoids. We establish that *Angptl4* mRNA levels are regulated by DEX treatment in cultured adipocytes and hepatocytes, and in the WAT and livers of mice. Using bioinformatics and ChIP, we identified a GR binding site in the genomic region of *Angptl4*. By finding that DEX treatment stimulated reporter activity in cells expressing this bind-

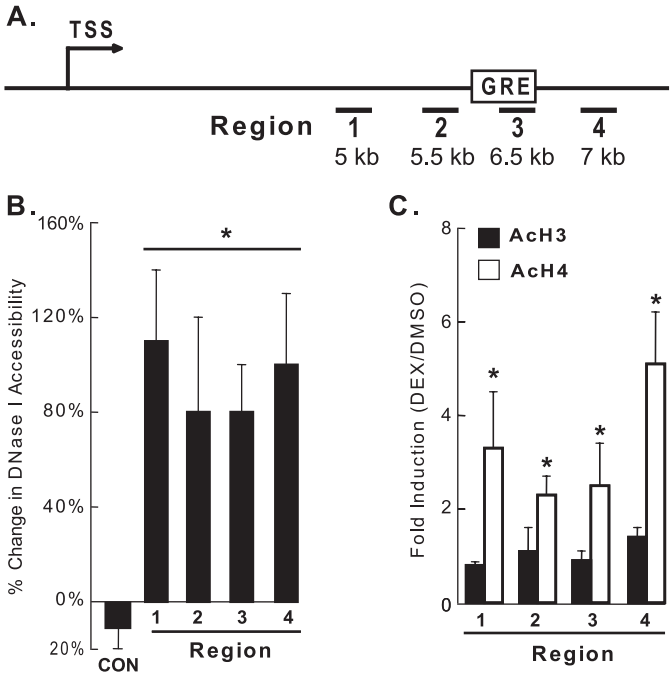

FIGURE 5. **DEX treatment increases DNase I accessibility and histone H4 acetylation in rat *Angptl4*.** *A*, schematic diagram of rat *Angptl4*, with *TSS* indicating the transcriptional start site, amplified genomic regions are *underlined* and *numbered* (1–4), and the position of the GRE shown. *B*, H4IIE cells were treated with DMSO or DEX (0.5 μM) for 30 min, and DNase I accessibility was analyzed as described ("Experimental Procedures"), showing increased cleavage of DNA in DEX-treated cells. *C*, H4IIE cells ($n = 4$ per group) were treated with DMSO or DEX (0.5 μM) for 30 min, and the levels of acetylated histones H3 and H4 were measured in regions 1–4 by ChIP. The fold-enrichment (DEX/DMSO) was used to show increased enrichment of AcH4 but not AcH3 in DEX-treated cells (*, $p < 0.05$). Data in *B* and *C* were normalized to a control genomic region in rat *Rpl19*, and each experiment was done at least 3 times. The error bars represent the S. E. for the percent change and the fold induction.

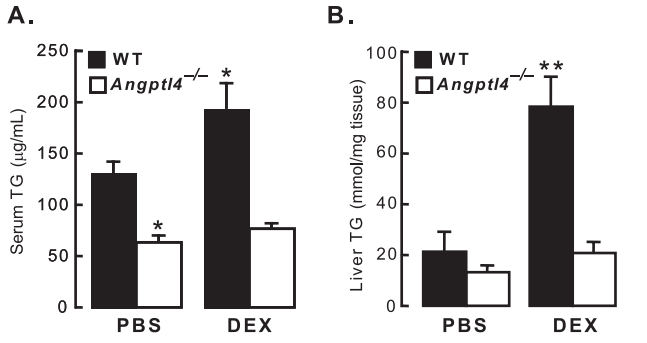

FIGURE 6. **The DEX-stimulated increase in serum and liver TG is impaired in *Angptl4*$^{-/-}$ mice.** *A*, wild-type and *Angptl4*$^{-/-}$ mice were treated daily with PBS (control; $n = 4$–5 per group) or DEX ($n = 5$ per group) for 4 days as described ("Experimental Procedures"), after which serum TG levels were measured. Shown is the fold-increase in serum TG of DEX-treated mice (*, $p < 0.05$ *versus* WT PBS) for both wild-type and *Angptl4*$^{-/-}$ mice. *B*, liver TG content measured by TLC from the same mice as in *A* (**, $p < 0.05$ *versus* WT PBS). The error bars represent the S. E. for the TG concentration.

ing site linked to luciferase, we determined that this site is a functional GRE. Furthermore, we used EMSA to show that this GRE interacts directly with GR. Our data suggest that the mechanism by which GR controls *Angptl4* transcription involves the modulation of DNase I accessibility and histone acetylation within the gene. We linked these effects to *in vivo* physiology by studying mice lacking ANGPTL4. These mice had reductions in DEX-induced hypertriglyceridemia and hepatic steatosis, indicating that ANGPTL4 is required for these effects. Overall, we show that *Angptl4* is a direct transcriptional target of GR and a contributor to the regulation of TG homeostasis by glucocorticoids in mice.

Other signals have also been shown to modulate *Angptl4* expression. For example, *Angptl4* transcription is increased by hypoxia in endothelial cells (28, 29). By contrast, microbiota suppress intestinal levels of *Angptl4* mRNA in mice (6). In addition to being regulated by glucocorticoids, as shown here, *Angptl4* transcription is also controlled by peroxisome proliferator-activated receptors α and γ (PPARα and PPARγ), which function as nutritional sensors in hepatocytes and adipocytes, respectively (19, 20). In particular, PPARα increases the expression of key genes involved in the metabolic response to fasting (30). However, the effect of fasting on *Angptl4* mRNA levels is not altered in mice lacking PPARα (19), suggesting that other pathways, including ones under GR regulation as shown here, may mediate this effect. Notably, *Ppar*α mRNA levels are also increased by glucocorticoids (31). Thus, it is conceivable that both *Angptl4* and *Ppar*α are part of a GR-regulated gene network that controls the metabolic adaptation to fasting.

Using rat H4IIE hepatoma cells, we analyzed the mechanisms governing the stimulation of *Angptl4* mRNA expression by glucocorticoids. We found that glucocorticoids increased the transcriptional rate of *Angptl4* and identified a GR binding site between 6267 and 6281 bp downstream of the transcriptional start site within the 3′-untranslated region. We confirmed the recruitment of GR to this site by ChIP and showed that this site can bind GR dimers efficiently. Furthermore, in cells transfected with a reporter plasmid containing this GR binding site, we were able to stimulate reporter activity with DEX treatment, indicating that this site functions as a GRE. Notably, this element is conserved between mouse, rat, and human, highlighting its importance as a mammalian regulatory element. Regarding the sequence location, it is not unusual for a GRE to be far away from the transcriptional start site. Recently, GREs were shown to be distributed both 5′ and 3′ to the transcriptional start site at distances over 5 kb (23). Responsive elements in estrogen receptor- and androgen receptor-regulated genes have been found to be distributed similarly (16, 32, 33). Recently, a study found a GR binding region in human *Angptl4* to be located as far as 8 kb upstream of the transcriptional start site using a ChIP on chip approach (23). The exact sequences mediating glucocorticoid responsiveness in this human GR binding region have not been identified, and we were unable to find sequences in the rat or mouse genomes resembling this specific region. Regardless, these human data coupled with our findings suggest the possibility that distinct transcriptional mechanisms may be employed to regulate *Angptl4* expression in rodents and humans.

Chromatin remodeling regulates the activity of several GREs (23, 25). To determine how glucocorticoids activate *Angptl4* transcription, we therefore tested whether DEX treatment affects the chromatin structure and histone acetylation of *Angptl4*. We found that DEX treatment increased the DNase I accessibility of genomic regions near the *Angptl4* GRE, indicating that activation by GR may open up the structure of chromatin in these regions and facilitate the binding of transcriptional

co-regulators. Glucocorticoids also specifically induced the acetylation of histone H4 in genomic regions near the *Angptl4* GRE, suggesting that acetylation of key regulatory elements within these regions may serve as another modulator of glucocorticoid-activated *Angptl4* transcription. That histone H4, but not H3, was acetylated by DEX treatment suggests the occupied GR recruits only a subset of histone acetyltransferases in activating *Angptl4* transcription, although it is possible that histone H3 acetylation is induced at other genomic regions not tested here. Overall, the increased DNase I accessibility and histone H4 acetylation in the identified GRE offer insight into the specific machinery important for regulating *Angptl4* transcription.

As seen previously (34), glucocorticoid treatment significantly increased TG levels in the serum (~1.5-fold) and livers (~4-fold) of mice (Fig. 6*A*, B). However, this response was significantly compromised in *Angptl4*$^{-/-}$ mice (Fig. 6, *A* and *B*). Thus, ANGPTL4, potentially by inhibiting LPL, plays a role in the mechanism by which glucocorticoids increase serum and hepatic TG levels. Our DEX treatment protocol matched that of Dolinsky *et al.* (34), who found that glucocorticoid treatment increased the rate of hepatic TG synthesis, but not very low density lipoporotein secretion. This could explain how the mice we treated developed higher TG levels in the liver than in the plasma. Although we did not observe a significant change in the epididymal fat mass of mice treated for 4 days with DEX (data not shown), it is well known that long-term glucocorticoid treatment promotes a re-partitioning of lipids between different WAT depots (1, 35). Future work should determine whether ANGPTL4 plays a role in this process.

The mechanisms(s) underlying how ANGPTL4 modulates glucocorticoid-stimulated hepatic steatosis are unclear. A likely possibility is that without ANGPTL4, a lipoprotein lipase inhibitor and a stimulator of WAT lipolysis, glucocorticoids cannot efficiently mobilize TG from WAT for use in hepatic TG synthesis. Alternatively, this process may involve an activity of ANGPTL4 distinct from its ability to inhibit LPL. A recent report showed that the fibrinogen-like domain of ANGPTL4, located at its carboxyl terminus, can suppress the basic fibroblast growth factor-induced activation of ERK1/2 MAP kinase in endothelial cells (36). Furthermore, analysis of mRNA expression showed that genes involved in fatty acid oxidation in the muscle were down-regulated in *Angptl4*$^{-/-}$ mice (37). It is unclear if the ERK1/2 MAP kinase or fatty acid oxidation pathways are similarly modulated in the livers and WAT of *Angptl4*$^{-/-}$ mice, and investigating this possibility is an important topic for future investigation.

It is worth noting that *Angptl4* is not the only GR target that participates in the regulation of liver TG metabolism. Recently, GR was shown to inhibit transcription of the hairy enhancer of split 1 gene (*Hes1*), which encodes a transcriptional repressor involved in glucocorticoid-induced hepatic steatosis (38). Inhibition of *Hes1* coordinately represses the expression of pancreatic lipase (*PNL*) and pancreatic lipase-related protein (*PNLRP*) 2, both of which encode TG hydrolases. Down-regulation of these two lipolytic genes in the liver can result in the accumulation of TG (38). These findings along with ours suggest that glucocorticoids potentially regulate the transcription of multiple networks of genes that can exert overlapping effects on hepatic lipid metabolism. Additionally, these GR target genes are likely tissue-specific, as glucocorticoid-dependent effects on lipid metabolism in the liver and WAT are quite different. Thus, gaining a complete picture of how glucocorticoids affect lipid homeostasis will require the systematic identification of all direct GR targets in both the WAT and liver. Our identification of *Angptl4* as a direct GR target is an important first step toward the systematic dissection of this metabolic regulatory process.

Our findings mark ANGPTL4 as a potential key mediator of the effects of glucocorticoids on TG homeostasis during physiologic fasting. Fasting TG levels are routinely measured in humans and are often elevated in patients with insulin resistance and type 2 diabetes. Recently, genetic sequence variations interfering with either the production of ANGPTL4 or with its capacity to inhibit LPL were associated with low plasma TG levels in up to 4% of individuals in a large population when combined with mutations in other members of the ANGPTL family (39). These findings, coupled with the work shown here, suggest that ANGPTL4 may mediate the metabolic effects of glucocorticoids on TG metabolism similarly in both in humans and mice.

Acknowledgments—We thank Dr. Keith Yamamoto for support on this project; Dr. Andras Nagy for providing Angptl4$^{-/-}$ *mice; Drs. Jeff Gordon and Peter Crawford for sharing the experience of breeding Angptl4*$^{-/-}$ *mice; Dr. Sebastiaan Meijsing for EMSA assays; Dr. Miles Pufall for purified GR DBD; and Dr. Donald Scott for the nuclear run-on assay protocol.*

REFERENCES

1. Macfarlane, D. P., Forbes, S., and Walker, B. R. (2008) *J. Endocrinol.* **197,** 189–204
2. Seckl, J. R., Morton, N. M., Chapman, K. E., and Walker, B. R. (2004) *Recent Prog. Horm. Res.* **59,** 359–393
3. Hato, T., Tabata, M., and Oike, Y. (2008) *Trends Cardiovasc. Med.* **18,** 6–14
4. Kersten, S. (2005) *Biochem. Soc. Trans.* **33,** 1059–1062
5. Li, C. (2006) *Curr. Opin. Lipidol.* **17,** 152–156
6. Bäckhed, F., Ding, H., Wang, T., Hooper, L. V., Koh, G. Y., Nagy, A., Semenkovich, C. F., and Gordon, J. I. (2004) *Proc. Natl. Acad. Sci. U.S.A.* **101,** 15718–15723
7. Mandard, S., Zandbergen, F., van Straten, E., Wahli, W., Kuipers, F., Müller, M., and Kersten, S. (2006) *J. Biol. Chem.* **281,** 934–944
8. Xu, A., Lam, M. C., Chan, K. W., Wang, Y., Zhang, J., Hoo, R. L., Xu, J. Y., Chen, B., Chow, W. S., Tso, A. W., and Lam, K. S. (2005) *Proc. Natl. Acad. Sci. U.S.A.* **102,** 6086–6091
9. Akiyama, T. E., Lambert, G., Nicol, C. J., Matsusue, K., Peters, J. M., Brewer, H. B., Jr., and Gonzalez, F. J. (2004) *J. Biol. Chem.* **279,** 20874–20881
10. Yoshida, K., Shimizugawa, T., Ono, M., and Furukawa, H. (2002) *J. Lipid Res.* **43,** 1770–1772
11. Romeo, S., Pennacchio, L. A., Fu, Y., Boerwinkle, E., Tybjaerg-Hansen, A., Hobbs, H. H., and Cohen, J. C. (2007) *Nat. Genet.* **39,** 513–516
12. Wang, J. C., Derynck, M. K., Nonaka, D. F., Khodabakhsh, D. B., Haqq, C., and Yamamoto, K. R. (2004) *Proc. Natl. Acad. Sci. U.S.A.* **101,** 15603–15608
13. Walker, B. R. (2006) *Diabet. Med.* **23,** 1281–1288
14. Walker, B. R. (2007) *Eur. J. Endocrinol.* **157,** 545–559
15. Desai, U., Lee, E. C., Chung, K., Gao, C., Gay, J., Key, B., Hansen, G., Machajewski, D., Platt, K. A., Sands, A. T., Schneider, M., Van Sligtenhorst, I., Suwanichkul, A., Vogel, P., Wilganowski, N., Wingert, J., Zam-

browicz, B. P., Landes, G., and Powell, D. R. (2007) *Proc. Natl. Acad. Sci. U.S.A.* **104,** 11766–11771
16. Bolton, E. C., So, A. Y., Chaivorapol, C., Haqq, C. M., Li, H., and Yamamoto, K. R. (2007) *Genes Dev.* **21,** 2005–2017
17. Wang, J. C., Shah, N., Pantoja, C., Meijsing, S. H., Ho, J. D., Scanlan, T. S., and Yamamoto, K. R. (2006) *Genes Dev.* **20,** 689–699
18. Snyder, F., and Stephens, N. (1959) *Biochim. Biophys. Acta* **34,** 244–245
19. Mandard, S., Zandbergen, F., Tan, N. S., Escher, P., Patsouris, D., Koenig, W., Kleemann, R., Bakker, A., Veenman, F., Wahli, W., Müller, M., and Kersten, S. (2004) *J. Biol. Chem.* **279,** 34411–34420
20. Yoon, J. C., Chickering, T. W., Rosen, E. D., Dussault, B., Qin, Y., Soukas, A., Friedman, J. M., Holmes, W. E., and Spiegelman, B. M. (2000) *Mol. Cell. Biol.* **20,** 5343–5349
21. So, A. Y., Cooper, S. B., Feldman, B. J., Manuchehri, M., and Yamamoto, K. R. (2008) *Proc. Natl. Acad. Sci. U.S.A.* **105,** 5745–5749
22. Luisi, B. F., Xu, W. X., Otwinowski, Z., Freedman, L. P., Yamamoto, K. R., and Sigler, P. B. (1991) *Nature* **352,** 497–505
23. So, A. Y., Chaivorapol, C., Bolton, E. C., Li, H., and Yamamoto, K. R. (2007) *PLoS Genet* **3,** e94
24. Li, B., Carey, M., and Workman, J. L. (2007) *Cell* **128,** 707–719
25. Fletcher, T. M., Ryu, B. W., Baumann, C. T., Warren, B. S., Fragoso, G., John, S., and Hager, G. L. (2000) *Mol. Cell. Biol.* **20,** 6466–6475
26. John, S., Sabo, P. J., Johnson, T. A., Sung, M. H., Biddie, S. C., Lightman, S. L., Voss, T. C., Davis, S. R., Meltzer, P. S., Stamatoyannopoulos, J. A., and Hager, G. L. (2008) *Mol. Cell* **29,** 611–624
27. Shahbazian, M. D., and Grunstein, M. (2007) *Annu. Rev. Biochem.* **76,** 75–100
28. Wang, B., Wood, I. S., and Trayhurn, P. (2007) *Pflugers Arch.* **455,** 479–492
29. Le Jan, S., Amy, C., Cazes, A., Monnot, C., Lamandé, N., Favier, J., Philippe, J., Sibony, M., Gasc, J. M., Corvol, P., and Germain, S. (2003) *Am. J. Pathol.* **162,** 1521–1528
30. Desvergne, B., Michalik, L., and Wahli, W. (2006) *Physiol. Rev.* **86,** 465–514
31. Lemberger, T., Staels, B., Saladin, R., Desvergne, B., Auwerx, J., and Wahli, W. (1994) *J. Biol. Chem.* **269,** 24527–24530
32. Carroll, J. S., Liu, X. S., Brodsky, A. S., Li, W., Meyer, C. A., Szary, A. J., Eeckhoute, J., Shao, W., Hestermann, E. V., Geistlinger, T. R., Fox, E. A., Silver, P. A., and Brown, M. (2005) *Cell* **122,** 33–43
33. Deblois, G., and Giguère, V. (2008) *Mol. Endocrinol.* **22,** 1999–2011
34. Dolinsky, V. W., Douglas, D. N., Lehner, R., and Vance, D. E. (2004) *Biochem. J.* **378,** 967–974
35. Masuzaki, H., Paterson, J., Shinyama, H., Morton, N. M., Mullins, J. J., Seckl, J. R., and Flier, J. S. (2001) *Science* **294,** 2166–2170
36. Yang, Y. H., Wang, Y., Lam, K. S., Yau, M. H., Cheng, K. K., Zhang, J., Zhu, W., Wu, D., and Xu, A. (2008) *Arterioscler. Thromb. Vasc. Biol.* **28,** 835–840
37. Bäckhed, F., Manchester, J. K., Semenkovich, C. F., and Gordon, J. I. (2007) *Proc. Natl. Acad. Sci. U.S.A.* **104,** 979–984
38. Lemke, U., Krones-Herzig, A., Berriel Diaz, M., Narvekar, P., Ziegler, A., Vegiopoulos, A., Cato, A. C., Bohl, S., Klingmüller, U., Screaton, R. A., Müller-Decker, K., Kersten, S., and Herzig, S. (2008) *Cell. Metab.* **8,** 212–223
39. Romeo, S., Yin, W., Kozlitina, J., Pennacchio, L. A., Boerwinkle, E., Hobbs, H. H., and Cohen, J. C. (2009) *J. Clin. Invest.* **119,** 70–79

ADDITIONS AND CORRECTIONS

THE JOURNAL OF BIOLOGICAL CHEMISTRY VOL. 287, NO. 6, p. 4394, February 3, 2012

VOLUME 284 (2009) PAGES 25593–25601
DOI 10.1074/jbc.A109.025452

Angiopoietin-like 4 (ANGPTL4, fasting-induced adipose factor) is a direct glucocorticoid receptor target and participates in glucocorticoid-regulated triglyceride metabolism.

Suneil K. Koliwad, Taiyi Kuo, Lauren E. Shipp, Nora E. Gray, Fredrik Backhed, Alex Yick-Lun So, Robert V. Farese, Jr., and Jen-Chywan Wang

PAGE 25599:

On the *y* axis in *panel A* of Fig. 6, the measurement for serum TG should be mg/dL (not μg/mL), and on the *y* axis in *panel B*, the measurement for liver TG should be nmol/mg tissue (not mmol/mg tissue). The corrected figure is presented below.

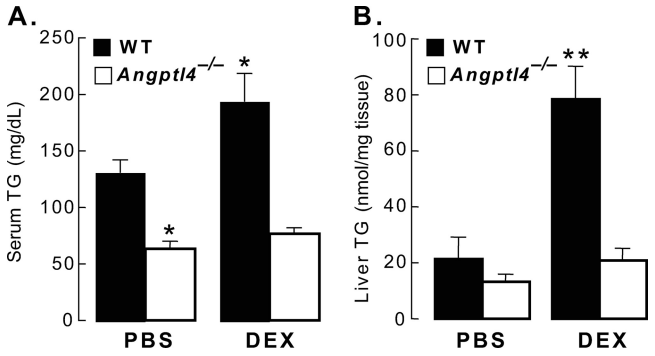

VOLUME 286 (2011) PAGES 36739–36748
DOI 10.1074/jbc.A111.245944

Functional characterization of a ficolin-mediated complement pathway in amphioxus.

Huiqing Huang, Shengfeng Huang, Yingcai Yu, Shaochun Yuan, Rui Li, Xin Wang, Hongchen Zhao, Yanhong Yu, Jun Li, Manyi Yang, Liqun Xu, Shangwu Chen, and Anlong Xu

The grant information footnote should read as follows. "This work was supported by Project 30901103 from the National Natural Science Foundation of China; Projects 2011CB946101 and 2007CB815800 of the National Basic Research Program (973), Project 2008AA092603 of the State High-Tech Development Project (863), and Project 2007DFA30840 of the International S&T Cooperation Program from the Ministry of Science and Technology of China; Key Project 0107 from the Ministry of Education; and projects from the Commission of Science and Technology of Guangdong Province and Guangzhou City and from the Sun Yet-sen University Science Foundation."

I would like to express my deepest gratitude to

My dearest mother, ***Gloria Y. C. Chen****, for all the supports through the years,*

Professor ***Jen-chywan Wally Wang*** *for the guidance through my graduate career, and*

Professors ***Paola S. Timiras*** *and* ***Chantilly A. Munson*** *for*

introducing me to the world of science.